

POLITECNICO DI MILANO

Scuola di Ingegneria Industriale e dell'Informazione
Corso di Laurea Magistrale in Ingegneria Biomedica



Cardiorespiratory Interactions in Newborns during Sleep: Linear and Nonlinear Multiparametric Analysis

Relatore: Prof. Maria Gabriella SIGNORINI

Correlatori: Maristella LUCCHINI
William FIFER, PhD

Tesi di Laurea di:
Nicolò PINI
Matr. 841423

Anno Accademico 2015-2016

Contents

List of figures	III
List of tables	VII
Ringraziamenti	IX
Acknowledgements	X
Sommario	XI
Summary	XXII
Chapter 1	1
1 Introduction	2
1.1 Sudden Infant Death Syndrome	2
1.2 Intrinsic risk: Prematurity	4
1.3 Extrinsic risk: Sleep Position	6
1.4 Fetal and newborn cardiovascular systems	8
1.4.1 Cardiovascular system generation	8
1.4.2 Circulation before birth	8
1.4.3 Circulation after birth	10
1.5 Autonomic Nervous System	12
1.6 Cardiorespiratory coupling	14
1.7 Sleep states	15
1.8 SIDS and cardiorespiratory control	16
Chapter 2	21
2 Materials and Methods	22
2.1 Study population and acquisition system	22
2.2 Time domain analysis	25
2.3 Entropy analysis: univariate and bivariate estimators	26
2.3.1 Approximate Entropy	27
2.3.2 Sample Entropy	28
2.3.3 Quadratic Sample Entropy	29

2.3.4	Transfer Entropy.....	30
2.4	Phase locking analysis	35
2.5	Directionality Index analysis	41
2.6	Statistical analysis.....	44
Chapter 3	45
3	Results	46
3.1	Time domain	46
3.2	Sample Entropy and Quadratic Sample Entropy	50
3.3	Transfer Entropy	55
3.4	Phase synchronization.....	59
3.5	Directionality index	67
Chapter 4	79
4	Discussions	80
4.1	Time and Frequency domain	80
4.2	Sample Entropy and Quadratic Sample Entropy	82
4.3	Transfer Entropy	83
4.4	Phase synchronization.....	85
4.5	Directionality Index	86
4.6	Conclusions.....	88
4.7	Further developments and future work	90
Bibliography	92

List of figures

Figure 1.1.1 Triple-risk model for SIDS by Filiano et al.	3
Figure 1.2.1 Preterm birth rates with respect to the total life birth in each state in 2015.....	4
Figure 1.3.1 Trend of SIDS rate, the diminishing trend can be observed as a consequence of the Back to Sleep Campaign. The green line indicates the percentage of babies sleeping supine with respect to the total percentage of premature infants in the USA.....	6
Figure 1.4.1 The heart and peripheral circulations in fetus	9
Figure 1.4.2 Heart and peripheral circulation before and after birth	10
Figure 1.4.3 A schematic of the fetal circulation before birth and the changes in flow in a newborn subject. Before birth the major supply of preload for the left ventricle is derived from the placental circulation, which passes from several structures and enters the left side of the heart; thereby bypassing the right side of the heart and the lungs (panel A, pathway is shown by red arrow). As most blood exiting the right ventricle passes through the ductus arteriosus (A, red arrow) and enters the descending aorta, very little blood flows into the fetal lungs before birth.	11
Figure 1.8.1 Five Steps in the terminal respiratory pathway associated with the SIDS results from one or more failures in protective mechanisms against a life-threatening event during sleep in the vulnerable infant during a critical period.....	18
Figure 1.8.2 The serotonergic system is considered to be critical for the modulation and integration of diverse homeostatic functions. The medullary level of the brain stem (black line in Panel A) includes regions involved in the regulation of upper-airway control, respiration, temperature, autonomic function, and the sympathetic nervous system. In the medulla of an infant with the sudden infant death syndrome (SIDS), tissue autoradiography shows a generalized reduction in binding to the 5- hydroxytryptamine type 1A receptor (Panel B), as compared with that in a control infant at the same postconceptional age (Panel C). ARC denotes arcuate nucleus, DMX dorsal motor nucleus of the vagus nerve, GC ganglion cells, HG hypoglossal nucleus, NA noradrenaline, NTS	

nucleus tractus solitarius, PGCL paragigantocellularis lateralis, PreBot pre-Bötzinger complexes, and ROb raphe obscurus.....	20
Figure 2.3.1 Scheme of the main steps involved in TE calculation:	34
Figure 2.4.1 From top to bottom: examples of a 60-second segment of RR series, respiration, synchrogram and relative λ index of 3:1 synchronization order	36
Figure 3.1.1 Boxplot of time domain parameters computed from RR series (RR mean, RR IQR, SDNN, RMSDD, IBI mean, IBI IQR) and from respiratory signal (IBI mean, IBI IQR).....	47
Figure 3.1.2 Boxplot of time domain parameters computed from RR series (RR mean, RR IQR, SDNN, RMSDD, IBI mean, IBI IQR) and from respiratory signal (IBI mean, IBI IQR).....	49
Figure 3.2.1 Boxplots of Sample Entropy computed for different embedding dimensions when state-related analysis is performed, active (red) versus quiet (green) in newborns and one month infants.....	51
Figure 3.2.2 Boxplots of Sample Entropy computed for different embedding dimensions when state-related analysis is performed, AS (red) versus QS (green) in newborns and one month infants.....	52
Figure 3.2.3 Boxplots of Quadratic Sample Entropy computed for different embedding dimensions when state-related analysis is performed, AS (red) versus QS (green) in newborns and one month infants.....	53
Figure 3.3.1 Boxplots of Transfer Entropy computed for newborn cohort. Comparisons are made considering same direction and different sleep state or same sleep state and different direction, N represents the number of segments in the considered population.....	56
Figure 3.3.2 Boxplots of Transfer Entropy computed for one month cohort. Comparisons are made considering same direction and different sleep state or same sleep state and different direction, N represents the number of segments in the considered population	57
Figure 3.3.3 Boxplots of Transfer Entropy computed for both newborns and one month infants. Comparisons are made considering same direction and sleep state at	

different time points, N represents the number of segments in the considered population.....	58
Figure 3.4.1 Boxplots of total percentage of synchronization, sum of ratios with respect a single breathing cycle and two consecutive breathing cycles	60
Figure 3.4.2 Boxplots of total duration of synchronization, sum of ratios with respect a single breathing cycle and two consecutive breathing cycles	61
Figure 3.4.3 Boxplots of total percentage of synchronization, sum of ratios with respect a single breathing cycle and two consecutive breathing cycles	62
Figure 3.4.4 Boxplots of total duration of synchronization, sum of ratios with respect a single breathing cycle and two consecutive breathing cycles	63
Figure 3.4.5 Entity of increase in synchronization between AS and QS for subjects with both state during the recorded baseline. Each colored line represents a subject	65
Figure 3.4.6 Bar graph of specific ratio of synchronization comparing same sleep state for different time points	66
Figure 3.5.1 Scatter plot of breathing frequency and directionality index for newborns ...	67
Figure 3.5.2 Boxplots of directionality index and breathing frequency in AS versus QS considering newborns.....	68
Figure 3.5.3 Scatter plot of breathing frequency and directionality index for one months	69
Figure 3.5.4 Boxplots of directionality index and breathing frequency in AS versus QS considering one months.....	70
Figure 3.5.5 Scatter plot of breathing frequency and directionality index in AS for both newborns and one months	72
Figure 3.5.6 Boxplots of directionality index and breathing frequency comparing newborns versus one months in AS	72
Figure 3.5.7 Scatter plot of breathing frequency and directionality index in QS for both newborns and one months.....	73
Figure 3.5.8 Boxplots of directionality index and breathing frequency comparing newborns versus one months in QS	73
Figure 3.5.9 Histogram of newborn cohort grouped based on breathing frequency, darker green indicates bins where the distributions overlap	75

Figure 3.5.10 Boxplots of directionality index and breathing comparing newborns grouped based on breathing frequency	75
Figure 3.5.11 Histogram of one month cohort grouped based on breathing frequency, darker green indicates bins where the distributions overlap	76
Figure 3.5.12 Boxplots of directionality index and breathing frequency comparing one months grouped based on breathing frequency	77
Figure 3.5.13 Boxplots of breathing and directionality index comparing newborns and one months at different time points	78

List of tables

Table 2.1.1	Subject information, percentages are computed with respect to the total number of subjects for each cohort; 151 newborns and 33 one month infants	23
Table 3.1.1	Time domain parameters extracted from RR series and respiratory signal. IBI measures the mean distance between adjacent respiratory onsets and IBI IQR the interquartile range of this distribution. P-values are relative to statistics comparing AS and QS parameters within the same age	46
Table 3.1.2	Time domain parameters extracted from RR series and respiratory signal. P-values are relative to statistics comparing same sleep state (AS and QS) parameters for the two different time points	48
Table 3.2.1	Sample Entropy and Quadratic Sample Entropy considering 300 beats of RR series only. P-values are relative to statistics comparing AS and QS parameters within the same age	51
Table 3.2.2	Sample Entropy and Quadratic Sample Entropy considering 300 beats of RR series only. P-values are relative to statistics comparing same sleep state (AS and QS) parameters for the two different time points	54
Table 3.3.1	Transfer Entropy considering 300 beats of RR series and respiratory sampled at RR instants. P-values are relative to statistics comparing AS and QS parameters within the same age and directionality or within the same age and different directionality.....	55
Table 3.3.2	Transfer Entropy considering 300 beats of RR series and respiratory sampled at RR instants. -values are relative to statistics comparing same sleep state (AS and QS) parameters for the two different time points	58
Table 3.4.1	Total synchronization parameters extracted from the analysis of phase relationship between RR series and respiratory signal. P-values are relative to statistics comparing AS and QS parameters within the same age.....	59
Table 3.4.2	Total synchronization parameters extracted from the analysis of phase relationship between RR series and respiratory signal. P-values are relative to	

statistics comparing same sleep state (AS or QS) parameters for the two different time points	62
Table 3.4.3 Paired comparison of AS versus QS in newborns and one months.....	64
Table 3.5.1 Computed directionality index and extracted breathing frequency. P-values are relative to statistics comparing AS and QS parameters within the same age	67
Table 3.5.2 Extracted directionality index and breathing frequency computed. P-values are relative to statistics comparing same sleep state (AS or QS) parameters for the two different time points	71
Table 3.5.3 Percentage indicating the portion of subjects associated with a negative directionality index and positive directionality index	74
Table 3.5.4 Extracted breathing frequency and computed directionality index. P-values are relative to statistics comparing AS and QS parameters within the same age	74
Table 3.5.5 Computed directionality index and extracted breathing frequency. P-values are relative to statistics comparing newborns and one months grouped based on breathing frequency threshold.....	77

Ringraziamenti

Questa tesi è la realizzazione di un progetto di collaborazione tra il Politecnico di Milano e Columbia University Medical Center, ideato e sviluppatosi durante l'anno accademico 2015-2016.

In particolare, hanno reso possibile questa esperienza il costante supporto e l'entusiasmo di William Fifer PhD, Direttore del Clinical Developmental Neuroscience Division at the Sackler Institute for Developmental Psychobiology, mio relatore durante i mesi di permanenza a New York.

Un ringraziamento al gruppo di lavoro del laboratorio di ricerca per la loro disponibilità.

Esprimo la mia profonda gratitudine alla mia correlatrice Maristella Lucchini, dottoranda presso il Politecnico di Milano, per il suo incessante aiuto, la pazienza ed il supporto durante questi mesi.

Un ringraziamento speciale va alla mia relatrice Maria Gabriella Signorini, Professore Associato presso il Dipartimento di Bioingegneria del Politecnico di Milano, per aver creduto in me ed avermi permesso di vivere questa esperienza unica, nonché per il supporto costante fin dall'inizio di questa tesi.

Infine un ringraziamento al sostegno economico fornito dal Politecnico di Milano per l'erogazione della borsa di studio "Tesi all'estero".

Acknowledgements

This thesis is the realization of a collaboration project between the Politecnico di Milano and Columbia University Medical Center, conceived and developed during the academic year 2015-2016.

Particularly, this has been possible thanks to the consistent support and enthusiasm of William Fifer PhD, Director of the Clinical Developmental Neuroscience Division at the Sackler Institute for Developmental Psychobiology, my Advisor during my stay in New York.

I would like to thank the entire staff of the research lab for their availability.

I would like to express my deep gratitude to my advisor Maristella Lucchini, PhD student at Politecnico di Milano, for her endless help, her patience and her support during these months.

A special thank goes to my advisor Maria Gabriella Signorini, Professore Associato at the Dipartimento di Bioingegneria del Politecnico di Milano, for believing in me and giving me this unique opportunity along with her constant presence since the beginning of this thesis.

Lastly, thanks to the Politecnico di Milano for the economic support given through the scholarship “Tesi all’estero”.

Sommario

Introduzione e scopo del lavoro

La sindrome della morte improvvisa infantile (Sudden Infants Death Syndrome, SIDS) è descritta come la morte improvvisa di un neonato sano durante il sonno e rappresenta una delle maggiori cause di mortalità infantile nei paesi sviluppati. Nonostante il marcato declino dell'incidenza della SIDS a partire dal 1990, grazie a campagne globali di educazione sul tema, SIDS rimane una delle maggiori cause di morte per i neonati di età 1-12 mesi di età. A causa del suo drammatico impatto, questa sindrome è stata studiata per lungo tempo, ma i meccanismi fisiologici di base rimangono ancora da essere chiariti.

Attualmente, la spiegazione più supportata in letteratura riguardo SIDS, è il modello del triplo rischio (Triple-risk model), proposto da Filiano e Kinney.

L'ipotesi di Filiano e Kinney riguardo SIDS è basata sulla concomitanza di tre fattori: 1) un neonato fragile, 2) un periodo critico dello sviluppo, 3) un fattore di stress esogeno.

I neonati hanno una maggiore probabilità di morire di SIDS se posseggono tutti questi tre fattori: la vulnerabilità congenita dei neonati rimane latente finché questi ultimi entrano nel periodo critico della SIDS e sono soggetti ad uno stress esterno.

Lo sviluppo del controllo cardiorespiratorio può essere classificato come un fattore di rischio, in accordo con il modello del triplo rischio. In particolare può essere pensato come una sottoclasse del cosiddetto controllo omeostatico.

A seguito di queste considerazioni, il presente studio si propone di analizzare una popolazione di neonati a termine sani ed una popolazione di infanti sani di un mese di età. Il lavoro di tesi si concentra sull'analisi dell'interazione cardiorespiratoria, la sua relazione con gli stati del sonno e la sua evoluzione dalla nascita ad un mese di vita. Lo scopo della ricerca è la descrizione dell'accoppiamento cardiorespiratorio di tipo fisiologico, al fine di metterne in luce le differenze rispetto all'accoppiamento cardiorespiratorio delle vittime di SIDS.

Lo studio di questa interazione è eseguita su soggetti durante il sonno. Il sonno ha un ruolo fondamentale nello sviluppo del sistema nervoso e nella regolazione omeostatica.

Il sonno nei neonati e negli infanti può essere classificato in tre tipi: Sonno Quiet (Quiet Sleep, QS) (equivalente a NREM), Sonno Attivo (Active Sleep, AS) (equivalente a REM) e Sonno Indeterminato (Indeterminate Sleep, IS).

È stato ipotizzato che gli infanti morti di SIDS avrebbero mostrato anomalie nell'organizzazione degli stati del sonno precedentemente allo loro morte.

Il meccanismo alla base di SIDS appare avere origini nell'ambiente fetale con il risultato di danni neuronali e di sviluppo del sistema nervoso autonomo (Autonomic Nervous System, ANS). Questo meccanismo ancora sconosciuto in seguito, comprometterebbe l'adeguata risposta alle sfide respiratorie e pressorie durante il sonno.

Questo deficit coinvolge alterazioni dei recettori delle regioni coinvolte nel controllo chemocettivo, cardiovascolare e cardiorespiratorio.

Risulta fondamentale evidenziare che l'indagine dell'accoppiamento cardiorespiratorio è in grado di fornire una conoscenza non invasiva dei meccanismi di interazione fra il sistema cardiaco e respiratorio ed è in grado di aiutare a comprendere i fattori che contribuiscono all'occorrenza di SIDS.

Lo studio descritto in questa tesi è stato possibile grazie alla collaborazione fra il centro clinico di eccellenza Columbia University Medical Center (CUMC) e il Politecnico di Milano, Dipartimento DEIB.

L'indagine di tesi è stata condotta al Politecnico di Milano e al CUMC durante i miei 6 mesi di permanenza nella città di New York. L'incontro fra il contributo dell'ingegneria biomedica e le competenze mediche hanno permesso di proporre nuove soluzioni per la quantificazione dell'interazione cardiorespiratoria e la validazione dei risultati ottenuti.

Materiali e Metodi

Il dataset dei neonati include 151 infanti nati al Morgan Stanley Children's Hospital di New York at CUMC fra 38 e 40 settimane di età gestazionale (Gestational Age (GA)), mentre il gruppo degli infanti di un mese di età include 33 soggetti che si sono sottoposti ad un follow-up ad un mese, la selezione di questi ultimi soggetti è basata sul medesimo criterio

relativo all'età gestazionale. Nessuno degli infanti è stato ricoverato nell'unità di terapia intensiva neonatale (Neonatal Intensive Care Unit, NICU) o è stato diagnosticato di gravi patologie o disordini genetici conosciuti.

Fra i vari segnali registrati, in questo contesto sono stati analizzati ECG e segnale respiratorio. Gli stati del sonno sono stati codificati, sulla base del respiro, da medici esperti nel settore.

Durante i 10 minuti di acquisizione della baseline, i neonati dormivano in posizione supina, entro ~ 30 minuti in seguito all'allattamento. Sono stati analizzati segmenti di 3 minuti di durata durante i quale non vi sono cambiamenti nello stato del sonno: 514 epoche di durata tre minuti per la popolazione dei neonati (239 sonno quieto, 275 sonno attivo), mentre 247 epoche per gli infanti di un mese di età (144 sonno quieto, 103 sonno attivo).

I picchi R sono stati individuati sul tracciato ECG per mezzo dell'algoritmo di Pan-Tompkins. Un filtro adattativo è stato successivamente applicato al fine di rimuovere i battiti ectopici o artefatti.

Il segnale respiratorio è stato filtrato con un filtro passa-banda (0.05 – 3.5 Hz). I picchi di inspirazione sono stati individuati per mezzo di un software automatico di riconoscimento ed ogni segmento è stato controllato manualmente al fine di eliminare i picchi incorretti.

L'analisi dell'interazione cardiorespiratoria durante il sonno è svolta per mezzo di un approccio univariato ed uno bivariato, per mezzo di metodi lineari e non lineari. Lo scopo dell'analisi è la caratterizzazione dell'interazione in relazione agli stati del sonno e la corrispondente evoluzione dovuta all'età.

La prima analisi riguarda l'estrazione dei parametri univariati nel dominio del tempo, calcolati dalla serie RR e dal respiro. Vi è una mancanza di linee guida per l'applicabilità di questi metodi per i neonati. È evidente che modalità di analisi applicate agli adulti non possano essere applicate a questo contesto, considerato che la frequenza cardiaca media (Heart Rate, HR) dei neonati risulta circa doppia rispetto a quella degli adulti e presenta caratteristiche peculiari. Date queste considerazioni, l'analisi nel dominio del tempo per i neonati utilizza parametri adattati dal contesto dell'analisi per gli adulti.

Come indicato nella HRV Task Force, i parametri relativi ad HR sono RR medio, RR IQR, SDNN and RMSSD, calcolati per ogni segmento di durata 3 minuti. Riguardo il segnale respiratorio, i parametri calcolati sono Inter Breath Interval (IBI) medio and IBI IQR.

L'analisi nel dominio delle frequenze è effettuata considerando tre differenti bande specificatamente scelte for la popolazione di infanti di questo studio: Very Low Frequency (VLF), 0.01-0.04 Hz, Low Frequency (LF), 0.04-0.2 Hz, and High Frequency (HF), 0.35-1.5 Hz.

Riguardo l'analisi non lineare dell'interazione cardiorespiratoria, stimatori di entropia univariati e bivariati sono stati calcolati.

È ampiamente riportata in letteratura la capacità degli stimatori di entropia di discriminare i segnali fisiologici per mezzo di misure di complessità. In questa tesi sono stati calcolati parametri di entropia classici ed in aggiunta ad essi, nuovi indici capaci di descrivere la direzionalità dell'interazione fra sottosistemi.

Sample Entropy (SampEn) e Quadratic Sample Entropy (QSE) sono stimatori di entropia univariati basati sull'analisi della serie RR. Possono essere intesi come l'evoluzione dell'Approximate Entropy (ApEn) di Pincus. Entrambi mostrano un leggero bias nella stima in dipendenza alla lunghezza del segnale analizzato, per questa ragione in questa analisi, è stato considerato un numero fisso di battiti per ogni segmento.

L'approccio innovativo proposto in questo lavoro è l'utilizzo della Transfer Entropy (TE) per lo studio della coordinazione cardiorespiratoria. TE stima la direzionalità del trasferimento di informazione fra il segnale HR e il segnale respiratorio senza nessuna assunzione a priori riguardo la natura dell'interazione fra i sottosistemi, in questo modo è in grado di coglierne i contributi lineari e non lineari. La stima di TE riguarda il calcolo della funzione di densità di probabilità di entrambi i segnali e la funzione di densità di probabilità capace di descrivere la relazione reciproca fra serie RR e respiro.

TE è una misura di predicibilità e complessità. In questo contesto, TE calcolata per la direzionalità $1 \rightarrow 2$, quantifica il miglioramento nella predizione del futuro del segnale 2, nel caso in cui si tenga in considerazione non solo il passato del segnale stesso ma anche l'informazione del passato del segnale 1.

Al fine di fornire una differente prospettiva alla quantificazione dell'interazione cardiorespiratoria l'analisi conclusiva di questo lavoro si focalizza sull'interazione delle fasi della serie RR e del segnale respiratorio.

Gli stimatori presentati sono la quantificazione del locking di fase (phase locking) e l'indice di direzionalità (Directionality Index, DI).

Entrambi sono metodi non lineari bivariati che quantificano, per mezzo dell'analisi della fase di due sistemi, sincronizzazione e direzionalità rispettivamente. In accordo con questa ipotesi è possibile indagare la sincronizzazione cardiorespiratoria per mezzo dell'analisi di fase della serie RR e del segnale respiratorio rispetto ad una classica analisi sulle ampiezze.

Questo presupposto supporta l'assunzione che l'ampiezza di due oscillatori possa rimanere scorrelata nonostante le loro fasi interagiscano mutualmente.

La sincronizzazione è stata in prima luogo analizzata per mezzo del sincrogramma, uno strumento visuale che rappresenta le distanze relative fra i picchi R e i picchi di inspirazione respiratoria. Al fine di quantificare la presenza o l'assenza di interazione e valutare la forza dell'accoppiamento fra i sistemi in analisi, l'indice di sincronizzazione λ è stato calcolato.

L'analisi della sincronizzazione non è in grado di spiegare la modalità con cui i sistemi interagiscono e mutualmente perturbano loro stessi. L'indice di direzionalità è capace di stimare l'interazione causale fra HR e segnale respiratorio, osservando l'evoluzione delle fasi dei sottosistemi.

In questo studio, l'algoritmo Evolution Map Approach (EMA) è stato utilizzato. Questo metodo si basa sulla mutua predicibilità in modo simile alla causalità di Granger.

Risultati

In questa tesi, sono state eseguite due tipologie di analisi: una riguardante gli stati del sonno (state-related) ed una riguardante le età (age-related). Il primo caso tratta il confronto di un parametro in AS rispetto allo stesso parametro in QS considerando una specifica età (neonati oppure infanti di un mese d'età), il secondo caso riguarda invece il confronto di un parametro in uno specifico state del sonno valutato per le due differenti età.

L'analisi statistica è stata eseguita utilizzando il criterio IQR per l'outlier rejection. Le differenze fra gruppi sono state valutate per mezzo di un unpaired T-test se l'ipotesi di distribuzione Gaussiana per la distribuzione della popolazione risulta verificata; nel caso l'ipotesi di Gaussianità non sussiste, è stato utilizzando il test non parametrico Wilcoxon signed-rank.

I risultati ottenuti in questa tesi mostrano come i nuovi parametri descritti nella sezione precedente siano in grado di aumentare la conoscenza della sincronizzazione cardiorespiratoria e della regolazione del sistema nervoso autonomo durante il sonno.

Risulta importante sottolineare come questi indici siano da utilizzarsi in combinazione con gli stimatori nel dominio del tempo, nel dominio delle frequenze, con gli stimatori di entropia classici al fine di ottenere una descrizione completa dell'interazione fra sistema cardiaco e sistema respiratorio.

- **Dominio del tempo e dominio delle frequenze:** i risultati confermano un aumento di HR dalla nascita ad un mese di età come riportato da vari autori. I parametri estratti dalla serie RR e dal segnale respiratorio mostrano differenze significative per l'analisi state-related, ad eccezione del parametro RMSSD. Le differenze nella variabilità battito-battito possono essere estratte per mezzo dell'analisi in frequenza, il contributo delle alte frequenze aumenta in modo significativo comparando AS contro QS. Queste considerazioni sono valide per entrambe le popolazioni presentate in questa tesi. Riguardo l'analisi age-related, solo i parametri nel dominio del tempo relativi ad HR mostrano una evoluzione relativamente all'età.
- **Sample Entropy e Quadratic Sample Entropy:** è stato possibile osservare in studi precedenti che l'entropia è maggiore in QS rispetto che in AS. I risultati ottenuti in questo lavoro confermano un aumento di entropia in QS per entrambi gli stimatori. Queste considerazioni sono consistenti indipendentemente la dimensione di embedding (m), in questo contesto $m=1, 2, 3$. L'analisi age-related non mostra differenze nel confronto fra le due età.
- **Transfer Entropy:** in questa tesi, TE è stata utilizzata per la prima volta per caratterizzare il cambiamento in termini di flusso di informazione, per entrambi i tipi

di analisi: state-related e age-related (paper sottomesso, Entropy Journal 2017). In AS non è evidenziabile nessuna differenza di flusso di informazione comparando le direzionalità $RR \rightarrow RESP$ e $RESP \rightarrow RR$. Al contrario in QS, un aumento netto di informazione è rintracciabile in direzione $RESP \rightarrow RR$ rispetto alla direzionalità opposta. Le precedenti considerazioni sono valide per entrambe le età.

Riguardo l'analisi age-related, l'evoluzione in termini di flusso di informazione è rintracciabile in QS per entrambe le direzioni ($RR \rightarrow RESP$ e $RESP \rightarrow RR$), al contrario AS non mostra nessuna evoluzione in termini di trasferimento di informazione fra i sottosistemi, confrontando neonati e infanti di un mese d'età.

L'analisi state-related dell'interazione cardiorespiratoria per mezzo dell'analisi delle fasi del sistema cardiaco e respiratorio ha evidenziato interessanti peculiarità. È evidente un significativo aumento della sincronizzazione confrontando QS ed AS (poster session Dynamics Days, January 2017; conference paper EMBEC, June 2017).

Sono state individuate differenze in termini di direzionalità relativamente agli stati del sonno, i risultati supportano le analisi di TE sopra riportate. Le presenti conclusioni sono in contrasto con la precedente letteratura in cui è riportata una assenza di cambio di direzionalità nel confronto AS contro QS.

- **Locking di fase:** l'analisi state-related mostra un aumento di sincronizzazione significativo confrontando AS contro QS. L'aumento è calcolato in termini di percentuale di sincronizzazione (la durata di sincronizzazione percentuale rispetto alla durata del segmento analizzato) e di durata media di sincronizzazione (la durata media degli episodi di sincronizzazione durante il segmento analizzato). L'indagine age-related mostra un aumento di sincronizzazione in termini di percentuale, mentre la durata media della sincronizzazione resta invariata, questi risultati sono relativi solamente a QS.
- **Indice di direzionalità:** l'analisi state-related ha evidenziato un'assenza di direzionalità chiara in AS ed una predominanza di direzionalità $RESP \rightarrow RR$ in QS. I presenti risultati supportano le considerazioni ottenute per mezzo di TE, è da evidenziare però la differente modalità di indagine, basata sulla fase del segnale

cardiaco e respiratorio. L'analisi age-related non mostra alcuna evoluzione nel confronto fra neonati ed infanti di un mese di età. Un'ulteriore analisi indaga la direzionalità dell'interazione quando la suddivisione delle popolazioni è basata sulla frequenza respiratoria indipendentemente dallo stato del sonno. È evidente una direzionalità predominante (RESP→RR) per frequenze respiratorie < 0.6 Hz, mentre non è individuabile una direzionalità chiara per frequenze respiratorie ≥ 0.6 Hz.

Discussioni

I risultati presentati nelle sezioni precedenti hanno contribuito alla descrizione dell'interazione cardiorespiratoria attraverso metodi non invasivi di analisi del segnale.

Il tentativo di caratterizzare la relazione reciproca fra il sistema cardiaco e il sistema respiratorio ha confermato gli studi precedenti e ha fornito interessanti nuovi risultati.

I parametri nel dominio del tempo hanno evidenziato differenze fra gli stati del sonno, con un aumento di RR medio in QS rispetto ad AS esclusivamente nei neonati e una decrescita della variabilità cardiaca (Heart Rate Variability, HRV) sia nel caso dei neonati che negli infanti.

Considerando il confronto tra gli stati del sonno, i parametri nel dominio del tempo indicano una maggiore variabilità in AS (SDNN), mentre non vi sono differenze nella variabilità battito-battito (RMSSD) alla nascita, ad un mese di età è evidenziabile una lieve e significativa decrescita in QS rispetto ad AS.

In conclusione, la maggioranza dei parametri nel dominio del tempo mostra una adeguata capacità nell'individuare differenze in relazione agli stati del sonno.

Riguardo il confronto fra neonati ed infanti di un mese di età, solo i parametri nel dominio del tempo relativi all'analisi delle serie RR mostrano differenze significative, mentre i parametri estratti dall'analisi del segnale respiratorio mostrano una decrescita non significativa con l'età.

La complessità del segnale HR è stata analizzata per mezzo dell'entropia univariata: Sample Entropy (SampEn) e Quadratic Sample Entropy (QSE).

Un aumento di entropia in QS rispetto ad AS è consistente indipendentemente dalla dimensione di embedding, questo risultato conferma la predominanza del controllo

simpatico in QS. Un'ulteriore conferma a quest'ultima considerazione è stata proposta in studi precedenti, i quali interpretano una semplificazione della variabilità cardiaca e quindi una diminuzione della stima di entropia, in conseguenza di una diminuzione dell'attività parasimpatica ed attivazione del sistema simpatico.

TE è uno stimatore di entropia bivariato, il quale può essere impiegato per stimare il flusso di informazione fra due serie temporali.

I risultati riportati in questa tesi mostrano valori di TE maggiori in QS rispetto ad AS: QS può essere interpretato come una condizione in cui l'accoppiamento cardiorespiratorio è maggiormente evidente e la mutua influenza dei segnali risulta evidente. Inoltre, la principale direzione di interazione è RESP→RR in QS, mentre in AS non è rintracciabile una direzione preferenziale. Data le più lente e regolari frequenze respiratorie associate a QS, è possibile ipotizzare una più stabile relazione fra respiro e segnale cardiaco.

L'analisi della popolazione degli infanti di un mese d'età mostra risultati analoghi rispetto a quanto emerso dall'analisi dei neonati.

L'analisi age-related mostra una evoluzione in termine di flusso di informazione in QS per entrambe le direzionalità (RESP→RR, RR → RESP). AS risulta invece uno stato di minore accoppiamento cardiorespiratorio e la stima di TE non varia in modo significativo con l'età

I risultati ottenuti per mezzo dell'analisi di TE fornisco una descrizione innovativa ed una quantificazione del controllo cardiorespiratorio e della regolazione autonoma negli infanti.

L'analisi della sincronizzazione di fase permette la quantificazione dell'interazione cardiorespiratoria per mezzo dell'analisi della fase degli oscillatori cardiaco e respiratorio.

Il confronto fra AS e QS nei neonati mostra un incremento di sincronizzazione significativo in QS in accordo con studi precedenti i quali riportano gli stati del sonno come un aspetto fondamentale per la regolazione della sincronizzazione cardiorespiratoria, la quale è più frequente in QS.

La medesima analisi considerando gli infanti di un mese d'età evidenzia trend di aumento di sincronizzazione analoghi a quanto riportato nei neonati.

Nell'analisi age-related, un aumento di sincronizzazione è rintracciabile solo in QS. Il seguente risultato è coerente con l'analisi dei parametri del dominio del tempo e di TE, i quali riportano una evoluzione relativa all'età solo in QS.

L'analisi dell'indice di direzionalità (DI) permette una quantificazione della relazione di causalità fra HR e respiro, in modo simile alla stima di TE.

QS è caratterizzato da una prevalenza di direzionalità RESP→RR, mentre AS non mostra nessuna direzionalità preferenziale nell'interazione fra i due sistemi. Questi risultati sono simili all'analisi di TE: il respiro appare il principale driver dell'interazione in QS. Frequenze respiratorie più elevate ed associate ad AS non risultano in grado di modulare HR e la direzionalità conseguentemente si sposta verso la direzionalità opposta (RR→RESP). Risultati analoghi sono ottenuti considerando le due popolazioni: neonati e infanti di un mese d'età.

Gli indici tradizionali ed innovativi calcolati in questa tesi, hanno dimostrato la loro capacità di discriminare fra i differenti stati del sonno e descrivere l'interazione cardiorespiratoria attraverso una nuova prospettiva.

Alcune fra le più recenti teorie riguardo SIDS attribuiscono alla mancanza di coordinazione cardiorespiratoria un ruolo fondamentale nell'aumento del rischio associato alla patologia. È stato ipotizzato che gli stati del sonno (AS e QS) siano due condizioni che differiscono in termini di sincronizzazione cardiorespiratoria e la continua alternanza fra stati di maggiore e minore accoppiamento sia in grado di stressare il sistema nervoso autonomo al fine di renderlo capace di fronteggiare le numerose sfide cui è sottoposto.

I risultati ottenuti in questa tesi possono essere interpretati in accordo con l'ipotesi del sistema nervoso autonomo come capace di stressare se stesso. I soggetti analizzati in questa tesi erano distesi supini, e hanno presentato epoche di AS e di QS con una prevalenza di AS nei neonati. AS e QS sono stati descritti in questa indagine come due stati del sonno che differiscono in termini di sincronizzazione e direzionalità.

L'alternanza di questi due stati del sonno costituisce un fattore di stress positivo per il sistema nervoso autonomo, capace di stimolarne lo sviluppo.

Nonostante gli interessanti risultati, molte domande richiedono una futura approfondita indagine.

Al fine di studiare in profondità lo sviluppo del sistema nervoso autonomo in termini di sincronizzazione e direzionalità, sarebbe opportuno seguirne la crescita in funzione del tempo. La situazione ideale è rappresentata da una indagine dalla nascita fino all'anno di vita al fine di caratterizzare l'evoluzione fisiologica della coordinazione cardiorespiratoria durante il periodo critico per l'occorrenza di SIDS.

In seguito alla caratterizzazione della risposta fisiologica, un'indagine su soggetti prematuri potrebbe evidenziarne differenze nello sviluppo autonomo rispetto ai soggetti a termine.

Infine, l'analisi delle differenze nella coordinazione cardiorespiratoria in soggetti deceduti a causa di SIDS potrebbe aprire nuovi orizzonti nel monitoraggio e nella cura neonatale per mezzo di un'indagine non invasiva ed affidabile del sistema nervoso autonomo.

Summary

Introduction and aim of the work

Sudden Infants Death Syndrome (SIDS) is characterized by the sudden death of a healthy infant during a sleep period. It is one of the leading causes of infant mortality in developed countries. Despite the dramatic decline in the incidence of SIDS since 1990 following worldwide education programs, SIDS remains the major cause of death in infants of 1–12 months of age. Because of its dramatic impact, this syndrome has been studied for long, but the underlying physiologic mechanisms have not been cleared yet.

At the moment, the most supported explanation in literature regarding SIDS, is the Triple-risk model, proposed by Filiano and Kinney.

Filiano and Kinney's SIDS hypothesis is based on the concurrence of three factors: 1) a vulnerable infant, 2) a critical developmental period, 3) an exogenous stressor.

Infants are likely to die of SIDS if they possess all three factors: the already congenital infants' vulnerability lies latent until they enter the crucial period and are subject to an exogenous stressor.

Cardiorespiratory control development can be classified as risk factor according to Triple-risk model. In particular, it can be thought as a subclass of the so-called homeostatic control.

In light of this issue, the present study proposes to analyze a population of healthy full-term newborns and one month infants with a deep focus on cardiorespiratory interaction, its relationship with sleep state and its evolution from birth to one month of age. The aim of the investigation is the description of physiological cardiorespiratory coupling, within the future prospective of highlighting differences with respect to cardiorespiratory coupling of SIDS victims.

The investigation of this interaction is performed on subjects during sleep. Sleep plays a fundamental role in neurodevelopment and homeostatic regulation.

Sleep in newborns and infants can be classified in three type: Quiet Sleep (QS) (NREM equivalent), Active Sleep (AS) (REM equivalent) and Indeterminate Sleep (IS).

It has been hypothesized that infants who were to die of SIDS would show abnormalities of sleep state distribution prior to their deaths.

The mechanism underlying SIDS appears to have origins in the fetal environment resulting in neural damage and ANS development which later compromises responses to breathing or blood pressure challenges during sleep. The deficits appear to be related to alterations in neurotransmitter receptors within regions involved in chemoreception and cardiovascular and cardiorespiratory control.

It is crucial to stress the fact that cardiorespiratory coupling can provide a noninvasive insight of the mechanism underlying the interaction between the cardiac and respiratory system and help understanding the factors contributing to SIDS occurrence.

The study reported in this thesis was possible thanks to collaboration of the outstanding Columbia University Medical Center (CUMC) and Politecnico di Milano, DEIB Department.

The thesis investigation has been conducted at Politecnico di Milano and at CUMC during my 6-months staying in New York. The encounter between the biomedical engineering contribution and the clinical expertise has allowed proposing new solutions for a quantification of cardiorespiratory interaction and validation of obtained results.

Materials and Methods

The newborn dataset includes 151 infants born at the Morgan Stanley Children's Hospital of New York at CUMC between 38 and 40 weeks of gestation and the one month infants cohort includes 33 subjects who came back for a one month follow up, based on the same criterion about Gestational Age (GA). None of the infants were admitted to the Neonatal Intensive Care Unit (NICU) nor had any major illness or known genetic disorder.

Among the various recorded signal, in this work ECG and respiratory signal were analyzed. Sleep states were coded based on respiration by expert clinicians.

During the 10-minutes baseline acquisition, babies were sleeping in supine position within ~ 30 minutes following feeding. Segments of 3-minute length in a continuous sleep state were analyzed: 514 three-minute epochs were considered for newborns (239 quiet, 275 active), while 247 epochs were considered for one month infants (144 quiet, 103 active).

The R peaks were detected on the ECG with the Pan-Tompkins algorithm. An adaptive filter was then applied to remove ectopic beats or artifacts.

The respiration signal was filtered with a bandpass filter (0.05 - 3.5 Hz). Peaks of inspiration were detected with automated marking software and each record was corrected for incorrect marks manually.

The analysis of cardiorespiratory interaction during sleep is performed with a univariate and bivariate approach by means of linear and nonlinear methods. The aim of this investigation is to characterize this interaction depending on sleep state and track its age-dependent evolution.

The first performed investigation was the extraction of time domain univariate parameters, computed from RR series and respiration. There is a lack in guidelines for the application of these methods on neonates. As a matter of fact, indications given for adults are not applicable, since the average heart rate (HR) of neonate is almost double adult's one and it has peculiar characteristics. For this reason, time domain analysis takes adapted parameters from the adult approach.

As indicated in HRV Task Force, HR parameters employed in the analysis were RR mean, RR IQR, SDNN and RMSSD, computed on 3-minute length segments. On the other hand, computed respiratory parameters were Inter Breath Interval (IBI) mean and IBI IQR.

Frequency domain analysis were performed considering three different bands specifically chosen for this population of infants: Very Low Frequency (VLF), 0.01-0.04 Hz, Low Frequency (LF), 0.04-0.2 Hz, and High Frequency (HF), 0.35-1.5 Hz.

Regarding nonlinear investigation of cardiorespiratory coordination, univariate and bivariate entropy estimates were computed.

Entropy estimators have already shown their capability in discriminating physiological signals based on complexity measurements. In this work, classical entropy

parameters have been computed along with new indexes capable of describing directionality of interaction between subsystems within the information theory framework.

Sample Entropy (SampEn) and Quadratic Sample Entropy (QSE) are univariate entropy estimators based on RR series analysis. They can be seen as the evolution of Approximate Entropy (ApEn) by Pincus. Both SampEn and QSE have been reported to show a slight bias dependent on the length of the analyzed signal, due to this reason a fixed number of beats for each segment have been considered in this analysis.

The novel approach proposed in this work is the application of Transfer Entropy (TE) to investigate cardiorespiratory coordination. TE estimates the directionality of the information transfer between HR signal and respiratory signal without any assumption about the underlying nature of the interaction, in this way it is capable of catching both linear and nonlinear contributions. The estimation of TE deals with the computation of probability density function of both signals and the joint probability density function capable of describing the interrelationship between RR series and respiration.

TE is a measure of predictability and complexity. In this analysis when considering the direction $1 \rightarrow 2$, TE quantifies the improvement in predicting the future of signal 2 when the prediction takes into consideration not only the past of signal 2 but also information from the past of signal 1.

In order to provide a different prospective of cardiorespiratory quantification the last part of this work focuses on phase analysis of RR series and respiratory signal.

The last estimators presented in this work are phase locking quantification and directionality index (DI).

They both are nonlinear bivariate method to quantify synchronization and directionality respectively, by means of the analysis of systems' phase rather than a traditional amplitude analysis.

This assumption supports the idea that amplitude of (two or more) oscillators may remain uncorrelated whereas their phases do mutually perturb.

Synchronization has been primarily investigated by means of synchrogram, a visual tool displaying the relative distances between R peaks and respiratory onsets. In order to

quantify the presence or absence of the interaction and the strength of the coupling between the systems under analysis, the synchronization index λ has been computed.

Even when considering phase-locking analysis, synchronization does not explain how systems interact and mutually perturb themselves. Directionality index is capable of estimating a casual interrelationship between the HR and respiration, looking at the evolution of phase of the subsystems.

In this work the Evolution Map Approach (EMA) algorithm has been used. This method deals with mutual predictability similarly to Granger causality. Considering system 1 interacting with system 2, if system 1 affects system 2, the future of system 2 can be better predicted taking into account the past samples of both system with respect to information of system 1 only.

Results

In this work, state-related and age-related analyses have been performed. The former case regards the comparison of a parameter in AS versus QS when a specific age is considered (newborns or one month infants), in the latter case a parameter in a specific state (AS or QS) is compared at two different time points.

The statistical analysis has been performed employing IQR outlier rejection criterion. Differences between groups have been tested by means of an unpaired T-test in case of Gaussian distributed populations; on the contrary the non-parametric Wilcoxon signed-rank test has been performed if the hypothesis of Gaussian-like distribution was not verified.

Results obtained in this thesis show that novel parameters are capable of improving the knowledge about cardiorespiratory synchronization and ANS regulation during sleep.

It is important to stress that they need to be employed in combination with traditional time domain, frequency domain and classical entropy estimators to achieve a complete description of the interaction between the cardiac and respiratory systems.

- **Time domain and frequency domain:** results confirmed the HR increase from birth to one month of age as reported by many authors. Time domain parameters extracted from RR series and respiratory signal showed significant differences when

performing state-related analysis, with the exception of RMSSD. Beat-to-beat variability differences can be instead extracted by means of frequency analysis, high frequencies contribution is statistically increasing when comparing AS versus QS. These considerations are valid for both newborns and one month infants populations. Regarding age-related analysis, only time domain parameters extracted from HR showed an evolution with age when the two cohorts are compared.

- **Sample entropy and Quadratic Sample Entropy:** it has been observed by previous studies that entropy is higher in QS than in AS. Results obtained in this work, confirmed an entropy increase in QS with respect to AS for both SampEn and QSE. This finding is consistent regardless the employed embedding dimension (m), in this work $m=1, 2, 3$. Age-related analysis showed no differences when comparing newborns and one month infants.

- **Transfer Entropy:** in this work, TE analysis has been applied for the first time to characterize the information flow changes when performing state-related and age-related analyses (submitted paper, Entropy Journal 2017).

In AS no clear differences in information flow has been found when comparing RR→RESP and RESP→RR directionalities. In QS instead, a net TE increase is found for RESP→RR with respect to the opposite directionality. This result is valid both for newborns and one month infants.

Regarding the age-related analysis, the evolution of information flow is only seen in QS for both RR→RESP and RESP→RR directionalities, on the other hand AS did not show any evolution in term of information transfer between subsystems when comparing newborns versus one month infants.

The state-related investigation of cardiorespiratory interaction by means of phase analysis highlighted interesting peculiarities. A net increase in synchronization in QS with respect to AS is seen (poster session Dynamics Days, January 2017; conference paper EMBEC, June 2017).

Differences in directionality related to sleep states have been found, supporting this work results about TE. The obtained finding is in contrast with previous works reporting the absence of a clear change in directionality when comparing AS versus QS.

- **Phase locking:** state-related analysis showed a statistically significant increase in synchronization comparing AS versus QS. The increase is computed in term of percentage of synchronization (the percentage duration of synchronization with respect to length of the analyzed record) and mean duration in seconds (the mean duration of various synchronization episodes during the analyzed segment). Age-related investigation showed an increase in synchronization in term of percentage while the average duration stayed the same, in QS only.
- **Directionality Index:** state-related analysis highlighted the absence of a clear directionality in AS and a predominance of RESP→RR directionality in QS. This result support findings of TE analysis, within a different investigation procedure based on oscillators' phase. Age-related analysis shows no trend of evolution when comparing newborns and one month infants. A further analysis investigates the directionality of interaction when population grouping is performed based on breathing frequency rate regardless the sleep state. A predominant directionality (RESP→RR) is clearly seen for breathing frequency < 0.6 Hz, while no clear directionality is present when considering breathing frequency ≥ 0.6 Hz.

Discussions

The thesis results presented in the previous section have helped describing in details the cardiorespiratory interaction by means of noninvasive methods of signal processing.

The effort in characterizing the interrelationship between the cardiac and respiratory system confirmed previous studies and provided interesting new findings.

Time domain parameters from this data analysis enhance differences between sleep states, with an increase of RR mean in QS with respect to AS in newborns only, and a decrease of Heart Rate Variability (HRV) in both newborns and one month infants cohorts.

Considering the comparison between sleep states, time domain parameters indicate an increase in variability in AS (SDNN), while no difference was found in beat-to-beat variability (RMSSD) at birth and a slightly significant decrease in QS with respect to AS at one month of age.

Concluding, almost all the time domain parameters when performing state-related analysis have proved their ability to find significant differences between sleep states.

Regarding the comparison between newborns and one month infants within the same sleep state, only time domain parameters computed on RR series show significant differences while parameters extracted from respiratory signal show a non-significant decreasing trend with age.

The complexity of HR signal has been investigated by means of Univariate Entropy: Sample Entropy (SampEn) and Quadratic Sample Entropy (QSE).

An entropy increase in QS with respect to AS has been found for both SampEn and QSE despite the embedding dimension, confirming the predominance of parasympathetic control in QS. As a matter of fact, even previous studies have proposed that a simplification of HR dynamics and thus a lowering in entropy values, might follow a parasympathetic withdrawal and sympathetic activation.

Transfer entropy is a bivariate entropy estimator, which can be employed to assess the information flow between two time series.

Results reported in this work showed that TE is higher in QS than AS: QS can be seen as condition in which the cardiorespiratory coupling is more evident and the influence of RR over respiration and vice versa is noticeable. Moreover, the main direction of the information flow is RESP→RR in QS, while in AS no clear directionality is recognizable. Given that breathing in QS is slower and more regular, it potentially allows a more stable effect/relationship with HR.

The analysis performed on one month cohort shows analogous results of the ones obtained considering newborns.

An age dependent evolution in terms of information flow happens only in QS for both RR→RESP and RESP→RR directions. AS is per se a state of lower coupling between HR and respiration, changes in TE are not dramatically affected by age.

These findings provide an innovative description and quantification of cardiorespiratory control and ANS regulation in infants, based on information theory.

Phase synchronization analysis allows quantifying the cardiorespiratory interaction between the cardiac and respiratory systems by means of oscillators' phase analysis.

The comparison can be performed considering AS versus QS within the newborn cohort. A significant increase in synchronization in QS is noticeable and in agreement with previous studies, which established that sleep state is a relevant aspect for cardio-respiratory synchronization, which occurs more frequently in QS.

When one month population is analyzed, comparable trend of increase in synchronization are found.

When age-related analysis is performed, an increase in synchronization is found in QS only. This result is coherent with what previously found in time domain parameters and TE reporting an evolution with age in QS only.

Directionality index (DI) analysis performs a quantification of the causal directionality between HR and respiration similarly to Transfer Entropy.

QS is characterized by a prevalence of RESP→RR directionality while AS exhibit no clear directionality of interaction. These results are similar with what found in TE analysis: respiration appears to be the main driver in QS. Higher breathing frequencies associated with AS are no more capable of modulating the HR and the directionality shifts on the opposite direction, RR→RESP. The analogous analysis has been performed on one month infants: results are similar with what found for newborns.

The traditional and novel indexes have proven capability to discriminate between sleep states and to describe the cardiovascular interaction with a new insight.

Some of the most recent theories about SIDS started attributing the lack of cardiorespiratory control as the main driver of risk for SIDS. It has been hypothesized that AS and QS are two conditions that differs in term of cardiorespiratory synchronization and the continuous alternation between lower and higher coupling condition is capable of stressing the ANS, making it more ready to face several challenges.

It has been also reported that the state change from AS to QS increases the occurrence of sighs and gaps, two mechanisms those are crucial to overcome cardiorespiratory challenges and capable of driving the autoresuscitation mechanism.

The results obtained in this work could be interpreted with this hypothesis of ANS being the stressor of itself. The healthy and full-term subjects analyzed were lying supine and their sleep was characterized by both AS and QS with a prevalence of AS for newborns. AS and QS have been reported by this work as two different sleep states with different characteristics in term of synchronization and also directionality.

The alternation between these two sleep states constitutes a constant positive stressing condition that is probably capable of stimulating the ANS development.

Despite the interesting results many questions are still to be addressed.

In order to deeper investigate the ANS evolution in term of both synchronization and directionality, more time points are needed. The ideal situation would be tracking the ANS development from birth to one year of age to fully characterize the physiological behavior during the critical risk period for SIDS.

Once the quantification of interaction is established, an investigation on early and late preterm could help discovery the difference in term of ANS development on subjects born preterm.

The analysis on SIDS patients could highlight differences in coupling and synchronization and its quantification could open novel view about newborn state monitoring and care path by means of noninvasive and reliable investigations of ANS.

Chapter 1

In this chapter, Sudden Infant Death Syndrome (SIDS) will be defined and its epidemiology will be presented.

SIDS is characterized by the sudden death of a healthy infant during a sleep period. It is considered a multifactorial condition that associates inadequate cardiac, breathing, autonomic and/or arousal controls. The already immature control mechanisms can be aggravated by infections as well as by prenatal and postnatal life environmental factors.

These risk factors for SIDS were identified by epidemiological studies.

Afterwards, the fetal and newborn cardiovascular system evolution will be described, focusing on the Autonomic Nervous System (ANS) control.

Lastly, an overview of Cardiorespiratory Coupling (CRC) and sleep in infants is offered. Some of the most recent hypothesis about causes leading to SIDS are explained in term of lack of cardiorespiratory synchronization.

This work focuses on noninvasive signal processing techniques capable of assessing the physiological ANS coordination in a population of healthy newborns and one month infants.

Introduction

1.1 Sudden Infant Death Syndrome

Sudden Infant Death Syndrome (SIDS) is one of the leading causes of infant mortality in the developed countries and accounts for nearly 30% of deaths during the post neonatal period. Nonetheless, the physiologic mechanisms that underlie this syndrome are still unclear [1].

The first definition of SIDS was given by Bergman in 1970, who argued that SIDS did not depend on a “single characteristic that ordains an infant for death”, but on an interaction of risk factors with variable probabilities [2].

Later, Wedgwoog, Raring, Rognum and Saugstad developed the first “triple risk hypothesis” [2] which was succeeded by the most famous Triple Risk model by Filiano and Kinney. This model is based on invasive pathological studies of brainstem from SIDS victims.

Kinney et al. state that “many cases result from defects in brainstem-mediated protective responses to homeostatic stressors occurring during sleep in a critical developmental period” [2], [3], [4].

Given these hypothesis Kinney and Thach emphasize that SIDS occurs “only in infants with underlying abnormality”. The National Institute of Child Health and Development SIDS strategic plan 2000 quoting Kinney’s work, stated unequivocally that “SIDS is a developmental disorder. Its origins are during fetal development.” and later in 2001 “Knowledge acquired during the past decade supports the general hypothesis that infants who die from SIDS have abnormalities at birth that render them vulnerable to potentially life-threatening challenges during infancy” [4].

Filiano and Kinney’s SIDS hypothesis was based on the concurrence of three factors:

- 1) a vulnerable infant,
- 2) a critical developmental period for the homeostatic control with a peak at 2 - 4 postnatal months
- 3) an exogenous stressor,

as summarized in Figure 1.1.1 [5].

Infants are likely to die of SIDS if they possess all three factors: the infants’ vulnerability lies latent until they enter the crucial period and the infants are subject to an exogenous stressor [2].

During the first year of life, rapid changes in the maturation of cardiorespiratory control and in cycling between sleeping and waking occur, first as the fetus transitions to extrauterine life and subsequently as the infants adjust to postnatal life.

Regarding the investigation of SIDS risk evolution with age, it appears crucial to investigate changes from birth to one year of age [6].

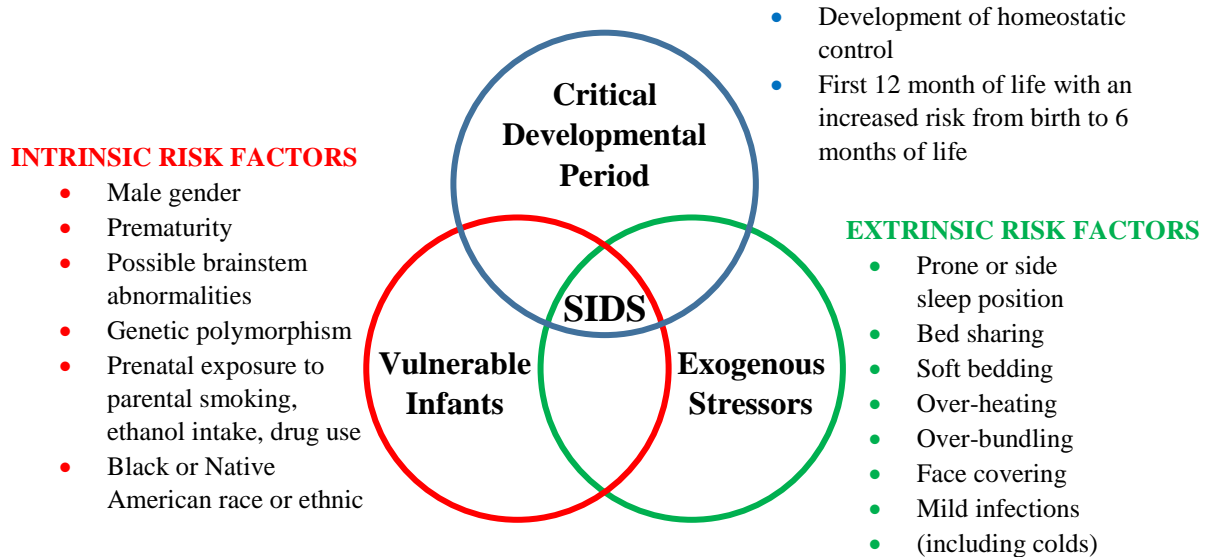


Figure 1.1.1 Triple-risk model for SIDS by Filiano et al.

In the following sections two main intrinsic risk stressors will be investigated: Prematurity and Sleep Position.

1.2 Intrinsic risk: Prematurity

Any infant born before the 37th weeks of Gestational Age (GA) is defined as premature. Premature infant can be further divided into extremely ($GA \leq 26$), early ($26 < GA \leq 34$) and late preterm ($34 < GA \leq 36$).

Reducing preterm birth is a national public health priority. Preterm birth rates decreased from 2007 to 2014 after about three decades of continuous increasing, from early 1980s through 2006. Despite this success, the preterm birth rate rose slightly in 2015 (Figure 1.2.1) and about 1 out of 10 babies (10%) was born premature in the United States. Additionally, racial and ethnic differences in preterm birth rates remain [6], [7], [8].

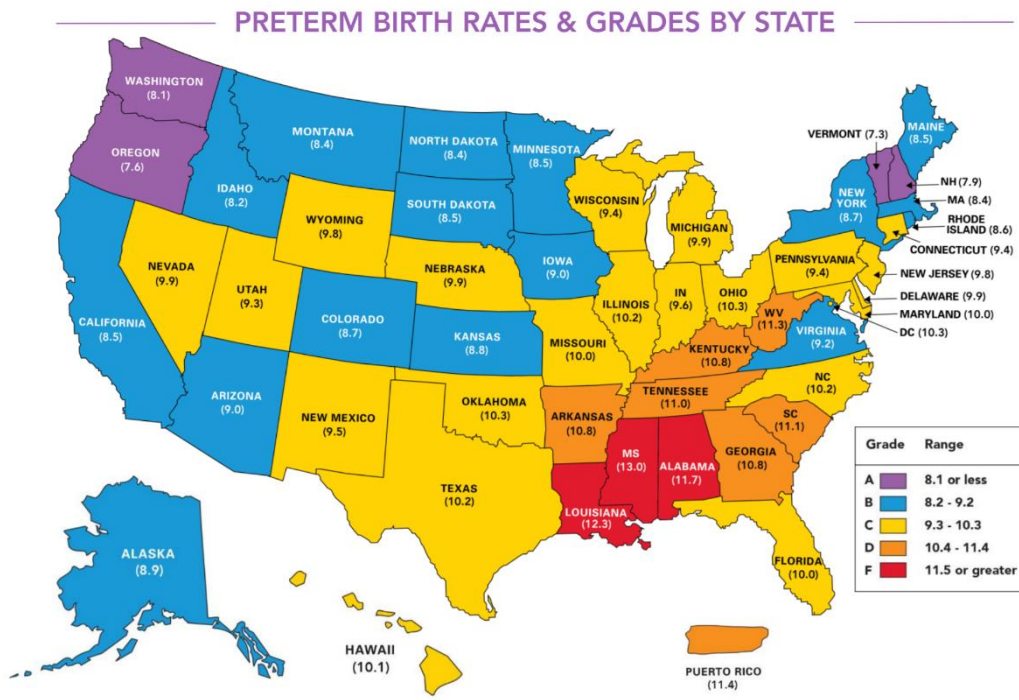


Figure 1.2.1 Preterm birth rates with respect to the total live birth in each state in 2015.

The USA score (considering the whole country) is C, with a 9.6 rate

Source: Grades determined by March of Dimes based on preterm birth rates from National Center for Health Statistics, 2015 final natality data

Prematurity is reported as intrinsic risk factor for SIDS in the Triple-risk model [9]. It should be reminded that preterm delivery is not a disease per se. Rather, preterm delivery raises the risk of adverse outcomes that would be present in normal delivery as well.

Prematurity sets the newborn to be exposed to the outer environment before his autonomic nervous system is fully developed and able to effectively face life challenging

situations like breathing and thermoregulation. A preterm baby is understandably more vulnerable than a full-term baby.

The immaturity of ANS has been hypothesized to be mainly reflected in cardiorespiratory coordination and consequently be responsible for SIDS episodes [10].

The lack of cardiorespiratory synchronization that represents per se a risk factor for SIDS, is mainly reflected in the frequent occurrence of apneic events. Apnea of prematurity is the most common disorder affecting infants born prematurely and the incidence and severity of apnea are also inversely related to GA.

Prolonged apneas in adults are generally resolved by arousal; however, in preterm infants this is not commonly found. Apnea of prematurity may not be inherently life threatening, but a deficient arousal response to the consequent asphyxia or hypoxia, could have fatal consequences. Abnormal arousal responsiveness to hypoxia and hypercarbia has been observed in infants with apnea of infancy, along with diminished ventilatory responsiveness [11], [12].

Preterm infants can experience a variety of cardiovascular disorders, ranging from major morphological defects to dysfunctional auto-regulation of blood vessels. Hypotension is a frequent concern in preterm infants, but there is no consensus as to what the blood pressure readings should be in preterm infants with gestational ages of less than 26 or 27 weeks.

Apnea and bradycardia are common in premature infants and are manifestations of immature cardiorespiratory control.

The non-physiological operation of these mechanisms exposes preterm infants to an increased risk of life-threatening events, which cannot be successfully resolved because the absence of mature cardiorespiratory coordination. The lack of responsiveness between cardiac and respiratory systems is at base of many models trying to depict the SIDS manifestation.

1.3 Extrinsic risk: Sleep Position

Prone position is thought to be one of the major risks for developing SIDS for a newborn. An association between prone sleep and an increased risk of SIDS was reported since the 1950s [1], [5].

The incidence of SIDS is highly reduced since the “Back to Sleep” campaign in 1994, initiated by the National Institute of Child Health and Development in the United States. In June 1992, the American Academy of Pediatrics (AAP) Task Force on Infant Positioning and SIDS published a recommendation that healthy full-term infants be placed laterally or supine to sleep. The SIDS rate in the United states declined by > 50 % in the 10 years after the initiation of the campaign (Figure 1.3.1) [13].

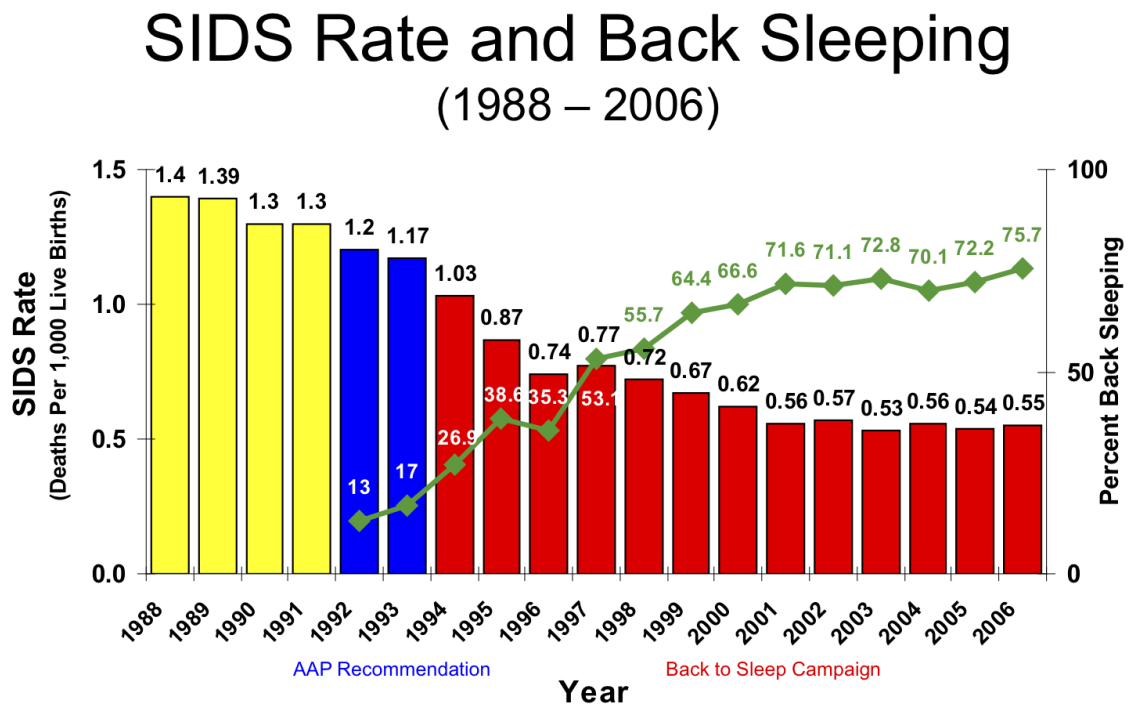


Figure 1.3.1 Trend of SIDS rate, the diminishing trend can be observed as a consequence of the Back to Sleep Campaign. The green line indicates the percentage of babies sleeping supine with respect to the total percentage of premature infants in the USA

SIDS Rate Source: CDC, National Center for Health Statistics
 Sleep Position Data: NICHD, National Infant Sleep Position Study

Several hypotheses relating prone sleep posture to SIDS were proposed. These include the consequence of the face-down position, such as nasal obstruction, posterior displacement of the mandible, increased upper airway resistance, rebreathing of carbon dioxide, the compromise of cerebral blood flow during cervical hyperextension, interactions between prone sleep and thermal balance, as well as depressed arousal responses.

When lying prone both premature infants and newborns were shown to have longer total sleep time, fewer arousals, less time spent in Active Sleep with respect to Quiet Sleep and less body movements. In supine position infants had more awakenings and arousals but more obstructive apneas [14].

A possible explanation for the increased risk of SIDS in the prone position is that infants sleep more deeply in that position and arouse less easily. It has been hypothesized that the ability to arouse from sleep is an important survival mechanism, which may be impaired in SIDS [15].

1.4 Fetal and newborn cardiovascular systems

1.4.1 Cardiovascular system generation

The cardiovascular system is one of the apparatus that develops firstly in the growing fetus. As the embryo becomes larger, the diffusion mechanism comes to be inadequate for the intake and outtake of oxygen, carbon dioxide and nutrients, triggering the development of a more complicate system for the growing organism.

The system is generated through a cascade of processes; first there is the vasculogenesis, which is the creation of the main vessels, followed by the angiogenesis, which is the generation of minor branches from the main vessels. Due to the expansion and elastic resistance of the walls of these vessels, the blood flow starts to be rhythmic and peristaltic patterns are originated.

The primitive heart is generated from an area of embryonic mesoderm as two tubes are fused together to form a single heart tube. The generation of the four chambers is mainly due to the vortexes, created by the blood flow in the heart.

By the 21st day after the conception, the cells around the heart begin to differentiate in myocardial cells, capable of stimulating a controlled response and at this point the heart begins to beat.

1.4.2 Circulation before birth

In fetus, the oxygen source role is played by the placenta instead of the lungs. To perform this task, the fetal circulation is provided with supplementary structures with respect to the adults, shown in Figure 1.4.1: the umbilical vein, which conveys the blood enriched with oxygen and nutrients to the underside of the liver, the ductus venosus, which connects the umbilical vein with the inferior umbilical vein and allows part of the blood to bypass the liver. Additionally, lungs are bypassed thanks to two structures, the foramen ovale that allows the blood to move directly from the right atrium to the left atrium, and the ductus arteriosus, which connects the pulmonary arterial trunk to the descending aorta.

The blood that is oxygenated and rich with nutrients is taken from the placenta in the umbilical vein that goes through the abdominal wall to the underside of the liver. Approximately half of the blood passes through the liver, the rest goes through the ductus venosus to the inferior vena cava where it mixes with blood low in oxygen content that comes from the lower trunk and extremities.

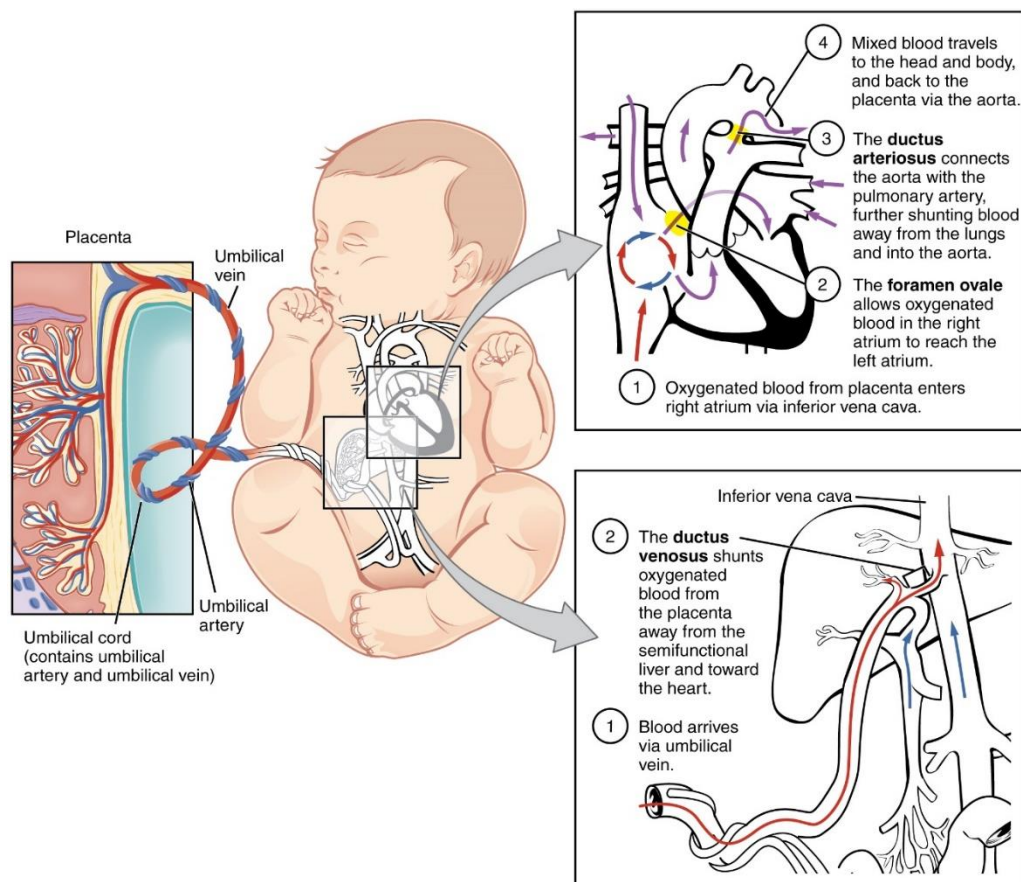


Figure 1.4.1 The heart and peripheral circulations in fetus

These two streams approximately maintain their separate identities inside the inferior vena cava: since the entry of the inferior vena cava is aligned with the foramen ovale, the blood stream coming from the umbilical vein manages to pass from the right atrium through the foramen ovale into the left atrium. The other stream goes into the right atrium, where it mixes with the blood coming from the upper parts of the body.

The reason why the foramen ovale remains open is that the high pulmonary vascular resistance (PVR) induces high pressure in the right atrium as well.

Figure 1.4.3 shows that the fetal circulation, differently from the adult one, operates in parallel; this is precisely because the pulmonary vascular resistance is very high, so only

about 10% of the right ventricle output contributes to the pulmonary circulation for the growth and metabolic needs of the lungs. The rest is diverted from the pulmonary artery to the aorta through the ductus arteriosus, which has a lower resistance. The ratio of the volume which goes to the lungs grows with the progression of the pregnancy.

The large volume of blood that passes through the foramen ovale into the left ventricle is joined by the blood coming from the pulmonary circulation and is pumped into the aorta.

1.4.3 Circulation after birth

An important step for a newborn is the transition from fetal circulation to neonatal circulation.

At the moment of birth, the blood flow starts to invade the pulmonary circulation and ceases to pass through the fetal structures. This process normally takes place within a minute from the birth, but it could take few weeks to stabilize.

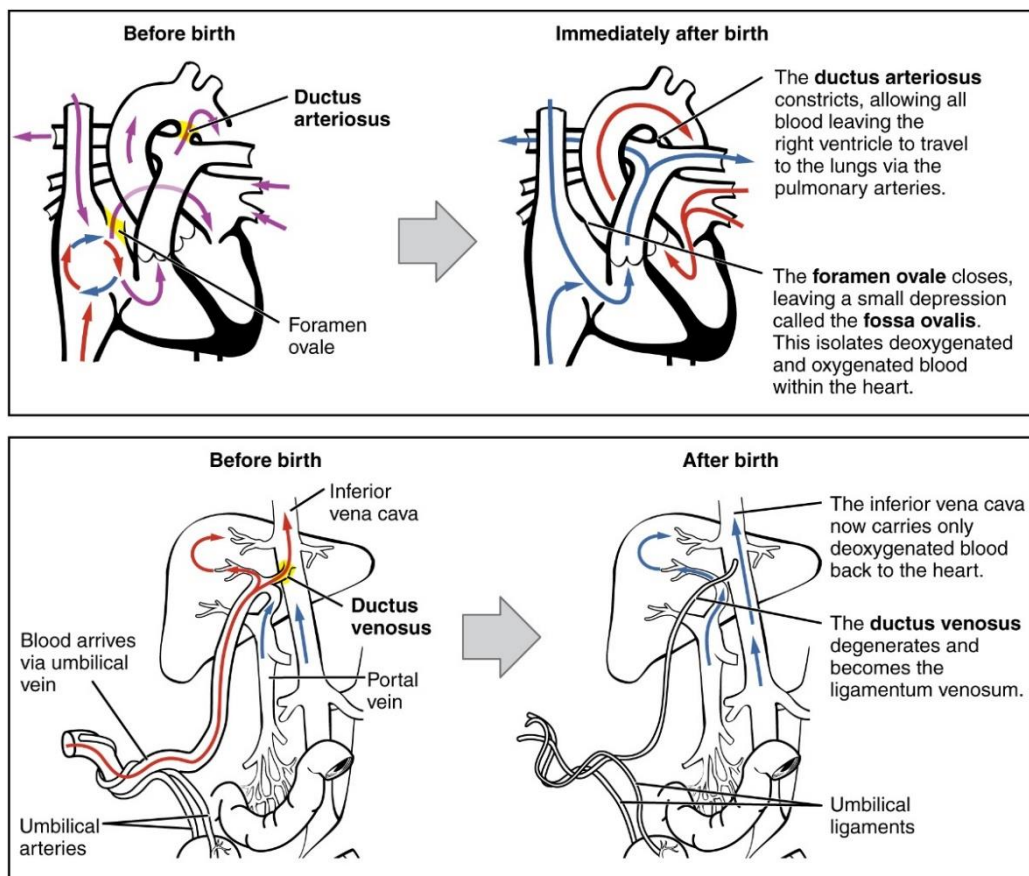


Figure 1.4.2 Heart and peripheral circulation before and after birth

The fetal shunt closes because umbilical circulation and consequently placental perfusion have ceased and because of lungs inflation, which generates an increase in pulmonary flow. This change is induced due to the fact that the lung circulation passes from high to low resistance. Another consequence of the ceased umbilical flow is the closure of the foramen ovale: decreased umbilical flow leads to a decreased venous return from the inferior vena cava so the pressure in the right atrium and the PVR fall. The increased pulmonary blood flow results in an increased return to the left atrium and consequent increase in pressure. Thus, the pressure gradient across the foramen ovale is reversed. The closure of the foramen is at first temporary then after few days should fuse and become permanent (Figure 1.4.2).

Figure 1.4.3 depicts by means of schematic approach the change in cardiorespiratory system comparing fetal and newborn circulation.

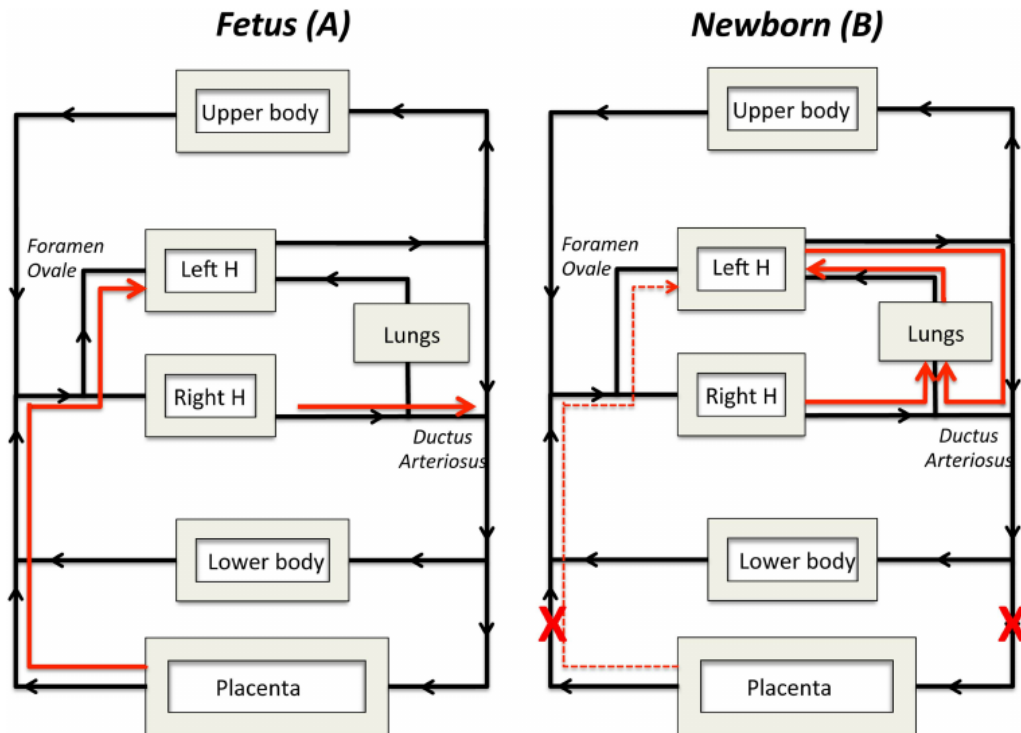


Figure 1.4.3 A schematic of the fetal circulation before birth and the changes in flow in a newborn subject. Before birth the major supply of preload for the left ventricle is derived from the placental circulation, which passes from several structures and enters the left side of the heart; thereby bypassing the right side of the heart and the lungs (panel A, pathway is shown by red arrow). As most blood exiting the right ventricle passes through the ductus arteriosus (A, red arrow) and enters the descending aorta, very little blood flows into the fetal lungs before birth.

After birth, the supply of blood for the left ventricle derived from the placental circulation is lost (B, broken red arrow) and so preload for the left ventricle becomes dependent on pulmonary venous return (B, red arrow). For this to occur, the lung must first aerate, which triggers a decrease in pulmonary vascular resistance, allowing all of right ventricular output to pass through the lungs (B, red arrow). In addition, flow through the ductus arteriosus reverses so that left ventricular output becomes a major contributor to pulmonary blood flow and, therefore to pulmonary venous return as well

1.5 Autonomic Nervous System

The Autonomic Nervous System (ANS) is an essential regulator of the homeostasis and a main actor in the control of circulatory and respiratory systems. The ANS, also known as visceral nervous system or vegetative nervous system, controls several body functions such as blood circulation, body temperature, respiration and digestion, maintaining the cardiovascular, thermal and gastrointestinal homeostasis.

These regulatory processes do not require a conscious intervention of higher brain centers, for this reason the ANS is also called involuntary nervous system. Anatomically and functionally the ANS consists of two complementary branches or subsystems, the Sympathetic Nervous System and the Parasympathetic Nervous System:

- **Sympathetic innervation:** this innervation is controlled by a complex neural network within the medulla and sympathetic nerves. Stimulation of the sympathetic nerves is usually driven by norepinephrine; the effect is a constriction of resistance and capacitance vessels, leading to increased systemic vascular resistance and decreasing venous capacitance, producing tachycardia and also an increase in the vigor of cardiac contractions.

In resting condition, the effect of sympathetic innervation on the HR is very low, because there is a predominance of vagal tone, thus the sympathetic nerves are a reserve mechanism to improve the pumping activity of the heart during intermittent stressful situations.

In contrast with the effect of the vagal stimulation, the sympathetic one decays very slowly when the stimulus is interrupted. Furthermore, the norepinephrine released even during intense stimulation, is enough to change the HR only by a small increment.

This is due to the fact that the neurotransmitters of the two branches of autonomic innervations, acetylcholine and norepinephrine, are released at different rates during stimulation and also sympathetic activity depends on the intracellular accumulation of second messengers.

- **Parasympathetic innervation:** the fibers of this innervation originate from the medulla of the brainstem, particularly from neurons called dorsal vagal nucleus. Efferent vagal fibers travel to the heart with two pathways, the left and right vagus nerves. The first one innervates the atrioventricular (AV) node, the second the sinoatrial (SA) node. Stimulation of the vagus nerve or injection of its mediator, acetylcholine, results in a reduction of HR and under resting conditions are tonically active, producing the so called ‘vagal tone’, which results in a HR much lower than the intrinsic firing rate of the SA pacemaker.

Moreover, some efferent parasympathetic fibers connect directly with blood vessels within specific organs and can cause vasodilatation.

The effect of this system is ephemeral because the acetylcholine released is hydrolyzed right away; moreover, the latency is very short since the acetylcholine can activate the specific K⁺ channels without the help of any secondary messenger.

When vagus nerve is stimulated, the HR reaches a steady state value within 1 or 2 cardiac cycles and, when stimulation is interrupted HR goes quickly back to its basal level.

These two aspects are very important because they allow the parasympathetic system to have a beat to beat control. The vagal tone is not necessarily constant, its influence increases progressively with GA.

1.6 Cardiorespiratory coupling

The analysis of causal and non-causal relationships within and between dynamic systems has become more and more a topic of great interest in the medical field. The understanding of driver–response relationships between regulatory systems and within subsystems is of growing interest. In particular, the detection and quantification of the strength and direction of couplings are two major aspects of investigations for a more detailed understanding of physiological regulatory mechanisms. The cardiovascular and cardiorespiratory systems are characterized by a complex interplay of several linear and nonlinear subsystems. Interactions of these physiological subsystems within the cardiovascular system can be described as closed loops with feed-forward (FF) and feed-back (FB) mechanisms [16].

Cardiorespiratory coupling (CRC) is an encompassing definition of various phenomena which result from shared inputs, common rhythms, and complementary functions related to the cardiovascular and respiratory systems. In addition to the well-recognized respiratory influence on autonomic activity, the autonomic system has an influence on respiratory pattern formation. The respiratory influence on autonomic activity is breath to breath, whereas the autonomic influence on respiration can be considered beat to beat [17].

Heartbeat, blood pressure, and ventilation share common frequencies. Many authors studied the quantification of HR and BP and the influence of respiration on these two variables.

In 1733 Rev. Stephen Hales reported that respiration modulates HR and BP. This observation was confirmed by Carl Ludwig (1847) who measured the increases in HR and BP during inspiration. The increase in HR during inspiration is referred as Respiratory Sinus Arrhythmia (RSA) and the increase in BP as Traube–Hering waves.

Heart rate (HR) and BP are modulated neurally, and both parasympathetic and sympathetic nerves have respiratory-modulated activity patterns. Multiple factors, including mechanical and neural coupling, underlie the increases in HR and BP [18].

1.7 Sleep states

Sleep plays a fundamental role in neurodevelopment mainly for the primary purpose of memory consolidation. The gold standards for scoring sleep stages in the newborn includes sleep behaviors, respiratory rates, eye movements, EEG and muscle tone. At birth, the circadian rhythm is not fully established; therefore, sleep can occur as easily during the daytime hours as during the night. The normal, full-term newborn sleeps approximately 16 to 18 hours per day. The longest continuous sleep period is 2.5 to 4 hours and the pattern of sleep and wakefulness is irregular.

Newborn sleep can be classified in three types: Quiet Sleep (QS) (analogous to NREM sleep), Active Sleep (AS) (REM equivalent) and Indeterminate Sleep (IS) [19], [20].

QS is characterized by minimal large or small muscle movements and rhythmic breathing cycles.

During AS instead, sucking motions, twitches, smiles, frowns, irregular breathing, and gross limb movements are seen.

IS is a period of sleep that cannot be defined as either Active or Quiet Sleep by predetermined criteria.

Sleep cycling is essential for brain wiring including receptors system, pathway processing, cortical processing, learning, cognition and memory. AS is predominant in the fetus and produces spontaneous synchronous firing of fetal sensory receptors for brain wiring. By term age, QS starts to be part of newborn sleep cycle and 1 hour sleep cycling between AS and QS is evident, with a mature cycling showing the predominance of QS at 3 months of age. During infancy, sleep cycles begin to block together and resemble adult sleep at 6 months. This maturation period coincides with the critical period for SIDS [21].

Infants at increased risk of SIDS show abnormal patterning of sleep-waking states. It was hypothesized that infants who were to die of SIDS would show abnormalities of sleep state distribution prior to their deaths. Victims of SIDS showed less arousals and more sleep than control infants during the early-morning hours. The finding of decreased waking time during the early morning is of particular importance since most SIDS deaths occur during this portion of the day. The findings of altered sleep patterns in SIDS victims suggest that central neural modulation is associated with SIDS risk. The mechanism underlying SIDS

appear to have origins in the fetal environment resulting in neural damage which later compromises responses to breathing or blood pressure challenges during sleep. The deficits appear to involve alterations in neurotransmitter receptors within regions involved in chemoreception and cardiovascular control.

It is crucial to stress the fact that cardiorespiratory coupling can provide an insight of the mechanism underlying the interaction between the cardiac and respiratory system. It has been reported by many authors [22], [23] that the interaction between these subsystems does deeply change depending on sleep state and the lack of this coupling may be address as one of the leading cause for SIDS.

The aim of this thesis is to investigate this interaction in a full-term cohort of newborns and one month infants in order to characterize the physiological interrelationship between the cardiac and respiratory system.

1.8 SIDS and cardiorespiratory control

Sighs, gasps, and the arousal response

Sleep has a marked influence on cardiorespiratory function. The mechanisms leading to SIDS may include a failure in the neural integration of the cardiovascular and respiratory systems, with a concomitant failure to arouse from sleep. Shannon and Kelly stated that “sudden death without an obvious cause implies the cessation of autonomic regulation of cardiovascular or respiratory activity or both”. In the following years, all SIDS hypotheses essentially invoked defective respiratory or autonomic mechanisms. The roles of respiratory and autonomic pathways in SIDS are not mutually exclusive, given that infants who subsequently died of SIDS have frequently been found to have subclinical deficits in both respiratory and autonomic function [10], [24], [25], [26].

Studies have shown that sleep states exert a marked influence on respiratory control and arousability. Infants are more likely to show arousals in AS compared with QS from both somatosensory and respiratory stimuli. Post-natal and gestational age at birth also have a marked influence on waking. Arousability is depressed by the major risk factors for SIDS

(prone sleeping, maternal smoking, prematurity and recent infection) and is increased by factors that decrease the risk for SIDS [27], [28], [29].

Sighs, gasps and arousals from sleep are important survival response to a life-threatening event such as hypotension or prolonged apnea. Arousal from sleep can occur spontaneously in response to internal physiological changes but can also be induced by external environmental factors. Arousal involves both autonomic and behavioral components. By arousing from sleep, heart rate, arterial pressure and ventilation are increased [30].

The cardiorespiratory responses at arousal are similar to ‘fight or flight’ reactions that also increase arterial pressure, heart rate and ventilation. These responses are relayed and integrated in specific regions of the hypothalamus and the brainstem. The underlying neuronal activity that elicits cortical activation also involves specific neurotransmitter-modulated discharge patterns of thalamocortical neurons. The insights gained are consistent with a final common pathway of cardio-respiratory distress that SIDS victims experience involving arousal and/or auto-resuscitation deficiencies [31].

One of the hypothesis capable of explaining the respiratory pathway to SIDS is shown in Figure 1.8.1 and it can be summarized in 5 steps [31]:

1. A life-threatening event which is more likely to occur in any infant during sleep, causes severe asphyxia, brain hypoperfusion. Such life-threatening events include rebreathing of exhaled or in the face-covered (supine) position, reflex apnea originating from the laryngeal chemoreflex. The vulnerable infant does not wake up and turn his/her head in response to asphyxia resulting in rebreathing or an inability to recover from apnea.
2. Progressive asphyxia leads to a loss of consciousness and areflexia, a so-called hypoxic coma.
3. Extreme bradycardia and hypoxic gasping ensue are seen. These phenomena that are evident in the terminal-event recordings in infants who were being monitored at home at the time of death from SIDS.

4. In the vulnerable infant, autoresuscitation is impaired because of ineffectual gasping, which results in uninterrupted apnea and death.

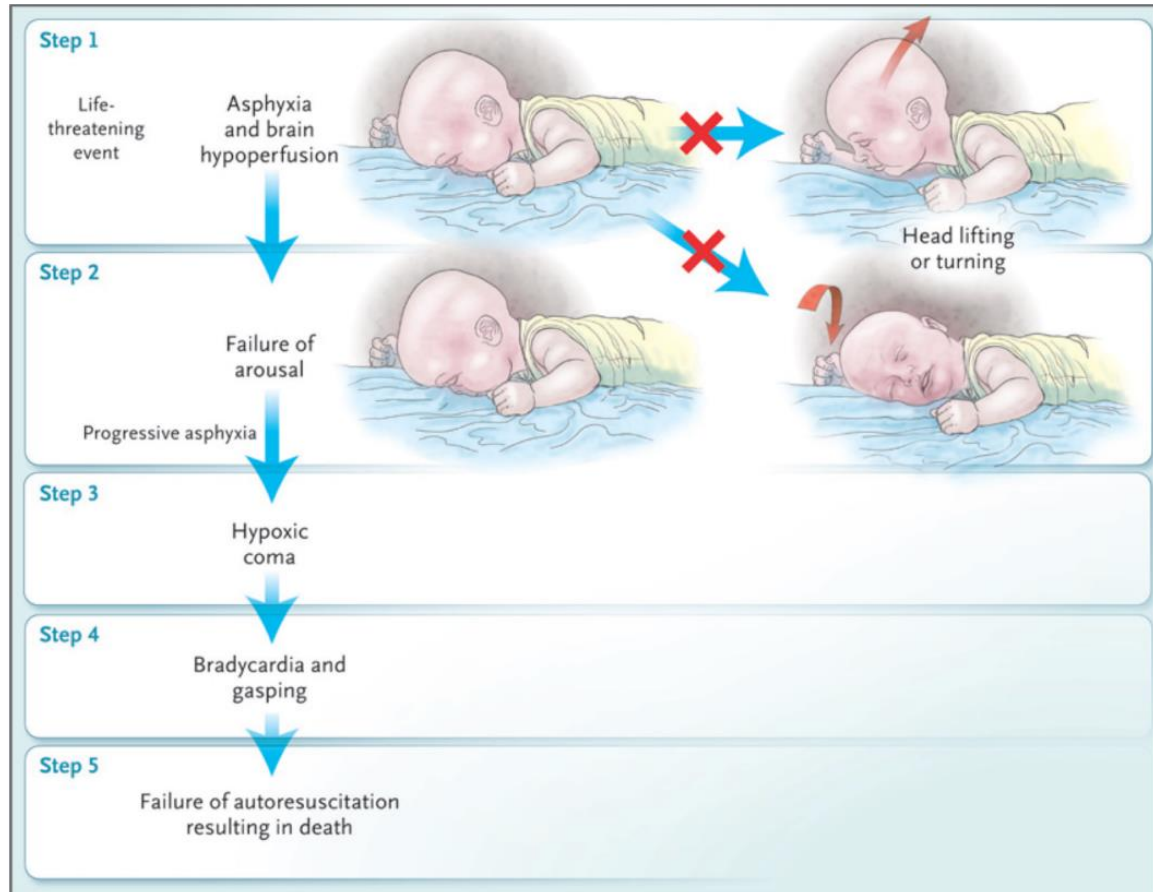


Figure 1.8.1 Five Steps in the terminal respiratory pathway associated with the SIDS results from one or more failures in protective mechanisms against a life-threatening event during sleep in the vulnerable infant during a critical period.

Arousal from sleep that is triggered by abnormal levels of carbon dioxide and oxygen is essential for the initiation of protective airway responses. Arousal involves a progressive activation of specific subcortical-to-cortical brain structures and consists of ascending and descending components that mediate cortical and subcortical arousal, respectively, with feedback loops between them. Cortical arousal involves noradrenergic, serotonergic (5-hydroxytryptamine), dopaminergic, cholinergic, and histaminergic neurons in the brain stem, basal forebrain, and hypothalamus, which excite the cerebral cortex and cause cortical activation. In severe hypoxia or ischemia, normal breathing fails and is replaced by gasping. Gasping increases the volume of air in the lungs, followed by oxygen transport to the heart, increased cardiac output, and finally brain perfusion and reoxygenation. Tracings from

infants who subsequently died of SIDS have indicated that their gasping was ineffectual, with large-amplitude breaths, abnormally complex gasps, and an inability to increase the heart rate. Some infants with acute life-threatening events may represent potential SIDS cases in which the failure in gasping is averted by successful intervention [31].

Cardiorespiratory recordings from infants who subsequently died of SIDS have shown episodes of tachycardia and bradycardia hours or days before death, suggesting a primary failure of autonomic mechanisms involving a lack of cardiorespiratory synchronization. In this context, it is important to monitor the cardiorespiratory interaction in order to identify a lack in coupling hours or even days before the critical event.

The biologic role of SIDS risk factors becomes comprehensible in light of the abovementioned pathways, since many risk factors can trigger asphyxia or other homeostatic stressors and exacerbate the underlying vulnerability in term of cardiorespiratory interaction. An increased risk of SIDS in the first 6 months of life probably reflects a convergence of immature homeostatic systems.

The search for the underlying vulnerability in SIDS infants has led to intense analysis of peripheral and central sites critical to protective responses to asphyxia and hypoxia.

The major focus of SIDS research has been on the brain stem because it contains critical neural networks that mediate respiration, chemosensitivity, autonomic function, sleep, and arousal as depicted in Figure 1.8.2. Abnormalities in various neurotransmitters or their receptors have now been reported in relevant brainstem regions in infants with SIDS. To date, the most robust evidence for a neurochemical abnormality comes from research on the medullary 5-hydroxytryptamine system, in that approximately 50 to 75% of infants with SIDS appear to have abnormalities in this system confirming brainstem abnormalities as an intrinsic risk factor. The medullary 5-hydroxytryptamine system, which is considered critical for the modulation and integration of diverse homeostatic functions, according to the level of arousal, is involved in ventilation and gasping, thermoregulation, autonomic control, responses to carbon dioxide and oxygen, arousal from sleep, and hypoxia-induced plasticity [25]. Abnormalities in 5-hydroxytryptamine neuronal number and differentiation, receptors, or transporter have been reported in the medulla of infants.

The investigation of these abnormalities can only be assessed by means of invasive procedures, not suitable to be performed on newborns or infants. Due to these reasons, the quantification of cardiorespiratory interaction in a noninvasive way, as proposed in this work, can provide an insight to the underlying interaction between cardiac and respiratory systems [31].

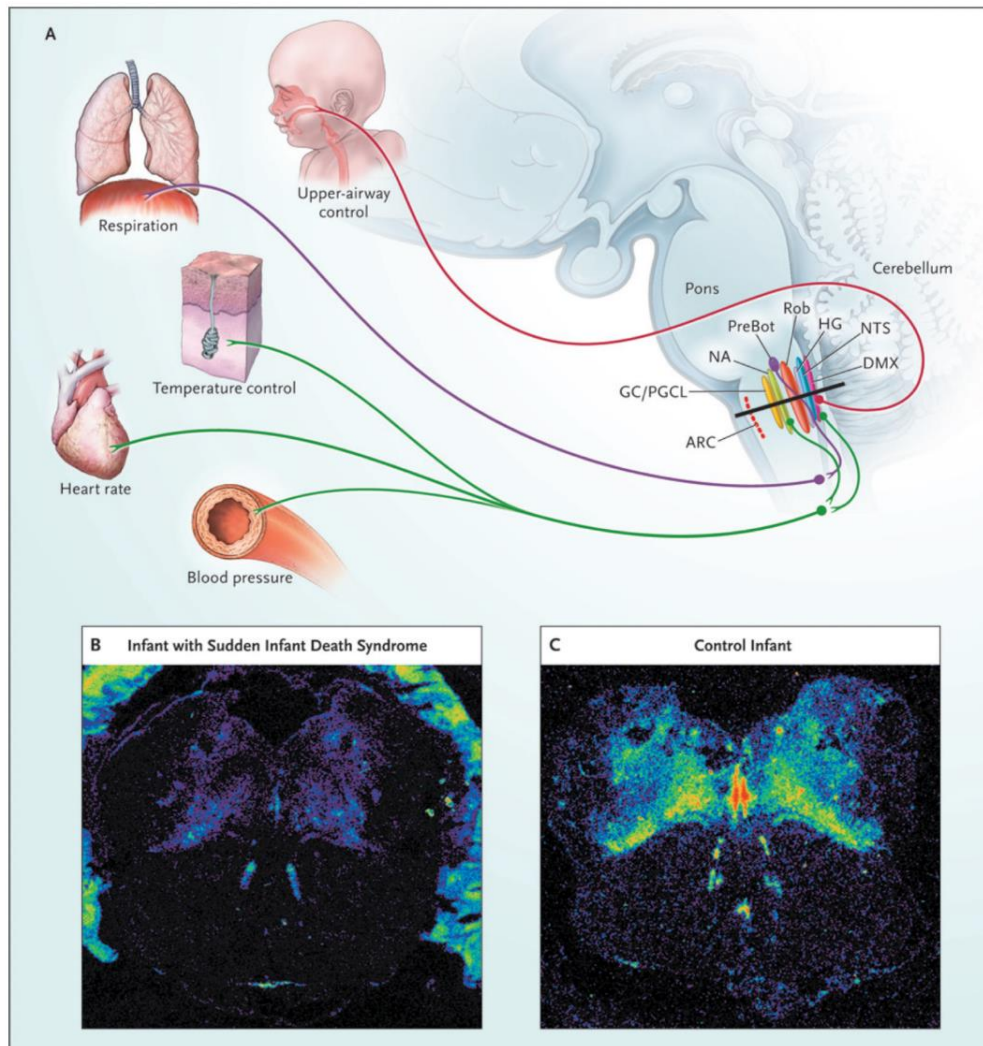


Figure 1.8.2 The serotonergic system is considered to be critical for the modulation and integration of diverse homeostatic functions. The medullary level of the brain stem (black line in Panel A) includes regions involved in the regulation of upper-airway control, respiration, temperature, autonomic function, and the sympathetic nervous system. In the medulla of an infant with the sudden infant death syndrome (SIDS), tissue autoradiography shows a generalized reduction in binding to the 5- hydroxytryptamine type 1A receptor (Panel B), as compared with that in a control infant at the same postconceptional age (Panel C). ARC denotes arcuate nucleus, DMX dorsal motor nucleus of the vagus nerve, GC ganglion cells, HG hypoglossal nucleus, NA noradrenaline, NTS nucleus tractus solitarius, PGCL paragigantocellularis lateralis, PreBot pre-Bötzinger complexes, and Rob raphe obscurus

Chapter 2

In this chapter, the populations employed for the analysis will be described. Information will be given about the infants involved in the first study and in the one month follow up, about the ECG and respiratory signal acquisition.

Afterwards, all the methods used in this work will be presented. Classical parameters such as time domain, univariate entropy estimators are computed analyzing the RR series, on the other hand bivariate entropy estimator, phase locking and directionality index are computed analyzing both RR series and respiratory signal.

Materials and Methods

2.1 Study population and acquisition system

The newborn dataset includes 329 infants born at the Morgan Stanley Children’s Hospital of New York at CUMC between 35 and 40 weeks of gestation. The subjects who met inclusion criteria were recruited and tested 12-84 hours after birth.

The newborn population analyzed in this work is subset of the original larger cohort, in this case the considered gestational age (GA) is 38-40 weeks, this interval of GA includes full-term subjects only.

Gestational age was determined by prenatal ultrasound in the first 20 weeks of gestation in combination with postnatal physical examination by the neonatal team as indicated in the newborn’s medical record.

The resulting number of full-term subjects is 206, 55 of the participating infants (26.70%) had poor ECG and/or respiratory recordings and were excluded from the analyses, the total number of newborn subjects after exclusions is 151.

In order to evaluate the subjects’ development, a second population has been considered. The one month infants cohort includes 93 subjects who came back for a one month follow up, 33 of them were selected for this work based on the same criterion about GA without any further exclusion related to the quality of ECG and/or respiratory.

Medical-record information about the two populations is summarized in Table 2.1.1.

None of the infants were admitted to the NICU nor had any major illness or known genetic disorder. All infants had a minimum Apgar score of 8 after 5 minutes of life. Review of the maternal medical chart revealed no evidence of major illness, genetic disorders, or past/present medicated/non-medicated psychiatric complaints.

Newborns			One month infants		
Sex [number of subjects], [%]			Sex [number of subjects], [%]		
Male	74	49.01%	Male	18	54.55%
Female	77	50.99%	Female	15	45.45%
Sex distribution by group (%) male vs female [number of subjects]			Sex distribution by group (%) male vs female [number of subjects]		
38 GA (28.47%)	19	24	38 GA (27.27%)	5	4
39 GA (37.09%)	28	28	39 GA (30.30%)	5	5
40 GA (34.44%)	27	25	40 GA (42.43%)	8	6
Birth weight [g]			Birth weight [g]		
Mean \pm SD	3343.08 \pm 407.22		Mean \pm SD	3388.03 \pm 435.75	
Min	2385		Min	2725	
Max	4525		Max	4525	
Hours of life [hours]			Hours of life [hours]		
Mean \pm SD	37 \pm 15		Mean \pm SD	38 \pm 17	
Min	14		Min	18	
Max	80		Max	80	
Maternal age [years]			Maternal age [years]		
Mean \pm SD	31 \pm 7		Mean \pm SD	31 \pm 6	

Table 2.1.1 Subject information, percentages are computed with respect to the total number of subjects for each cohort; 151 newborns and 33 one month infants

Three ECG leads were placed on the infant's chest (left abdomen, left and right scapula) and the signal was amplified and collected using the DATAQ Instruments ECG system (Medalex, NY, NY).

A respiratory inductance belt (Ambulatory Monitoring Inc., Ardsley, NY) was placed around the infant's abdomen. ECG and respiration signals were acquired at 500 and 200 samples per second, respectively.

During the 10-minutes baseline acquisition, babies were sleeping in supine position within ~ 30 minutes following feeding. Sleep states were classified into Active Sleep (AS), Quiet Sleep (QS), indeterminate (I) and awake (W) by an expert clinician [32].

The minimum length for a segment in order to be classified either as Active or Quiet is 120 seconds, indeterminate and awake segments were discarded from the analysis.

The sleep state coding assessment is performed on the respiratory signal analysis only. Sleep state coding procedure was supplemented by behavioral codes entered throughout the study and by review of videos to determine when infants were awake, crying, or fussy.

In this work for the purpose of signal processing analysis, segments of 3-minute length in a continuous sleep state were analyzed: 514 three-minute epochs were considered for newborns (239 Quiet, 275 Active), while 247 epochs were considered for one month infants (144 Quiet, 103 Active).

The R peaks were detected on the ECG with the Pan-Tompkins algorithm. An adaptive filter was then applied to remove ectopic beats or artifacts.

The respiration signal was filtered with a bandpass filter (0.05 - 3.5 Hz), peaks of inspiration were detected with automated marking software and each record was corrected for incorrect marks manually.

In the following sections, several linear and nonlinear parameters will be presented. In this thesis, the cardiorespiratory investigation starts with traditional methods: time and frequency domain. These tools have proven their capability of discriminating between sleep states and ANS development, within different degree of reliability. The results obtain by means of this analysis confirm previous findings by several authors.

Entropy estimators such as Sample Entropy and Quadratic Sample Entropy computed in this work are in accordance with previous findings, the novel contribution of this investigation is the estimation of information directionality by means of Transfer Entropy.

Regarding nonlinear phase analysis, phase locking and directionality index are powerful tools to be used in combination with traditional parameters. The contribution of these estimators is crucial to achieve a complete characterization of cardiorespiratory interaction. Their application in the neonatal field is the novel contribution presented in this work.

2.2 Time domain analysis

The simplest methods to evaluate the variations of HR and respiratory rate by means of a univariate approach are the time domain measurements. These quantities are computed for each segment, analyzing the distances between the R peaks for the ECG signal and peaks of inspiration for respiratory signal.

In this work some of the HRV Task Force [33] indexes are computed: RR mean, RR Interquartile Range (IQR), SDNN, RMSSD analyzing the RR series signal and Inter Breath Intervals (IBI) mean, IBI IQR analyzing the respiratory signal.

Considering the distribution of the RR distances, it is possible to compute their mean temporal distance and their interquartile range and obtain the above-mentioned RR mean and RR IQR.

SDNN is the standard deviation of the NN intervals, which is the square root of the variance. The variance is mathematically equivalent to total power of spectral analysis, thus SDNN represents all the cyclic components responsible for variability in the period considered. If the period analyzed is diminished, SDNN estimates shorter cycle lengths, thus SDNN depends on the duration of the recording period and for this reason it is inappropriate

to compare measures obtained from recordings of different length. On the other hand, RMSSD is the most frequently used measure derived from interval differences; it estimates short-term variations in HR.

IBI mean and IBI IQR are the corresponding measurements of RR mean and RR IQR when considering the differences between adjacent respiratory onsets.

2.3 Entropy analysis: univariate and bivariate estimators

In this work the entropy analysis is performed with both univariate and bivariate approaches. In the first case, the entropy estimation is based on the analysis of HR only, whereas in the bivariate case both HR and respiratory signal are considered.

Since the birth of this theory, many different entropies estimators have been developed [34]. One of the first methods to estimate univariate entropy is the KS entropy, developed by Kolmogorov and expanded by Sinai [35], which allowed classifying deterministic systems by rates of information generation. The main issues is that KS entropy is not developed for statistical applications, it requires infinite and noiseless signals, a combination of conditions those are impossible to be fulfilled in real applications in particular when dealing with biological signals [35].

Pincus proposed ApEn as solution to these issues and successfully applied it to relatively short and noisy data [36]. ApEn is a nonnegative entropy estimation of a time series, with larger values corresponding to more complexity, according to information entropy.

Richman and Randall [37] developed and characterized SampEn, a new family of statistics measuring complexity and regularity of clinical and experimental time-series data. SampEn statistics provide an improved evaluation of time-series regularity and is a useful tool in studies of the dynamics of human cardiovascular physiology.

2.3.1 Approximate Entropy

To face shortcomings of KS entropy, Approximate Entropy (ApEn) was introduced by Pincus [36] to provide applications on real, noisy and finite signals.

ApEn has four advantages in comparison to KS entropy: 1) the estimation is less affected by noise, 2) it is robust to occasional artifacts, 3) it requires a reasonable number of data points and 4) it is finite for both stochastic and deterministic processes.

In order to calculate ApEn the parameters N , m and r must be fixed for each calculation. N is the length of the time series, m is the length of template to be compared and r is the matches tolerance. It is convenient to set the tolerance as r -times the signal standard deviation, within this assumption it is possible to compare results obtained analyzing signals with different magnitudes.

For a time series of N points, $\{u(j) : 1 \leq j \leq N\}$ it is possible to subdivide the time series in $N - m + 1$ vectors $x_m(i)$ for $\{i : 1 \leq i \leq N - m + 1\}$, where $x_m(i) = \{u(i + k) : 0 \leq k \leq m - 1\}$ is the vector of m data points from $u(i)$ to $u(i + m - 1)$.

The distance between two such vectors is defined as $d[x(i), x(j)] = \max \{|u(i + k) - u(j + k)| : 0 \leq k \leq m - 1\}$, that represents the maximum difference of their corresponding scalar components. Let B_i be the number of vectors $x_m(j)$ within r distance of $x_m(i)$ and let A_i be the number of vectors $x_{m+1}(j)$ within r distance of $x_{m+1}(i)$.

Define the function $C_i^m(r) = B_i / (N - m + 1)$. In calculating $C_i^m(r)$, the vector $x_m(i)$ is called the template and an instance where a vector $x_m(j)$ is within r of it is called a template match. $C_i^m(r)$ is the probability that any vector $x_m(j)$ is within r of $x_m(i)$.

The function $\Phi^m(r) = (N - m + 1)^{-1} \sum_{i=1}^{N-m+1} \log(C_i^m(r))$ is the average of the natural logarithms of the functions $C_i^m(r)$ and the parameter $ApEn(m, r) = \lim_{N \rightarrow \infty} [\Phi^m(r) - \Phi^{m+1}(r)]$.

Given N data points, this parameter is estimated by defining the statistic $ApEn(m, r, N) = \lim_{N \rightarrow +\infty} [\Phi^m(r) - \Phi^{m+1}(r)]$.

ApEn measures the logarithmic likelihood that patterns that are close for m observations remain close on next incremental comparisons. Greater likelihood of regularity, produces smaller ApEn values, and conversely [36].

The main disadvantage of ApEn is the risk to obtain a number of matches equal to zero, thus a logarithm of zero is obtained. This constraint is overcome by allowing each template to match itself (self-matching), within this hypothesis ApEn is defined under all circumstances, because at least a single self matches is always defined. Although ApEn is a great methodological improvement, it is still affected by a bias effect and it depends strongly on the record length. This assumption leads to an entropy overestimation: self-matchings are counted even if they do not generate new information [37].

2.3.2 Sample Entropy

Sample entropy (SampEn) has been introduced by Richman and Moorman in order to overcome the limitations of ApEn [36]. SampEn quantifies the probability that two short templates that match within an arbitrary tolerance will continue to match at the next point. Considering a time series of N points x_1, x_2, \dots, x_n , for a length $m < n$ and starting point i , the template $x_m(i)$ is the vector containing the m consecutive intervals $x_i, x_{i+1}, \dots, x_{i+m-1}$.

For a matching tolerance $r > 0$, an instance where all the components of $x_m(i)$ are within a distance r of any other $x_m(j)$ in the record, is called a match (or template match). Let B_i denote the number of matches of length m with template $x_m(i)$ and A_i denote the number of matches of length $m + 1$ with template $x_{m+1}(i)$.

Let $A = \sum_i A_i$ and $B = \sum_i B_i$ denote the total number of matches of length $m + 1$ and m , respectively. The ratio $p = \frac{A}{B}$ is then the conditional probability (CP) that subsequent points of a set of closely matching m intervals remain close and match.

$SampEn(m, r)$ is the negative natural logarithm of this probability, it can be expressed as in [38] :

$$SampEn(m, r) = -\log(p) = -\log\left(\frac{A}{B}\right) = \log(B) - \log(A) \quad (1)$$

Equation 1 calculates the negative natural logarithm of a probability associated with the time series as a whole, it is always defined unless in the case of $B = 0$, when regularity has not been detected, or in case $A = 0$, which corresponds to a conditional probability of 0 and an infinite value of sample entropy [37].

The advantages of the SampEn are the exclusion of self-matches, the independence of record length and stronger consistency with respect to ApEn.

On the other hand, SampEn is strongly dependent on the choice of the tolerance r . Small values of r lead to higher and less confident entropy estimates because of the falling numbers of matches of length m and $m+1$ whereas larger values of r lead to entropy overestimation because of the high number of matches.

In this work, the newer insight about entropy is provided by Quadratic Sample Entropy (QSE) and Transfer Entropy (TE). The application of these measurements to infants has not been deeply investigated but results from this work suggest their applicability and reliability in the neonatal field.

2.3.3 Quadratic Sample Entropy

The main issue in computing an entropy estimator is the choice of r tolerance value. A new insight that deals with this limitation is presented in [39]. The idea is to convert the measured conditional probability to a density by normalizing it with a factor equal to $2r$, within this hypothesis, entropy estimation computed with different r can be compared directly. This measure is called Quadratic Sample Entropy (QSE) and it is defined as (Equation 2):

$$\begin{aligned} QSE &= -\log\left(\frac{p}{2r}\right) = -\log(p) + \log(2r) \\ &= \text{SampEn}(m, r) + \log(2r) \end{aligned} \quad (2)$$

Furthermore, r can be optimally varied for each data record. Another improvement to increase the statistical significance and the reliability of QSE parameter is to impose a minimum numerator counter. The minimum numerator count aim is to vary r until a pre-specified number of matches A are observed. Other additional restrictions, such as minimum denominator count on B , can be also used to control accuracy.

In this work SampEn and QSE have been computed considering the RR series of the two cohorts of newborns and one month infants. The length of the analyzed records is 300 beats and not 3-minute length as for time domain analysis.

This choice aims to avoid the influence of the length of the record on the entropy estimation. The same analysis has been performed considering 100 and 200 in order to test the reliability of the estimation.

2.3.4 Transfer Entropy

ApEn, SampEn and QSE are univariate entropy estimators based on RR series only. Transfer entropy (TE) is a multivariate method based on both RR series and respiratory signal [40], [41], [42]. It allows computing entropy not only evaluating the information flow from one system to another but also taking into account the directionality of interactions [43], [44].

In this work, TE has been computed within a bivariate framework, the interaction is either from RR series to respiration (RR→RESP) or vice versa (RESP→RR). TE evaluates the information flow from a source system X to a destination system Y, considering X and Y as two interacting dynamical subsystems. X_n, Y_n are the stochastic variables obtained by sampling the stochastic processes describing the state visited by the systems X and Y over time. Furthermore, Y_n^-, X_n^- are the vector variables representing the whole past of the processes.

Within this hypothesis, the transfer entropy from X to Y is defined as:

$$TE_{X \rightarrow Y} = \sum p(Y_n, Y_n^-, X_n^-) \cdot \log \frac{p(Y_n | Y_n^-, X_n^-)}{p(Y_n | Y_n^-)} \quad (3)$$

The conditional probability expressed in Equation 3, can be interpreted as the transition probability quantifying the information provided by the past of the process X about the present of the process Y that is not already provided by the past of Y.

It should be noted that the TE can be also expressed as a difference of two conditional entropies (CE) as in Equation 4:

$$TE_{X \rightarrow Y} = H(Y_n | Y_n^-) - H(Y_n | Y_n^-, X_n^-) \quad (4)$$

TE parameter is really powerful in detecting information transfer given that it does not require any particular assumption about the underlying models or their mutual interactions. It is able to discover purely non-linear interactions and to deal with a range of interaction delays [43].

Reconstruction of system's past states

In order to estimate CE and compute TE it is necessary to approximate the infinite-dimensional variable representing the past of the processes. This issue can be seen in terms of finding the best embedding set for both time series [45].

The idea is to reconstruct the past of the system represented by the processes X and Y, in order to obtain a vector $V = [V_n^Y, V_n^X]$ containing the most significant past variables to explain the present of the destination system.

Two possible approaches can be employed: uniform (UE) and non-uniform (NUE) embedding schemes. In the first case, components to be included in the embedding vectors are selected a priori and separately for each time series. For example, the vector Y_n^- is approximated using the embedding vector $V_n^Y = [Y_{n-m}, Y_{n-2m}, \dots, Y_{n-dm}]$, where d and m are respectively the embedding dimension and embedding delay (same reasoning to compute V_n^X from X_n^-).

Following this approach, TE estimation consists of two steps: collection of past states and estimation of entropy with a chosen estimator.

The main flaw related to estimation by means of UE is the arbitrariness and the redundancy, which may cause problems such as overfitting and detection of false influences.

The alternative strategy is the non-uniform embedding (NUE). This technique consists of a progressive selection among the available variables describing the past of the observed processes X, Y, considered up to a maximum lag, to identify the most informative variable for the destination variable Y_n .

At each step, selection is performed maximizing the amount of information that can be explained about Y by observing the variables with their specific lag up to the current step. Thus, a criterion for maximum relevance and minimum redundancy is applied for candidate

selection, and the resulting embedding vector V includes only the components of X_n^- and Y_n^- , which contribute most to the description of Y_n .

Moreover, the variables included into the embedding vector are by definition associated with a statistically significant contribution to the description of Y . Thus, the statistical significance of TE estimated with this approach results from the selection of at least one past component of the source process. Otherwise, the estimated TE will be zero and nonsignificant [45].

Joint probability distribution estimators

Another crucial aspect is the choice of the appropriate method to estimate the joint probability distribution capable of fully-describe the interrelationship between X and Y [46].

The first approach is the linear estimator (LIN) that assumes data are drawn from a Gaussian distribution. Under this assumption, the two CE terms defining the TE can be quantified by means of linear regressions involving the relevant variables taken from the embedding vector.

The second estimator is the classical binning estimator (BIN), which consists of coarse-graining the observed dynamics using Q quantization levels, and then computing entropies by approximating probability distributions with the frequencies of occurrence of the quantized values [47].

The third estimator is based on k -nearest neighbor techniques (NN) which exploit the statistics of distances between neighboring data points in the embedding space to estimate entropy terms. Regarding the method adopted in this work, a problem that could emerge dealing with uniform and non-uniform embedding procedures concerns the issue of dimensionality [48]. Indeed, increasing the candidates, the more the data points will be spread in the phase space, the more the probability density function will assume a constant value. Adopting the non-uniform embedding could overcome this potential. As a matter of fact, this method reduces the candidates of significant past states, preventing the risk of probability density function to assume a constant value.

This non-uniform embedding method was chosen in combination with nearest neighbor entropy estimator, since this arrangement was suggested to have high sensitivity and specificity both for linear and non-linear systems [49].

Nearest neighbor estimator

The nearest neighbor estimator method has been shown to be a powerful non-parametric method for classification, density and regression estimation [50]. It can be employed to estimate the entropy of a d -dimensional random variable X , $H(X)$, starting from its N realizations. Considering the probability distribution $P_k(\varepsilon)$ for the distance between x_i and its k -th nearest neighbor, the probability $P_k(\varepsilon)d\varepsilon$ is equal to the chance that there is one point lying within a distance $r \in [\frac{\varepsilon}{2}, \frac{\varepsilon}{2} + d\varepsilon]$ from x_i , that there are $k - 1$ other points at smaller distances from it and that $N - k - 1$ points have larger distance from x_k .

Within these assumptions, the expectation value of the mass p_i of ε -sphere centered at x_i can be expressed as:

$$E(\log(p_i)) = \int_0^{\infty} P_k(\varepsilon) \log(p_i(\varepsilon)) d\varepsilon \quad (5)$$

The expectation is evaluated over the position of all other $N - 1$ points, with x_i kept fixed. By means of further manipulations of this probability it is possible to compute $H(X)$, $H(Y)$, $H(X, Y)$, in the latter case the mass function is two-dimensional.

In this work the MuTE toolbox was employed to estimate Transfer Entropy values [49]. TE has been computed considering RR series and respiratory signal that was resampled at the R peak instants in order to defined two synchronous series. The adopted method is nearest neighbor with non-uniform embedding (NNUE).

The main steps for TE estimation procedure are summarized in Figure 2.3.1. Red boxes are relative to method choice adopted in this work [51].

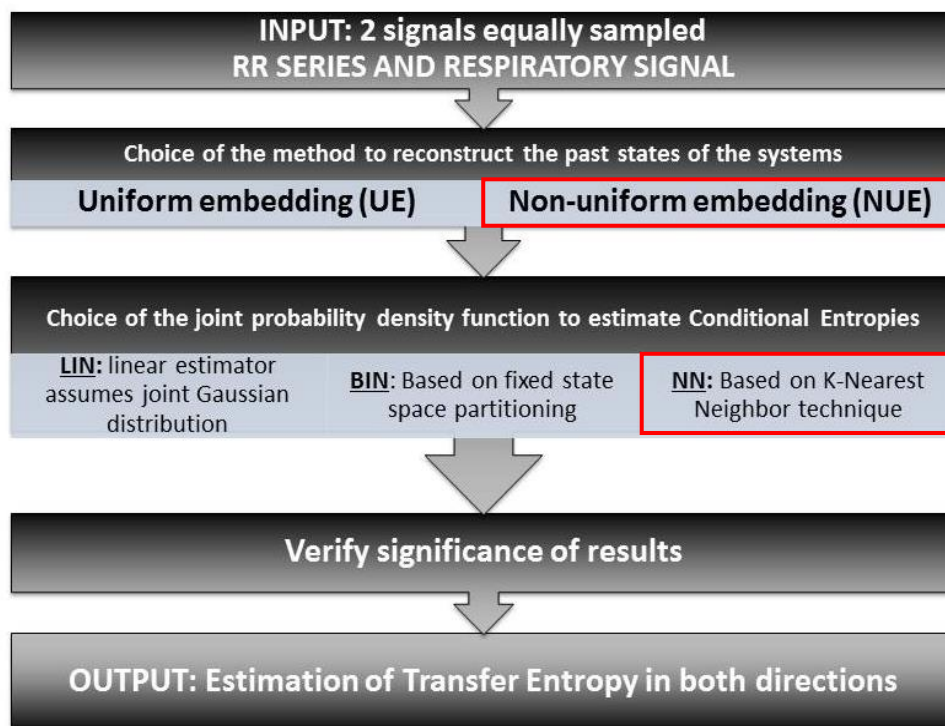


Figure 2.3.1 Scheme of the main steps involved in TE calculation:

- 1) selection of the 2 signals of interest equally spaced. TE will be calculated evaluating the directionality signal 1→signal 2 and vice versa
- 2) choice of the method to approximate the infinite-dimension past states of the systems (UE vs. NUE)
- 3) choice of Conditional Entropy estimator (LIN vs. BIN vs NN) and TE estimation
- 4) verification of TE results significance

2.4 Phase locking analysis

Generation of rhythms is an intrinsic property of many physiological systems, cardiac and respiratory systems are proper examples [52], [53]. It is well known that cardiac and respiratory system are not independent and they interact in a complex interplay of both linear and nonlinear interrelationships. Normally their interaction is weak and transient: the most well-known example is the respiratory sinus arrhythmia (RSA) [54], but in specific physiological conditions a tight coupling between the two subsystems takes place.

The univariate approaches employed to analyze HRV and respiration are not capable of investigating the interactions between the two subsystems. Bivariate methods have been developed to analyze coordination between complex interacting systems in both linear and nonlinear fashion. It is important to highlight that classical linear approaches are insufficient to quantify the strength and the nonlinear nature of cardiorespiratory interactions because the main assumption is linearity.

Many studies describe the cardiorespiratory interaction as characteristic of two weakly coupled chaotic oscillators [55], [56], [57]. Within this hypothesis it is possible to investigate cardiorespiratory synchronization by means of a phase analysis of RR series and respiratory signal rather than a classical amplitude analysis. This assumption is supported by the idea that amplitude of oscillators may remain uncorrelated whereas their phases do mutually perturb.

The first step towards the analysis of cardiorespiratory coordination is the calculation of temporal distances between the event markers of the two subsystems, in this context the temporal series of R peaks and inspiratory onsets [58]. The investigation can be performed considering various cardiorespiratory coordination ratio, where ratios refer to different n:m ratios (cardiac cycles : breathing cycles) [59].

Defining R_i ($i = 1, \dots, n_R$) as the series of R peaks and I_j ($j = 1, \dots, n_I$) as the series of inspiratory onsets detected in a 3-minutes long segment, it is possible to compute the absolute (t_i) and relative (φ_i) distance between the current respiratory event and the successive R peaks as:

$$t_i = R_i - I_j \quad (6)$$

$$\varphi_i = \left(\frac{R_i - I_j}{I_{j+1} - I_j} + j \right) \cdot \text{mod } b \quad (7)$$

Figure 2.4.1 shows a 60-second segment of RR series (first panel) and the synchronous respiratory signal (second panel). The third panel of Figure 2.4.1 shows the relative distances φ_i for $b = 1$, a single respiratory cycle.

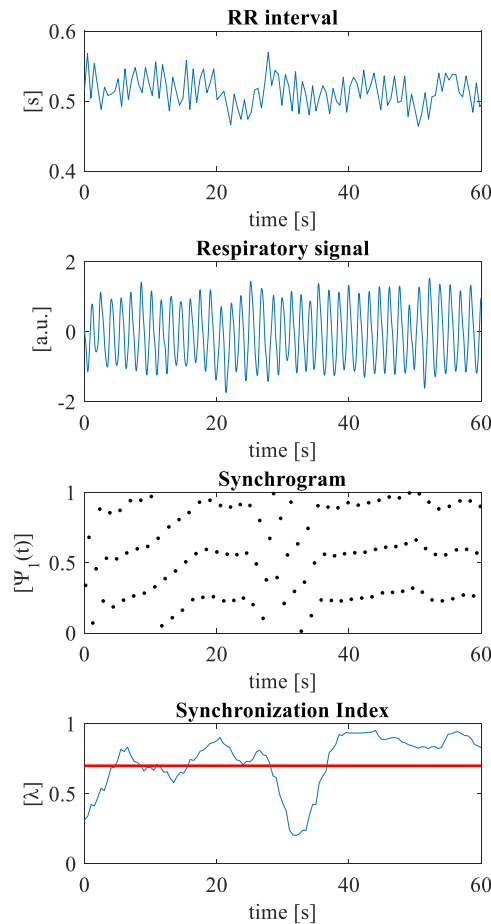


Figure 2.4.1 From top to bottom: examples of a 60-second segment of RR series, respiration, synchrogram and relative λ index of 3:1 synchronization order

This kind of presentation is called Synchrogram and it visually shows the relative distance with respect to time on x-axis and respiratory cycle on y-axis.

A synchrogram may show structures of parallel horizontal line: this configuration reveals epochs in which relative distances φ_i stay constant over consecutive breathing cycles. In this situation the cardiorespiratory interaction is said to be phase-locked [60], [61]. For example, the synchrogram in Figure 2.4.1 shows the main epochs of phase locking from 15 to 25 and from 40 to 60 seconds. In order to detect the number of successive coordinated beats, it is sufficient to count the number of horizontal lines. In this case, it is possible to assess a 3:1 ratio of synchronization.

After a visual representation of phase locking, it is necessary to quantify the degree of phase locking [62]. Considering two weakly coupled oscillators as the cardiac and respiratory systems, their phase variable can be defined as ϕ_1 and ϕ_2 respectively, so that their phase dynamics are expressed as:

$$\frac{d\phi_1}{dt} = \omega_1 + \varepsilon g_1(\phi_1, \phi_2) \quad (8)$$

$$\frac{d\phi_2}{dt} = \omega_2 + \varepsilon g_2(\phi_2, \phi_1) \quad (9)$$

where the variables ϕ_1 and ϕ_2 are defined not on the $[0, 2\pi]$ circle but on the whole real line, ω_1 and ω_2 are the natural angular frequency of the system, g_1 and g_2 are the 2π -periodic coupling terms and ε is the coupling coefficients.

In this work, instantaneous phase of the ECG is estimated as [63]:

$$\phi_1(t) = 2\pi k + 2\pi \frac{t - t_k}{t_{k+1} - t_k} \quad (10)$$

where t_k are the times of appearance of the k -th R peak.

The respiratory signal was detrended and filtered with a Savitzky-Golay filter and then its instantaneous phase ϕ_2 was estimated applying the Hilbert transform.

All the instantaneous phases were resampled at 100 Hz.

Considering a general case of n:m phase locking it is possible to define the generalized phase difference:

$$\varphi_{n,m}(t) = n\phi_1(t) - m\phi_2(t) \quad (11)$$

and its instantaneous variation considering the above defined phase variables:

$$\frac{d\varphi_{n,m}}{dt} = n\omega_1 - m\omega_2 + \varepsilon G(\phi_1, \phi_2) \quad (12)$$

where G is a function taking into account the mutual relationship between ϕ_1 and ϕ_2 .

Equation 12 admits two different kinds of solutions: the phase variable relationship can be either unbounded or bounded. When investigating the phase locking, it is crucial to achieve a bounded expression linking ϕ_1 and ϕ_2 :

$$|n\phi_1(t) - m\phi_2(t) - \delta| < \text{const} \quad (13)$$

where δ is a term that takes into account the average phase shift.

In the ideal synchronous situation, the difference between phase variables stays stable at a constant specific value (Equation 13). When dealing with real data derived from physiological systems, noise is always present and its influence needs to be taken into account. It is possible to assess that during synchronization in presence of noise, the difference $\phi_1 - \phi_2$ fluctuates around a constant.

Under the assumption about the synchronous state between two subsystems, it is possible to extract an index capable of quantifying the presence or absence of the interaction and measuring the strength of the coupling between the systems under analysis.

In order to achieve a quantitative estimator of synchronization, the phase variables are redefined as cyclic:

$$\tilde{\phi}_1 = \phi_1 \bmod 2\pi \quad (14)$$

$$\tilde{\phi}_2 = \phi_2 \bmod 2\pi \quad (15)$$

The phase $\tilde{\phi}_2$ of the second oscillator is then observed each time instant t_i when $\tilde{\phi}_1$ fulfills the condition $\tilde{\phi}_1 = \theta$, and then the following is computed (Equation 16):

$$\eta_i = \tilde{\phi}_2(t) \Big|_{\tilde{\phi}_1(t)=\theta} \quad (16)$$

where θ is a specific and constant value of first oscillator's phase.

This quantity corresponds to the construction of the Poincaré section that reduces Equation 16 to a circle map. Considering a 1:1 free-noise phase locking situation $\eta_i = \text{const}$, whereas in presence of noise the values of η_i are scattered around a constant.

The distribution of η_i can be characterized by computing the intensity of its first Fourier mode. A binning procedure of the first oscillator's phase allows to estimate the index over multiple values of θ in order to obtain a reliable estimation of phase relationship between oscillators.

In case of N points binning, the index Λ_l computed for the l-th bin can be expressed as:

$$\Lambda_l^2 = M_l^{-2} \left(\sum_{i=1}^{M_l} \cos \eta_i \right)^2 + M_l^{-2} \left(\sum_{i=1}^{M_l} \sin \eta_i \right)^2 \quad (17)$$

In this work the cyclic phase of the first oscillator was divided in 10 equally spaced bins.

The average of Λ_l over all N bins allows to compute the synchronization index λ :

$$\lambda = N^{-1} \sum_{i=1}^N \Lambda_l \quad (18)$$

The synchronization index λ (Equation 18) varies from 0 (absence of synchronization) to 1 (presence of synchronization) in the free-noise case [25]. Due to the constant presence of noise when dealing with physiological systems, the value of λ does not attain unity: it remains close to 1 in synchronization region and progressively decreases when synchronization vanishes.

In order to consider a generalized phase locking ratio, it is sufficient to rescale both phase variables. For example, in the case of $n:m$ locking, phases are rescaled such as: $\phi_1 \rightarrow \phi_1/n$ and $\phi_2 \rightarrow \phi_2/m$, obtaining the synchronization index λ that now can also be rewritten as $\lambda_{n,m}$.

According to this definition, $\lambda_{n,m}$ measures the conditional probability for $\tilde{\phi}_2$ to have a certain value, provided $\tilde{\phi}_1$ is in a certain bin.

In this study, the λ index was calculated on windows of 1000 samples overlapping by 50 samples. λ values equal or above the threshold of 0.7 were considered indicating a situation in which coupling is present. Bottom panel of Figure 2.4.1 shows an example of $\lambda_{3,1}$ (blue line) and the threshold (red line). In the intervals 15-25 sec and 40-60 sec, the index value is close to 1. This is in accordance with the synchrogram exhibiting horizontal lines in the same intervals Figure 2.3.1.

It is well-known [56], [61] that different rhythms can be found when considering the interacting relationship between the cardiac and respiratory phase.

It is also well-known that shifts in synchronization are likely to occur even considering short time scale as in the work. Due to these reasons a global index of synchronization, called $n:1$ can be computed by summation of 3:1, 4:1, 5:1, 6:1 ratios, this measurement summarizes the synchronization contribution of different rhythms in the whole signal. Analogous reasoning allows to compute $n:2$ summing 3:2, 5:2 ratios.

Once $n:1$ and $n:2$ have been computed it is possible to assess the time spent in synchronization for each segment. This latter quantity can be computed as the percentage of time spent in synchronization with respect to the 3-minute duration of segments, or in a different way, by computing the average duration (in seconds) of each epoch of synchronization.

2.5 Directionality Index analysis

Interactions between subsystems can be investigated by means of traditional and more novel signal-processing techniques e.g., cross-spectra, mutual information. These measurements provide a symmetric estimation of interaction strength, not suitable for evaluation of causality. Even when considering phase-locking analysis, synchronization does not explain how systems interact and mutually perturb themselves.

Other approaches deal with the concept of phase interaction of irregular oscillators: the main requirement is that the systems under analysis can be modeled as weakly coupled oscillators and the causal interaction can be assessed looking at the evolution of phase of the subsystems. The cardiorespiratory system can be modeled by two weakly interacting rhythmical oscillators. Subsystems have their own intrinsic rhythms even if they are completely uncoupled. Interaction takes place when the systems mutually perturb themselves during transient and finite time intervals.

Under this assumption, it is possible to fully describe weakly coupled oscillators dynamics by means of a phase model capable of describing underlying physiological mechanisms. The model generating cardiorespiratory rhythmic behavior is mostly unknown and it can be only passively observed. It is possible to have an insight looking at its macroscopic oscillations which are observable and they can be employed to describe the dynamic of the nonlinear oscillators [65].

In this work, a simple model of two coupled phase oscillators is proposed. Each system can be represented by its own phase variable ϕ so that its time variation $\dot{\phi}$ can be expressed as $\dot{\phi} = \omega$, where $\omega = 2\pi/T$ is the natural frequency of the considered oscillator and T the period of oscillation. The phase space of the model is two-dimensional, and it can be expressed as:

$$\dot{\phi}_1 = \omega_1 + \varepsilon_1 \cdot f_1(\phi_2, \phi_1) + \zeta_1(t) \quad (19)$$

$$\dot{\phi}_2 = \omega_2 + \varepsilon_2 \cdot f_2(\phi_1, \phi_2) + \zeta_2(t) \quad (20)$$

in Equation 19 and Equation 20 subscript 1 refers to cardiac system and subscript 2 to respiratory system.

The continuous phase variables ($\dot{\phi}_1, \dot{\phi}_2$) take into account the natural angular frequency of the system (ω_1, ω_2). The random terms (ζ_1, ζ_2) instead, account for amplitude fluctuations and perturbations which are intrinsic characteristics of every biological systems. The coupling terms consist of 2π -periodic functions (f_1, f_2) and the parameters describing the strength of interaction between subsystems ($\varepsilon_1, \varepsilon_2$); in case of weakly coupled systems the conditions $\omega_1 \gg \varepsilon_1$ and $\omega_2 \gg \varepsilon_2$ are usually verified.

Given the assumption that phase variables can be computed directly from the measured time series, it is possible to obtain an approximated reconstruction of both cardiac and respiratory oscillators in order to understand the causal relationship between the subsystems.

In this work, the Evolution Map Approach (EMA) [64], [66] algorithm has been used. This method deals with mutual predictability similarly to Granger causality. Considering system 1 interacting with system 2, if system 1 affects system 2, the future of system 2 can be better predicted taking into account the past samples of both system with respect to information of system 1 only. EMA was shown capable of revealing asymmetric directionality strength from short noisy records and quantify which of the systems under analysis influence its counterparts more strongly.

The idea is to observe the evolution of phase variables over a specific temporal window of length τ . Both ϕ_1 and ϕ_2 are unwrapped phase variables, defined as continuous quantities represented on the whole real line, not limited from 0 to 2π .

In this work the phase variable increments are computed using a fourth order Savitzky–Golay filter. Given these hypotheses, the phase increments of oscillator 1 and oscillator 2 can be expressed as:

$$\Delta_1(k) = \phi_1(t_k + \tau) - \phi_1(t_k) \quad (21)$$

$$\Delta_2(k) = \phi_2(t_k + \tau) - \phi_2(t_k) \quad (22)$$

where Δ_1 and Δ_2 can be computed from phase variables ϕ_1 and ϕ_2 and they represent the phase variable increments over time.

In order to reconstruct the real weakly coupled oscillators from a single recorded realization, it is necessary to fit the dependences of Δ_1 and Δ_2 over ϕ_1 and ϕ_2 upon considering phase variable increments generated by an unknown two-dimensional noisy map:

$$\Delta_1(k) = \omega_1\tau + \mathcal{F}_1[\phi_2(t_k), \phi_1(t_k)] + \xi_1(t_k) \quad (23)$$

$$\Delta_2(k) = \omega_2\tau + \mathcal{F}_2[\phi_1(t_k), \phi_2(t_k)] + \xi_2(t_k) \quad (24)$$

The deterministic part \mathcal{F}_1 and \mathcal{F}_2 of the map can be estimated fitting the dependences of Δ_1 and Δ_2 over ϕ_1 and ϕ_2 by the least mean square approach.

Giving the assumption that phase variables are cyclic, the most appropriate choice of family function is the finite Fourier series:

$$\mathcal{F}_1 \approx F_1 = \sum_m A_m \cdot e^{im\phi_1 + in\phi_2} \quad (25)$$

$$\mathcal{F}_2 \approx F_2 = \sum_n A_n \cdot e^{im\phi_1 + in\phi_2} \quad (26)$$

in this work the maximum order of Fourier expansions is set to 3, in the following computation $|m| \leq 3$ and $|n| \leq 3$.

F_1 and F_2 computed in Equation 25 and in Equation 26 are capable of describing the deterministic (ω and \mathcal{F}) and stochastic (ξ) link between phase variables and their increments. They can be also seen as smoothing functions because they are capable of filtering out the noise by means of the least square fitting.

The cross-dependency coefficients of phase dynamics of the two systems can be extracted from F_1 and F_2 as:

$$c_1^2 = \iint_0^{2\pi} \left(\frac{\partial F_1}{\partial \phi_2} \right)^2 d\phi_1 d\phi_2 \quad (27)$$

$$c_2^2 = \iint_0^{2\pi} \left(\frac{\partial F_2}{\partial \phi_1} \right)^2 d\phi_1 d\phi_2 \quad (28)$$

In summary, the directionality index can be expressed as:

$$d^{(1,2)} = \frac{c_2 - c_1}{c_1 + c_2} \quad (29)$$

The EMA algorithm computes a normalized directionality index. It varies from 1 in case of unidirectional coupling from system 1 to system 2, to -1 in the opposite case of unidirectional coupling is from system 2 to system 1. The positive intermediate values of d express a stronger or weaker 1→2 coupling strength, the negative intermediate values a coupling strength in the opposite direction (2→1). In the case of absence of interaction when $c_2 = c_1$, d is equal to zero.

In this work the DACOMO toolbox by Rosenblum et al. has been used to compute directionality index [66], [67], [68].

2.6 Statistical analysis

IQR outlier rejection criterion has been employed in this work. Differences between groups have been tested by means of T-test in case of Gaussian-like distributed populations, on the contrary the non-parametric Wilcoxon signed-rank test has been applied if the hypothesis of Gaussian-like distribution was not verified.

Chapter 3

In this chapter results obtained with methods illustrated in Chapter 2 will be presented.

In this work state-related and age-related analyses have been performed, the former case regards the comparison of a parameter in AS versus QS when a specific age is considered (newborns or one month infants), in the latter case a parameter in a specific state (AS or QS) is compared at two different time points.

In the first part of this chapter time domain and entropy parameters will be presented. The reliability of these results is compared with previous works by several authors.

In the second part of this Chapter the bivariate analysis is reported.

For each estimated parameter both state-related and age-related have been performed and the corresponding statistical analyses are reported.

Results

3.1 Time domain

Time domain parameters of RR series and respiratory signal have been calculated on 3-minute length segments, both in AS and QS.

As reported in [33] a 5-minute length segment is sufficient to extract short-term time domain parameters in adults. Due to this assumption and given the higher heart rate for newborns and one month infants, 3-minute segments are optimal to compute short-term parameters with the same degree of reliability.

In order to perform the parameter computation, both RR and respiratory signal quality has to be controlled; low quality segments containing for instance ectopic beats, interruptions, movement or noise artifacts have been discarded from the analysis.

A single set of time domain parameters is extracted, averaging the results over multiple segments if a subject presents more than one in a specific sleep state, N represents the number of subjects of a considered population.

In Table 3.1.1, mean and standard deviation of time domain parameters are shown. Differences between AS and QS considering the two cohorts of newborns and one month infants have been tested.

	Newborns			One months		
	Active sleep	Quiet sleep	<i>p-value</i>	Active sleep	Quiet sleep	<i>p-value</i>
RR mean [s]	0.49 ± 0.05	0.51 ± 0.04	< 0.01	0.41 ± 0.03	0.43 ± 0.02	n.s.
RR IQR [s]	0.04 ± 0.02	0.03 ± 0.01	< 0.01	0.03 ± 0.01	0.02 ± 0.01	< 0.01
SDNN [ms]	34.84 ± 15.73	25.33 ± 10.56	< 0.01	23.07 ± 6.29	14.10 ± 6.38	< 0.01
RMSSD [ms]	16.22 ± 9.63	16.10 ± 8.28	n.s.	11.04 ± 4.18	8.81 ± 4.97	< 0.05
IBI mean [s]	1.24 ± 0.25	1.50 ± 0.27	< 0.01	1.31 ± 0.23	1.62 ± 0.34	< 0.01
IBI IQR [s]	0.45 ± 0.15	0.27 ± 0.10	< 0.01	0.41 ± 0.15	0.26 ± 0.09	< 0.01

Table 3.1.1 Time domain parameters extracted from RR series and respiratory signal. IBI measures the mean distance between adjacent respiratory onsets and IBI IQR the interquartile range of this distribution. P-values are relative to statistics comparing AS and QS parameters within the same age

AS and QS can be seen as two states in which the ANS regulation acts differently and differences in time domain parameters confirm this.

As reported in Table 3.1.1 the majority of these indexes are significantly different when comparing the two sleep states.

Figure 3.1.1 shows boxplots of the above mentioned quantities highlighting increasing and decreasing trends.

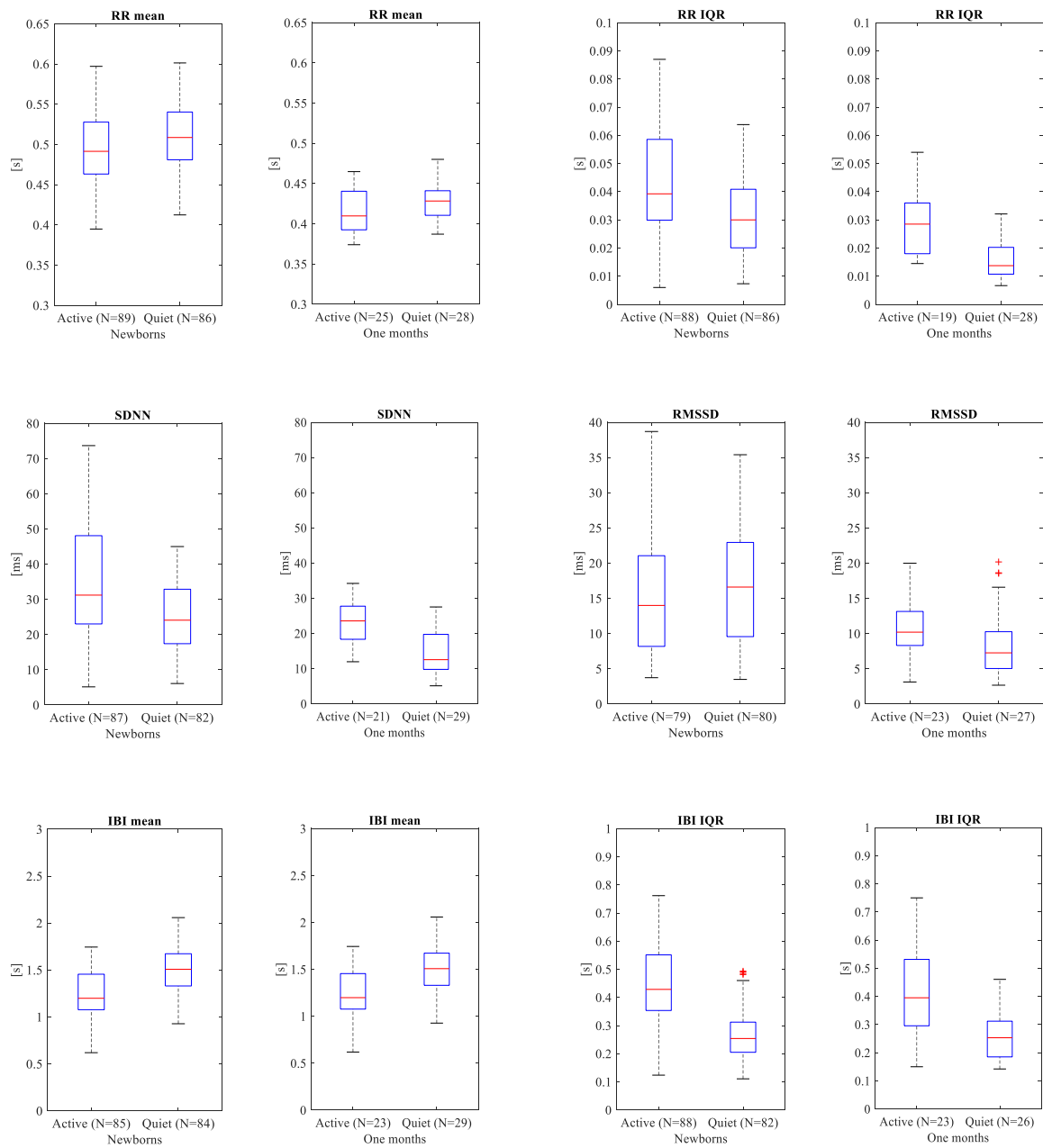


Figure 3.1.1 Boxplot of time domain parameters computed from RR series (RR mean, RR IQR, SDNN, RMSSD, IBI mean, IBI IQR) and from respiratory signal (IBI mean, IBI IQR)

A further investigation can be performed considering the comparison between the newborns and one month infants populations within the same sleep state as reported in Table 3.1.2.

	Active sleep			Quiet sleep		
	Newborns	One months	<i>p-value</i>	Newborns	One months	<i>p-value</i>
RR mean [s]	0.49 ± 0.05	0.41 ± 0.03	< 0.01	0.51 ± 0.04	0.43 ± 0.02	< 0.01
RR IQR [s]	0.04 ± 0.02	0.03 ± 0.01	< 0.01	0.03 ± 0.01	0.02 ± 0.01	< 0.01
SDNN [ms]	34.84 ± 15.73	23.07 ± 6.29	< 0.01	25.33 ± 10.56	14.10 ± 6.38	< 0.01
RMSSD [ms]	16.22 ± 9.63	11.04 ± 4.18	< 0.05	16.10 ± 8.28	8.81 ± 4.97	< 0.05
IBI mean [s]	1.24 ± 0.25	1.31 ± 0.23	n.s.	1.50 ± 0.27	1.62 ± 0.34	n.s.
IBI IQR [s]	0.45 ± 0.15	0.41 ± 0.15	n.s.	0.27 ± 0.10	0.26 ± 0.09	n.s.

Table 3.1.2 Time domain parameters extracted from RR series and respiratory signal. P-values are relative to statistics comparing same sleep state (AS and QS) parameters for the two different time points

Figure 3.1.2 shows the boxplot graphs of time domain parameters considering the population described in Table 3.1.2.

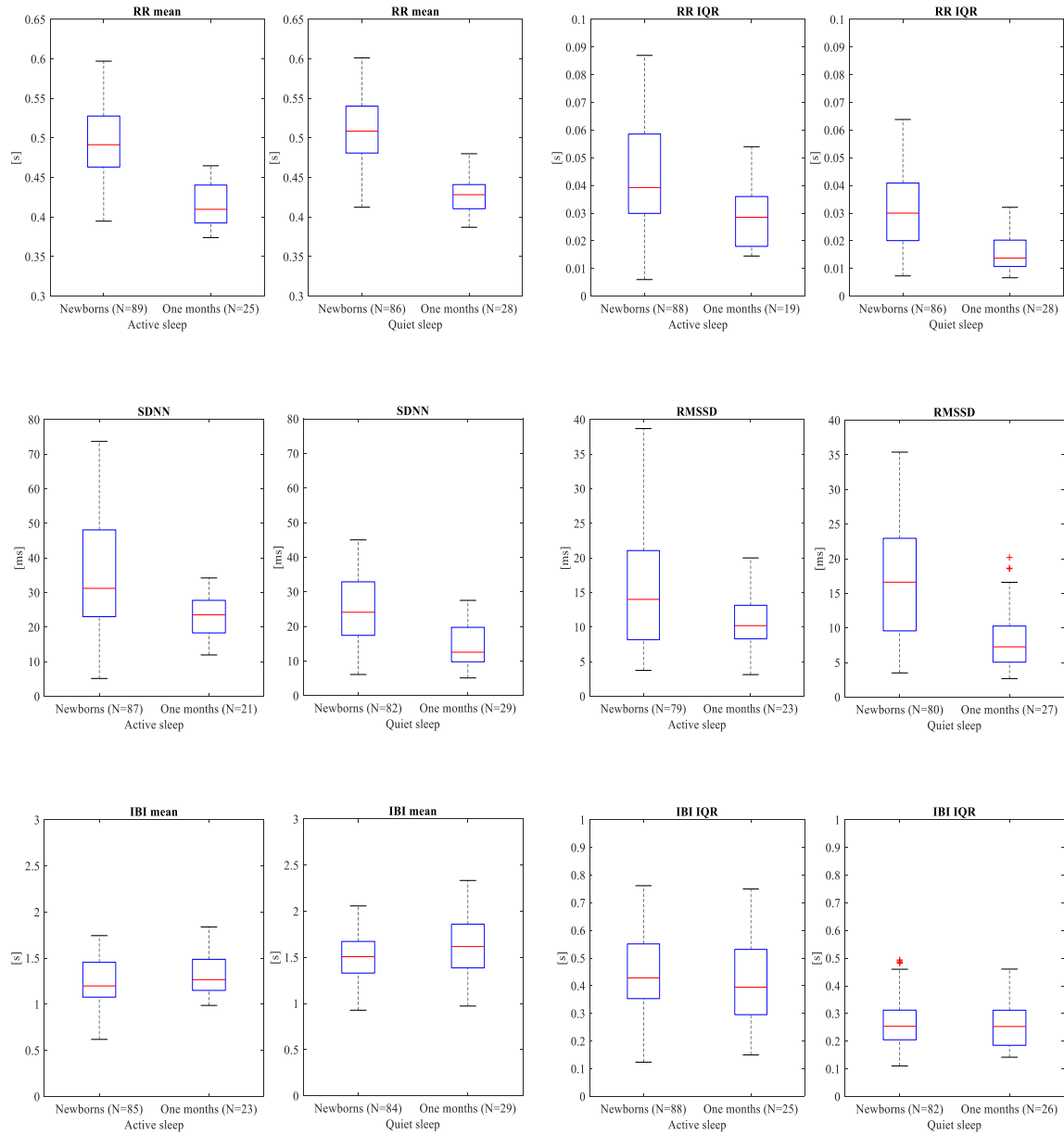


Figure 3.1.2 Boxplot of time domain parameters computed from RR series (RR mean, RR IQR, SDNN, RMSSD, IBI mean, IBI IQR) and from respiratory signal (IBI mean, IBI IQR)

3.2 Sample Entropy and Quadratic Sample Entropy

Sample Entropy (SampEn) and Quadratic Sample Entropy (QSE) are univariate entropy estimators computed on RR series. They are reported by many authors as dependent on the length of the considered signal [36], [37].

Due to this issue, 300-beat long segments are analyzed in order to obtain an unbiased estimation. The mean duration of segments is 148.30 ± 14.01 seconds for newborns in AS, 151.63 ± 12.29 seconds for newborns in QS, 124.02 ± 8.55 seconds for one month infants in AS and 129.87 ± 10.04 seconds for one month infants in QS.

Time domain analysis was performed considering the 300-beat segment for both newborns and one month infants, in order to perform a reliable comparison.

Time domain results considering 300-beat segments are consistent with time domain results when 3-minute segments were considered (Table 3.1.1 and Table 3.1.2). The only differences are found when comparing RR mean in newborns and IBI mean in QS between newborns and one month infants, analogous trends are found but resulting in a non-significant comparison.

Table 3.2.1 and Table 3.2.2 show Sample Entropy and QSE considering different embedding dimensions ($m=1, 2, 3$). The tolerance parameter r is set to 20% of RR series standard deviation for SampEn while for QSE is optimally chosen with the minimum count of matches method. The minimum required number of matches is 0 for SampEn while for QSE is set to $\frac{n^2}{5}$, where n is the number of points of the considered time series.

Table 3.2.1 shows SampEn and QSE computed for the three embedding dimension when newborns and one month infants are tested for differences related to sleep states.

	Newborns			One months		
	Active sleep	Quiet sleep	<i>p-value</i>	Active sleep	Quiet sleep	<i>p-value</i>
SampEn1 [bits]	1.76 ± 0.26	2.00 ± 0.14	< 0.01	1.70 ± 0.28	1.94 ± 0.15	< 0.01
SampEn2 [bits]	1.63 ± 0.31	1.84 ± 0.20	< 0.01	1.59 ± 0.30	1.86 ± 0.16	< 0.01
SampEn3 [bits]	1.52 ± 0.37	1.70 ± 0.25	< 0.01	1.50 ± 0.35	1.74 ± 0.24	< 0.01
QSE1 [bits]	7.89 ± 0.21	8.05 ± 0.16	< 0.01	7.83 ± 0.25	8.05 ± 0.18	< 0.05
QSE2 [bits]	8.00 ± 0.21	8.07 ± 0.15	< 0.01	7.88 ± 0.25	8.09 ± 0.14	< 0.01
QSE3 [bits]	8.00 ± 0.21	8.11 ± 0.14	< 0.01	8.00 ± 0.26	8.12 ± 0.15	< 0.01

Table 3.2.1 Sample Entropy and Quadratic Sample Entropy considering 300 beats of RR series only. P-values are relative to statistics comparing AS and QS parameters within the same age

Each of the computed entropy measurements is significant when comparing newborns and one month infants for differences between AS and QS, despite the embedding dimension.

It is important to highlight that each of the indexes show an increasing trend (Figure 3.2.1 and Figure 3.2.3) from AS (red) to QS (green), N represents the number of subjects of a considered population. Same time domain and entropy results are found when segments of 100 and 200 beats were analyzed.

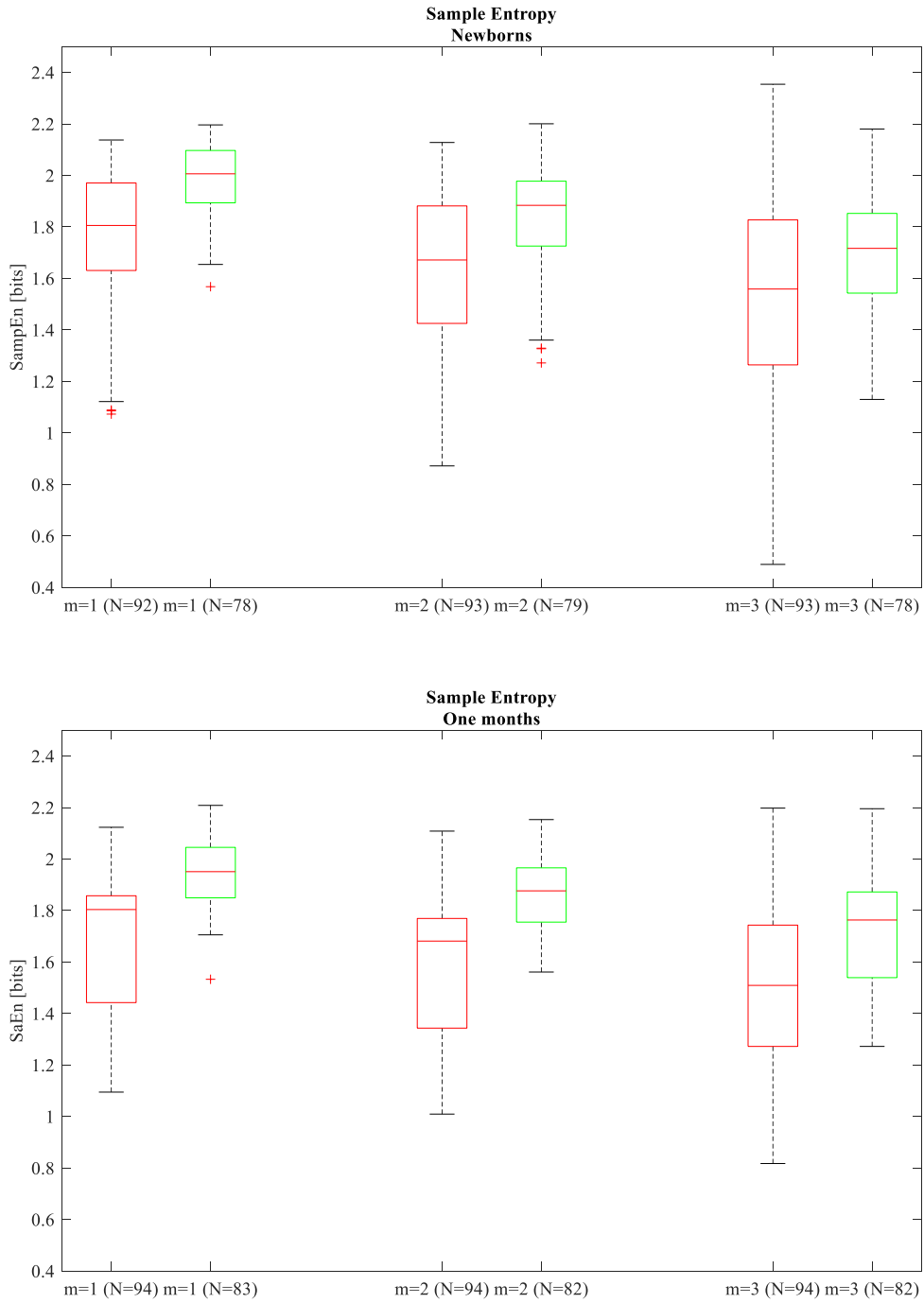


Figure 3.2.2 Boxplots of Sample Entropy computed for different embedding dimensions when state-related analysis is performed, AS (red) versus QS (green) in newborns and one month infants

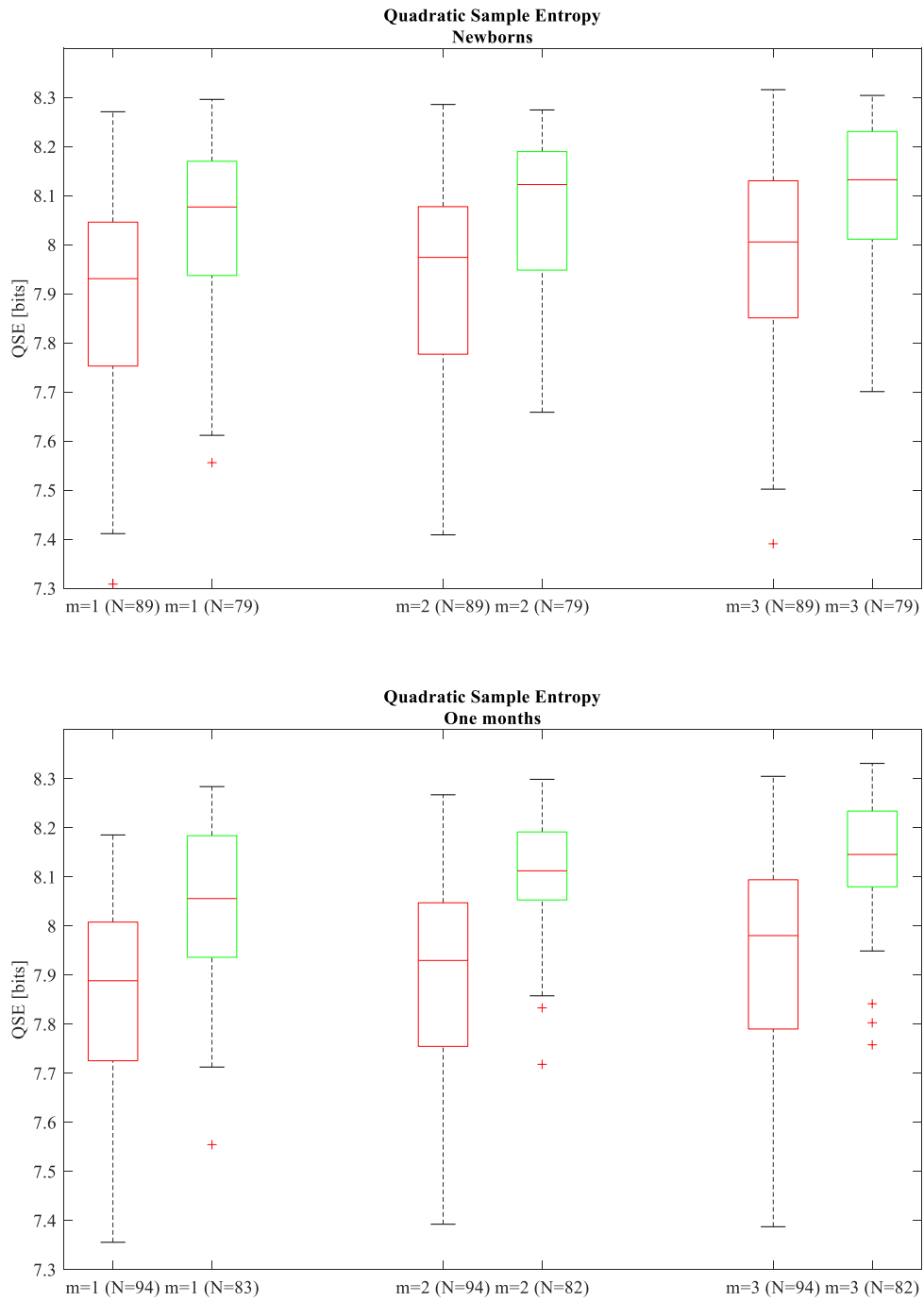


Figure 3.2.3 Boxplots of Quadratic Sample Entropy computed for different embedding dimensions when state-related analysis is performed, AS (red) versus QS (green) in newborns and one month infants

The comparison of newborns and one month infants within the same sleep state does not show any differences at newborn and one month time points as reported in Table 3.2.2.

Both entropy estimators remain stable within the same sleep stage when comparing newborns and one month infants.

	Active sleep			Quiet sleep		
	Newborns	One months	<i>p-value</i>	Newborns	One months	<i>p-value</i>
SampEn1 [bits]	1.76 ± 0.26	1.69 ± 0.28	n.s.	1.98 ± 0.14	1.94 ± 0.15	n.s.
SampEn2 [bits]	1.63 ± 0.31	1.59 ± 0.30	n.s.	1.84 ± 0.20	1.86 ± 0.16	n.s.
SampEn3 [bits]	1.52 ± 0.37	1.49 ± 0.35	n.s.	1.69 ± 0.25	1.74 ± 0.24	n.s.
QSE1 [bits]	7.89 ± 0.21	7.83 ± 0.2479	n.s.	8.05 ± 0.17	8.05 ± 0.18	n.s.
QSE2 [bits]	7.92 ± 0.21	7.88 ± 0.25	n.s.	8.07 ± 0.15	8.10 ± 0.14	n.s.
QSE3 [bits]	8.00 ± 0.21	7.91 ± 0.26	n.s.	8.11 ± 0.14	8.12 ± 0.15	n.s.

Table 3.2.2 Sample Entropy and Quadratic Sample Entropy considering 300 beats of RR series only. P-values are relative to statistics comparing same sleep state (AS and QS) parameters for the two different time points

3.3 Transfer Entropy

Transfer entropy (TE) is a method to assess directionality of information transferred between two time series. TE is a bivariate entropy estimator measuring the flow of information between RR series and respiratory signal. In this context, the same 300-beat database has been used in order to achieve a standardized entropy measurement over multiple subjects.

In Table 3.3.1, TE values for newborns and one month infants are reported. It is important to highlight that comparison can be performed within the same age group comparing AS versus QS when the information flow is from RR series to respiration (RR→RESP) and vice versa from respiration to RR series (RESP→RR).

	Newborns			One months		
	Active sleep	Quiet sleep	<i>p-value</i>	Active sleep	Quiet sleep	<i>p-value</i>
RR→RESP [bits]	0.03 ± 0.02	0.04 ± 0.02	< 0.05	0.04 ± 0.02	0.06 ± 0.02	< 0.01
RESP→RR [bits]	0.04 ± 0.02	0.09 ± 0.06	< 0.01	0.03 ± 0.02	0.10 ± 0.06	< 0.01
<i>p-value</i>	n.s.	< 0.01		n.s.	< 0.01	

Table 3.3.1 Transfer Entropy considering 300 beats of RR series and respiratory sampled at RR instants. P-values are relative to statistics comparing AS and QS parameters within the same age and directionality or within the same age and different directionality

Top row of Figure 3.3.1 shows the sleep state comparison of TE when the information flow is RR→RESP on the left and RESP→RR on the right. In this case both the populations are statistically different when tested. In both cases there is an increase in terms of information flow in QS with respect to AS [51].

When comparison are performed within the same sleep state but for opposite directions, no differences are found in AS, whereas in QS RESP→RR directional flow is more informative than RR→RESP, as shown in the bottom row of Figure 3.3.1 [51].

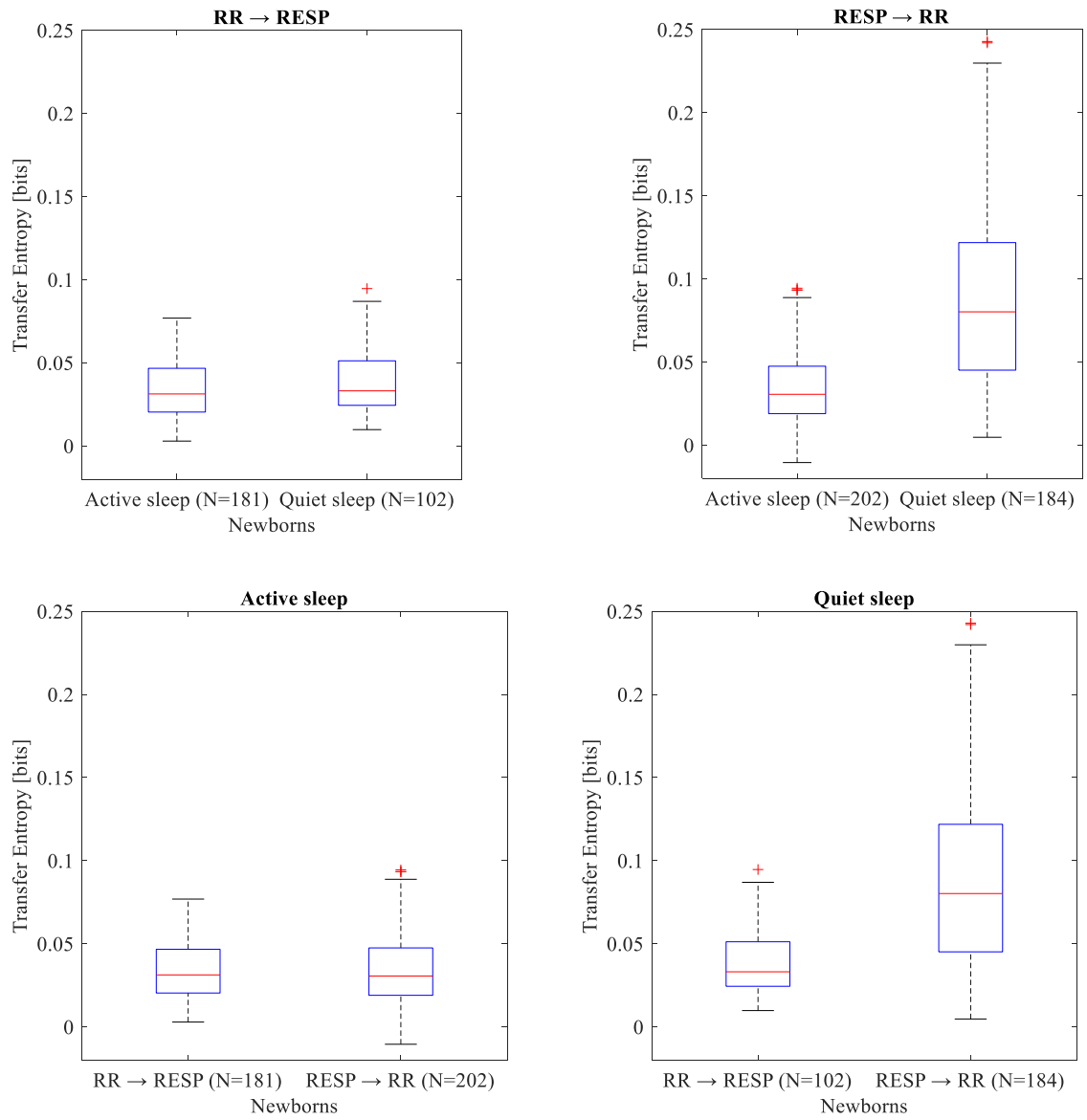


Figure 3.3.1 Boxplots of Transfer Entropy computed for newborn cohort. Comparisons are made considering same direction and different sleep state or same sleep state and different direction, N represents the number of segments in the considered population

Figure 3.3.2 shows the same comparisons of Figure 3.3.1 considering one month infants, significant differences of AS versus QS are comparable with what found in newborn cohort.

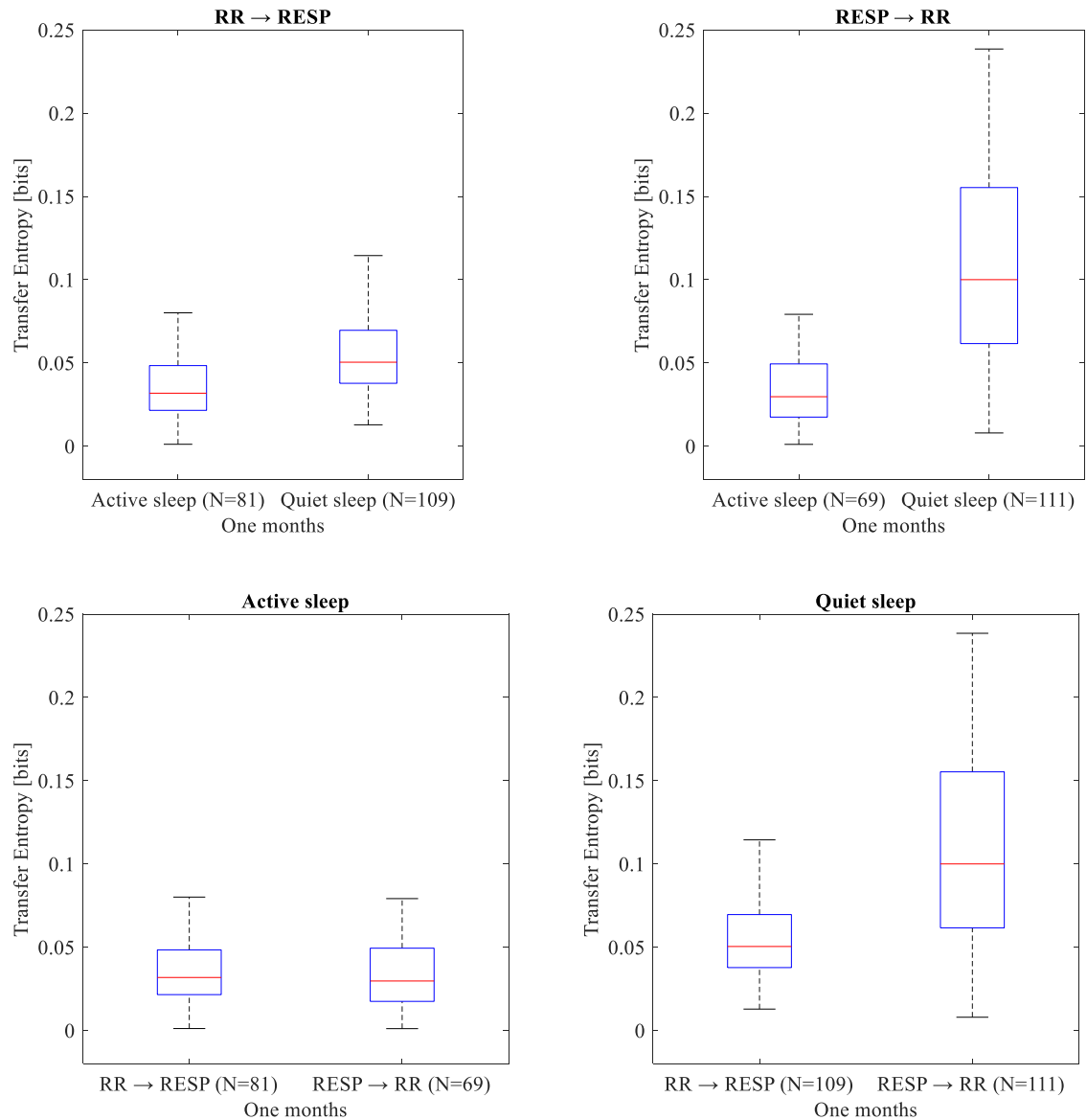


Figure 3.3.2 Boxplots of Transfer Entropy computed for one month cohort. Comparisons are made considering same direction and different sleep state or same sleep state and different direction, N represents the number of segments in the considered population

Looking at the evolution of TE in the first month of life, it appears clear that major differences occur in QS, with an increase in information flow in both directions with age (Figure 3.3.3).

Considering the evolution of TE in AS from newborn age to one month age, no differences in information flow are found neither from RR series to respiration nor from respiration to RR series (Figure 3.3.3) [51].

	Active sleep			Quiet sleep		
	Newborns	One months	<i>p</i> -value	Newborns	One months	<i>p</i> -value
RR → RESP [bits]	0.03 ± 0.02	0.04 ± 0.02	n.s.	0.04 ± 0.02	0.06 ± 0.02	< 0.01
RESP → RR [bits]	0.04 ± 0.02	0.03 ± 0.02	n.s.	0.09 ± 0.06	0.10 ± 0.06	< 0.05

Table 3.3.2 Transfer Entropy considering 300 beats of RR series and respiratory sampled at RR instants. - values are relative to statistics comparing same sleep state (AS and QS) parameters for the two different time points

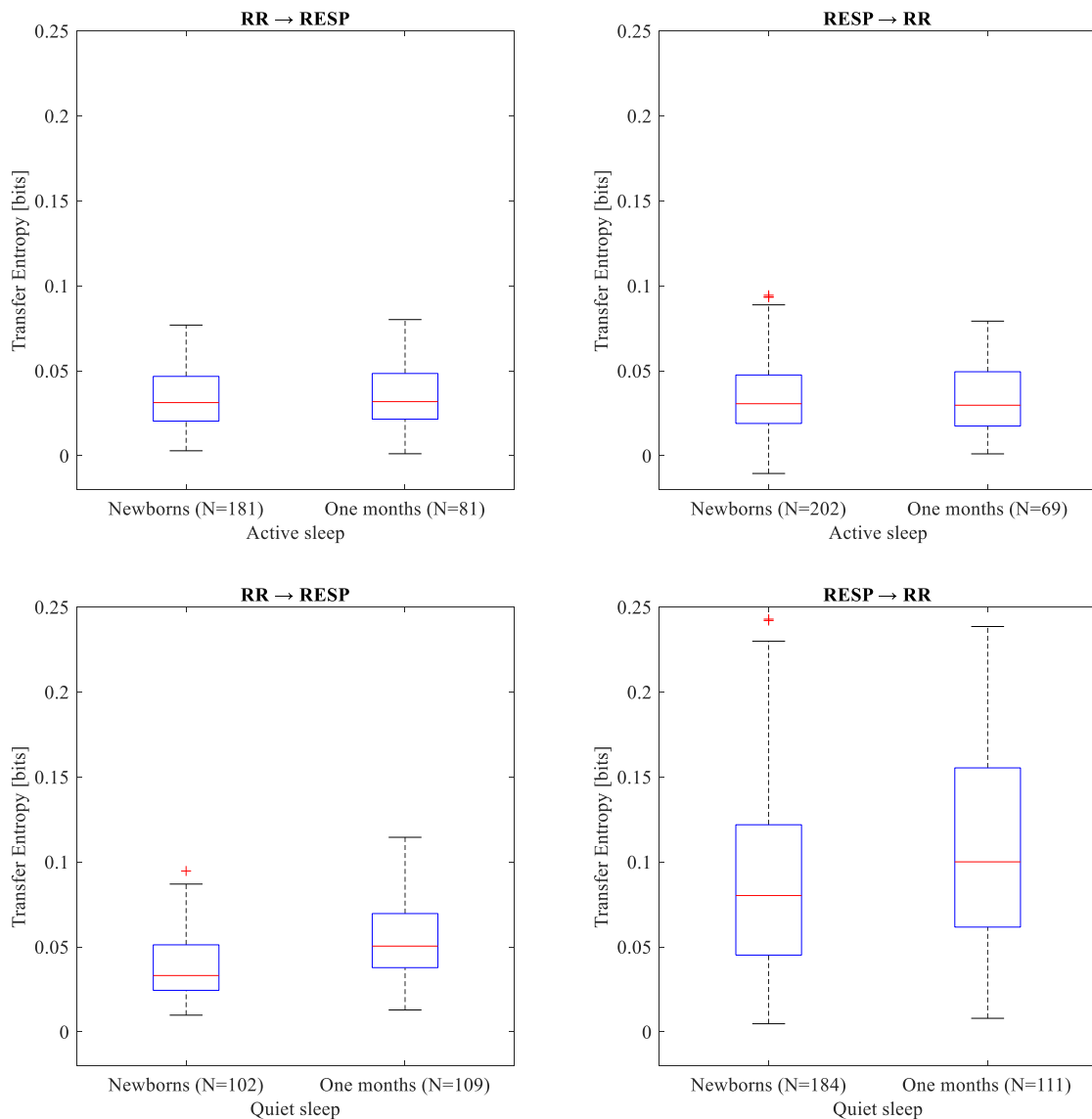


Figure 3.3.3 Boxplots of Transfer Entropy computed for both newborns and one month infants. Comparisons are made considering same direction and sleep state at different time points, N represents the number of segments in the considered population

3.4 Phase synchronization

The phase synchronization parameters are computed to highlight differences in cardiorespiratory coupling when comparing AS versus QS or subjects within the same sleep state at different time points.

As reported in Materials and Methods section, various n:m (cardiac cycles : breathing cycles) are considered in the analysis.

In Table 3.4.1, total synchronization parameters, considering a single breathing cycle or two consecutive breathing cycles, have been computed in terms of both percentage and duration. Statistical comparisons aim at assessing differences between AS and QS within subjects of the same age, N represents the number of subjects in the considered population.

	Newborns			One months		
	Active sleep	Quiet sleep	<i>p-value</i>	Active sleep	Quiet sleep	<i>p-value</i>
Total synch. n:1 [%]	0.06 ± 0.05	0.23 ± 0.14	< 0.01	0.08 ± 0.05	0.30 ± 0.17	< 0.01
Total synch. n:2 [%]	0.01 ± 0.01	0.14 ± 0.01	< 0.01	0.03 ± 0.03	0.19 ± 0.12	< 0.01
Total synch. n:1 duration [s]	5.27 ± 3.47	9.28 ± 4.72	< 0.01	5.55 ± 3.14	10.03 ± 4.27	< 0.01
Total synch. n:2 duration [s]	1.63 ± 1.74	6.53 ± 3.66	< 0.01	1.39 ± 1.21	6.94 ± 3.51	< 0.01

Table 3.4.1 Total synchronization parameters extracted from the analysis of phase relationship between RR series and respiratory signal. P-values are relative to statistics comparing AS and QS parameters within the same age

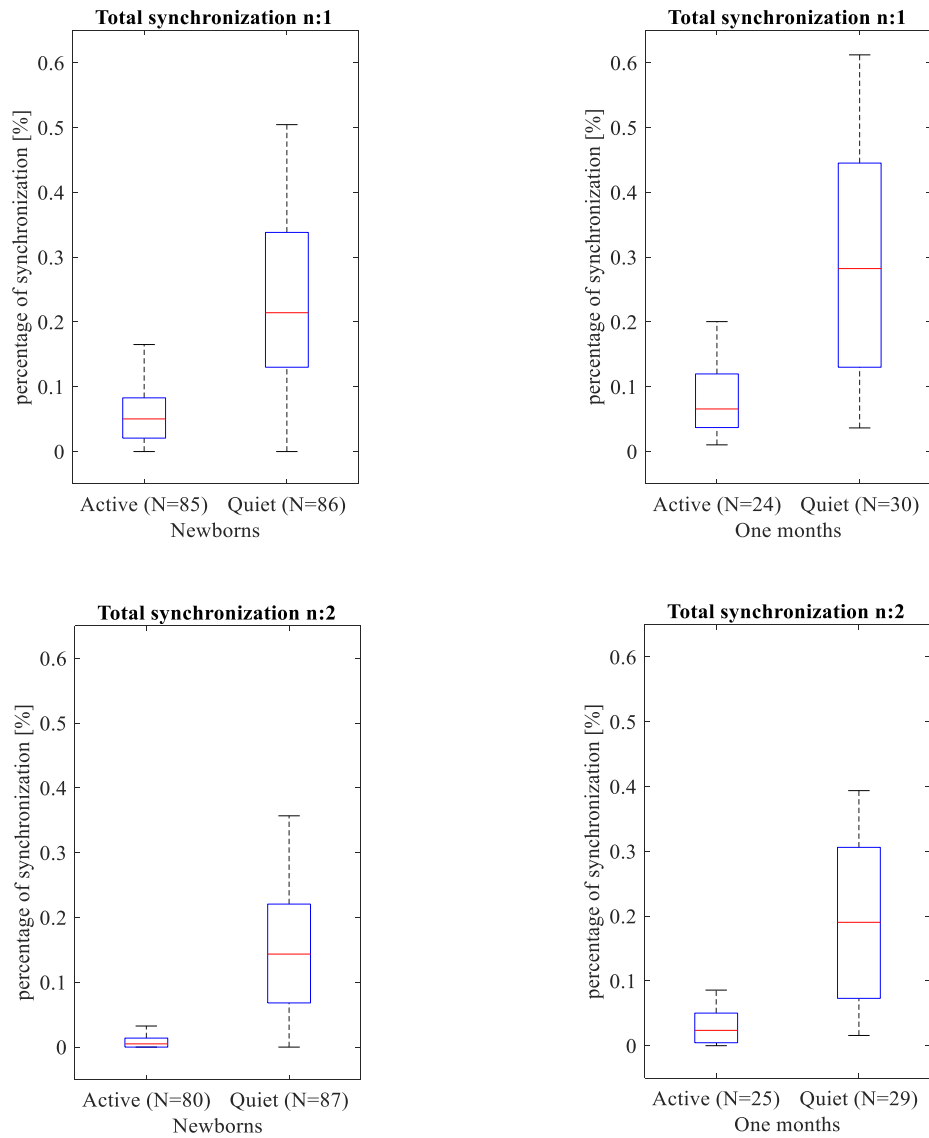


Figure 3.4.1 Boxplots of total percentage of synchronization, sum of ratios with respect a single breathing cycle and two consecutive breathing cycles

When comparing AS versus QS in term of synchronization percentage, differences are statistically significant for n:1 and n:2 parameters considering both newborn and one month subjects. The mean increase of n:1 and n:2 is 17% and 13% considering newborns cohort while 22% and 16% considering one month cohort. These percentage values correspond to 30, 40, 23, 29 seconds respectively, when considering 3-minutes length segments as in this analysis [69].

The total synchronization percentage of n:2 index is lower than n:1, in the former case λ index is required to stay stable for two respiratory cycles while for n:1 the circular variance index is computed considering a single breathing cycle.

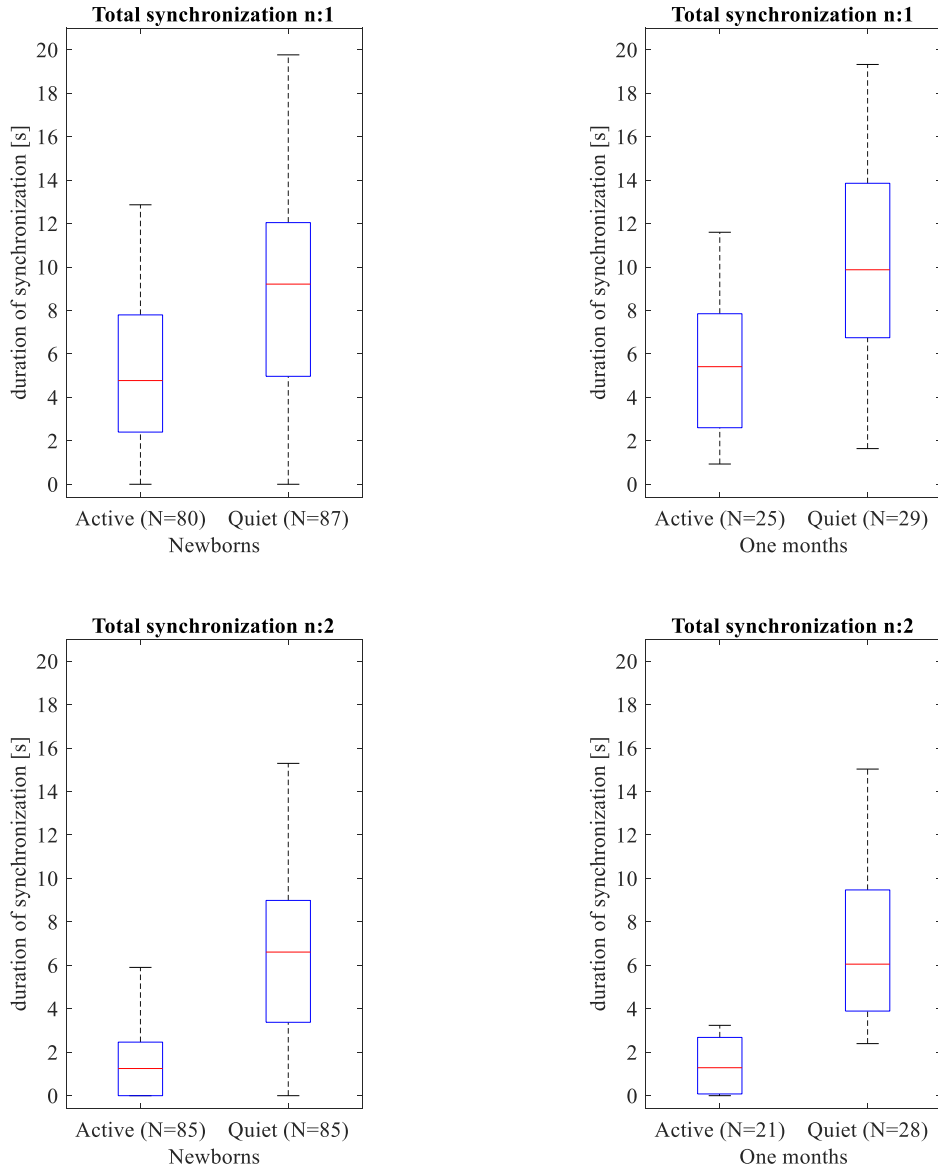


Figure 3.4.2 Boxplots of total duration of synchronization, sum of ratios with respect a single breathing cycle and two consecutive breathing cycles

In Table 3.4.2 total synchronization parameters are evaluated when age-related analysis is performed.

	Active sleep			Quiet sleep		
	Newborns	One months	<i>p</i> -value	Newborns	One months	<i>p</i> -value
Total synchron. n:1 [%]	0.06 ± 0.05	0.08 ± 0.05	n.s.	0.23 ± 0.14	0.30 ± 0.17	< 0.05
Total synchron. n:2 [%]	0.01 ± 0.01	0.03 ± 0.03	< 0.01	0.14 ± 0.01	0.19 ± 0.12	< 0.05
Total synchron. n:1 duration [s]	5.27 ± 3.47	5.55 ± 3.14	n.s.	9.28 ± 4.72	10.03 ± 4.27	n.s.
Total synchron. n:2 duration [s]	1.63 ± 1.74	1.39 ± 1.21	n.s.	6.53 ± 3.66	6.94 ± 3.51	n.s.

Table 3.4.2 Total synchronization parameters extracted from the analysis of phase relationship between RR series and respiratory signal. P-values are relative to statistics comparing same sleep state (AS or QS) parameters for the two different time points

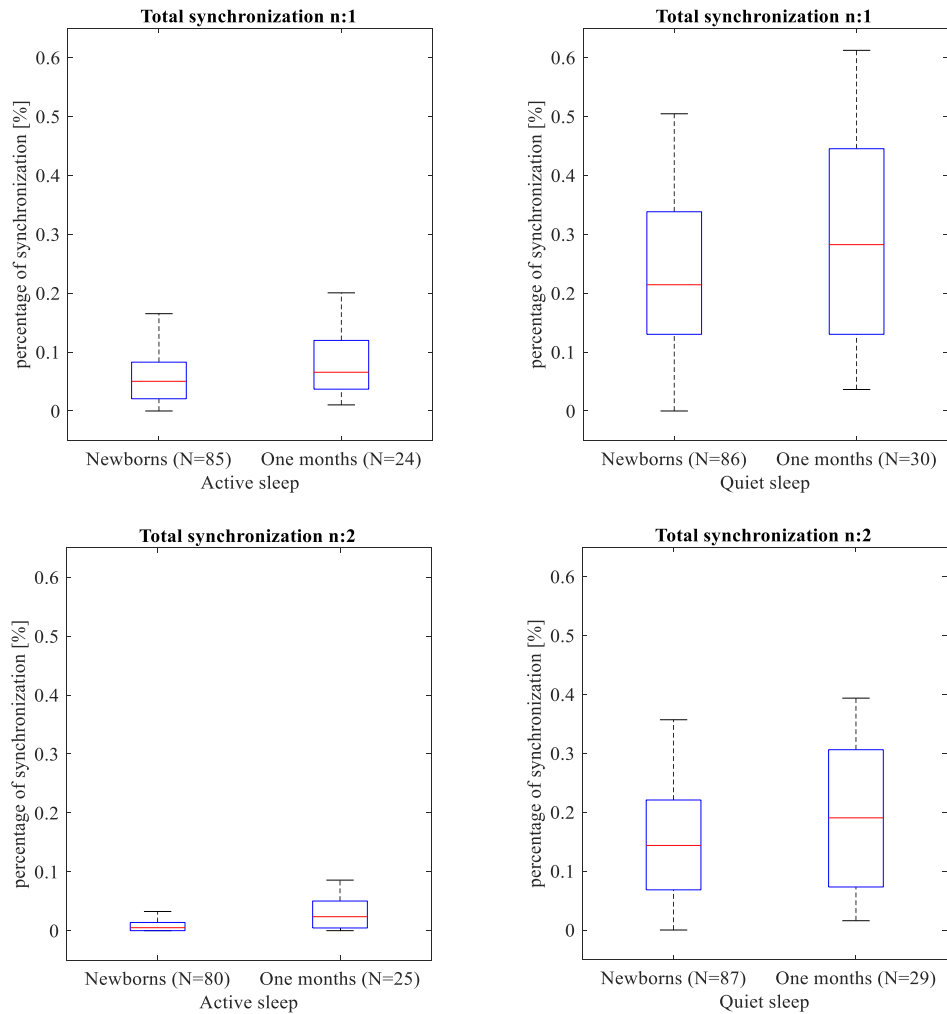


Figure 3.4.3 Boxplots of total percentage of synchronization, sum of ratios with respect a single breathing cycle and two consecutive breathing cycles

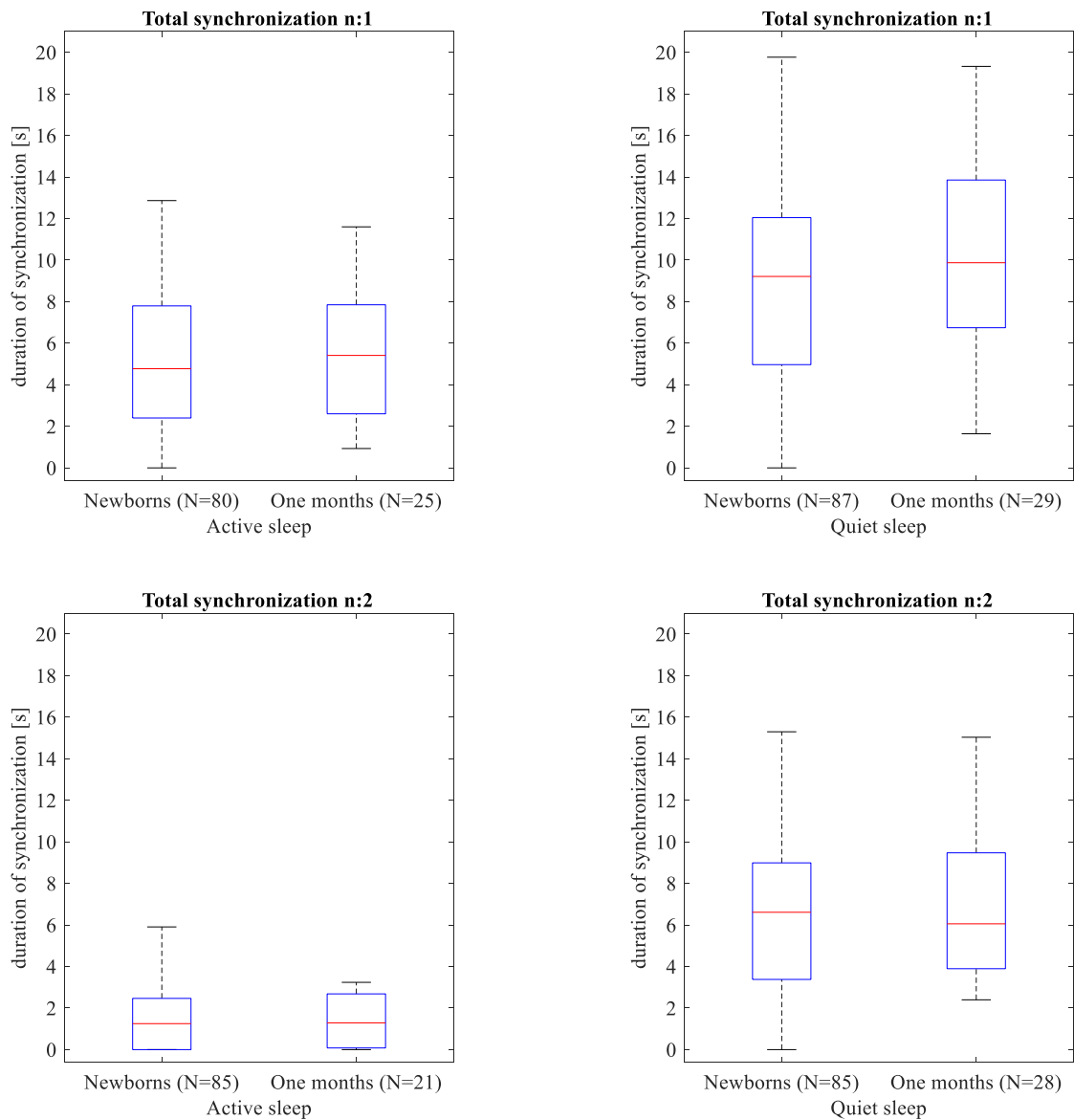


Figure 3.4.4 Boxplots of total duration of synchronization, sum of ratios with respect a single breathing cycle and two consecutive breathing cycles

In Figure 3.4.4 comparison between newborns and one month infants within the same sleep state are shown. When testing the populations in terms of duration of synchronization no differences are found despite the number of considered breathing cycles.

Given the fact the percentage of synchronization is increasing, as depicted in Figure 3.4.3, it is possible to assess that events of coupling in the cardio respiratory system are more likely to occur with increasing age but the average duration of the synchronization is not statistically changing.

Within the available database, it is possible to investigate the total percentage in synchronization for those subjects having both AS and QS epochs for the recorded baseline

In Table 3.4.3 the mean total synchronization n:1 and n:2 considering newborn and one month populations are shown.

The parameter “increase” represent the mean and standard deviation increase in synchronization for those subjects having a greater total synchronization in QS with respect to AS. In this context populations are tested by means of a paired T-test, upon passing the Lilliefors normality test, otherwise in case of non-normal distribution, the populations are tested with a Wilcoxon signed-rank test.

	Active sleep	Quiet sleep	Increase	<i>p-value</i>
Newborns Total synch. n:1 [%]	0.07 ± 0.06	0.20 ± 0.15	0.16 ± 0.10	< 0.01
Newborns Total synch. n:2 [%]	0.03 ± 0.04	0.13 ± 0.11	0.11 ± 0.09	< 0.01
One months Total synch. n:1 [%]	0.09 ± 0.06	0.28 ± 0.16	0.21 ± 0.12	< 0.01
One months Total synch. n:2 [%]	0.03 ± 0.03	0.18 ± 0.12	0.15 ± 0.11	< 0.01

Table 3.4.3 Paired comparison of AS versus QS in newborns and one months

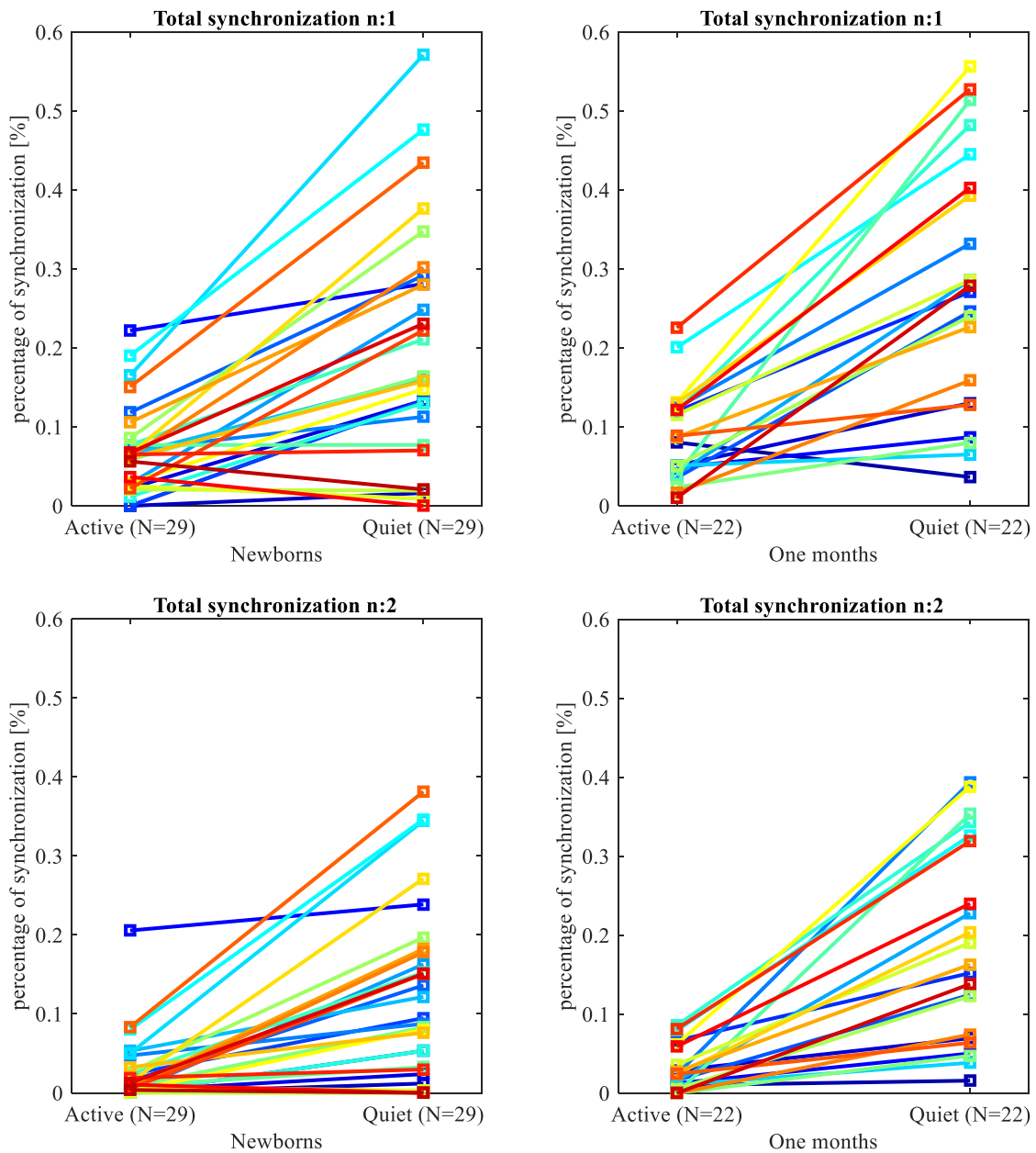


Figure 3.4.5 Entity of increase in synchronization between AS and QS for subjects with both state during the recorded baseline. Each colored line represents a subject

In this analysis, the number of subject in newborns cohort is 29, 86.21% (25 out of 29) and 89.66% (26 out 29) exhibit an increase in synchronization from AS to QS when n:1 and n:2 are computed, while when considering one month cohort the percentage number of subjects increasing synchronization are 95.45% (21 out of 22) for n:1 ratio and 100.00% (22 out of 22) for n:2 ratio.

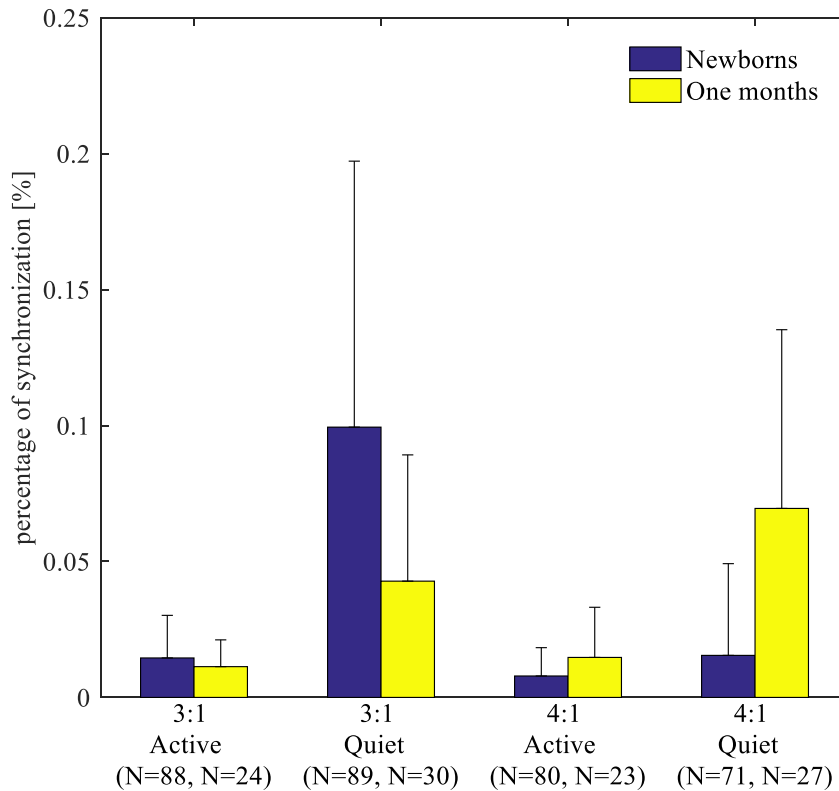


Figure 3.4.6 Bar graph of specific ratio of synchronization comparing same sleep state for different time points

Figure 3.4.6 shows the comparison within the same sleep state for newborns and one month when considering specific synchronization ratio, such as 3:1 and 4:1.

When the two cohorts are tested for both ratios in AS no significant differences are found; this result is coherent with absence of significance for total synchronization $n:1$ as reported in Table 3.4.2. Regarding 3:1 ratio and 4:1 ratio in QS, significant differences are found: p-values are < 0.05 and < 0.01 respectively.

This shift in synchronization, from 3:1 to 4:1, is coherent with results about the RR mean as reported in Table 3.1.2, the mean distance between R peaks decreases both in AS and QS from newborn to one month age. Consequently at one month time point the heart rate increases, so that 4:1 ratio is more likely to occur with respect to 3:1 [70].

3.5 Directionality index

Directionality index method to assess causality is an important step forward in revealing and understanding interaction between the cardiac and respiratory systems. A state-related and age-related analysis have been performed in order to assess the directionality of interaction, comparing AS versus QS and newborns versus one month infants.

In Table 3.5.1 directionality index and breathing frequency in AS and QS for both newborns and one month infants are compared, N represents the number of subjects in the considered population.

	Newborns			One months		
	Active sleep	Quiet sleep	<i>p</i> -value	Active sleep	Quiet sleep	<i>p</i> -value
Directionality index [s]	0.10 ± 0.30	-0.23 ± 0.30	< 0.01	0.06 ± 0.20	-0.15 ± 0.29	< 0.01
Breathing freq. [Hz]	0.82 ± 0.21	0.68 ± 0.14	< 0.01	0.76 ± 0.16	0.64 ± 0.15	< 0.01

Table 3.5.1 Computed directionality index and extracted breathing frequency. P-values are relative to statistics comparing AS and QS parameters within the same age

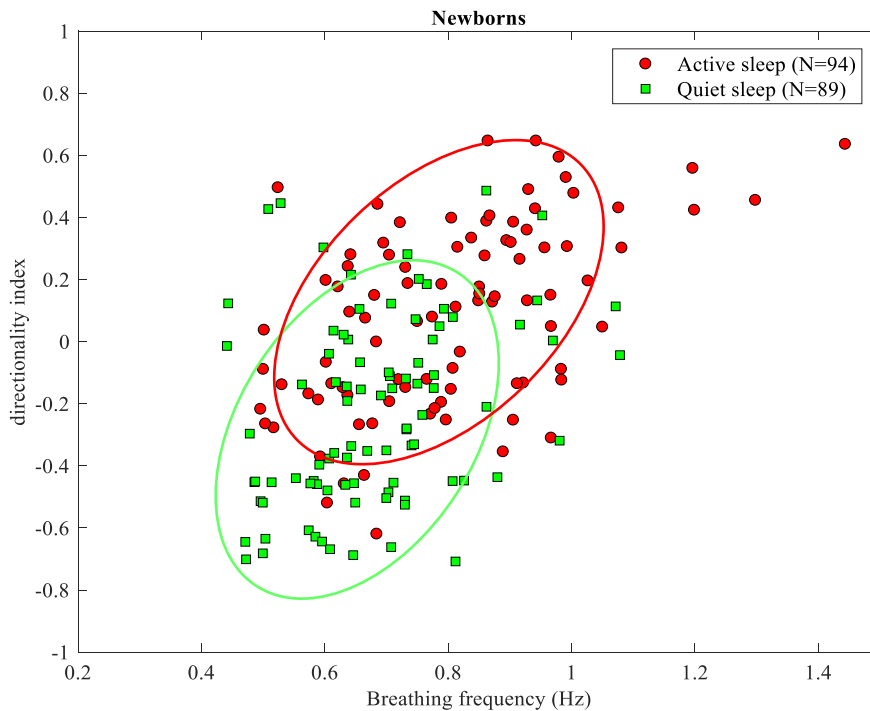


Figure 3.5.1 Scatter plot of breathing frequency and directionality index for newborns

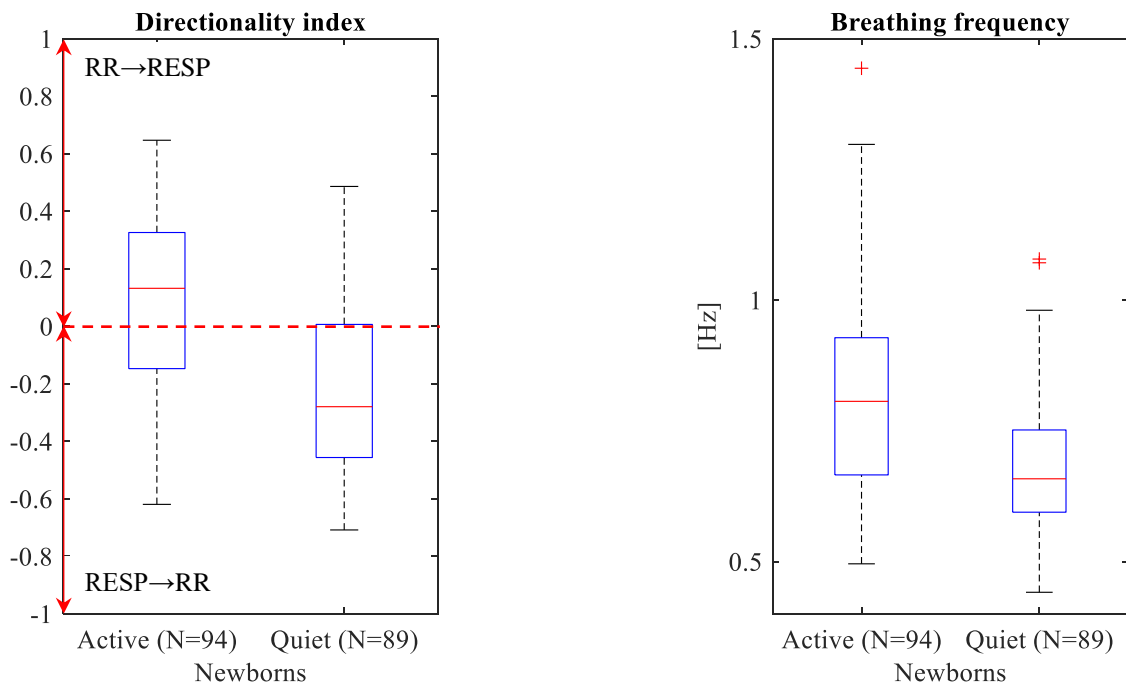


Figure 3.5.2 Boxplots of directionality index and breathing frequency in AS versus QS considering newborns

Figure 3.5.1 and Figure 3.5.2 show scatterplot and boxplots of stage-related analysis: slower breathing frequencies are associated with QS and faster breathing frequencies with AS.

At intermediate frequencies, such as the interval 0.6-0.8 Hz, an overlapping area is present where subjects with both AS and QS are found.

When breathing frequency and directionality index are tested for differences between sleep states, both measures are found statistically different. It is important to recall that a negative directionality index is an interacting condition in which respiration is driving HR (RESP→RR) while HR drives respiration (RR→RESP) when directionality index is positive.

Considering state-related analysis for one month infants, Figure 3.5.3 shows slower breathing frequencies associated with QS and faster breathing frequencies with AS. At intermediate frequencies, such as the interval 0.5-0.8 Hz, an overlapping area is present where subjects with both AS and QS are found, similarly to newborns scatter plot (Figure 3.5.1).

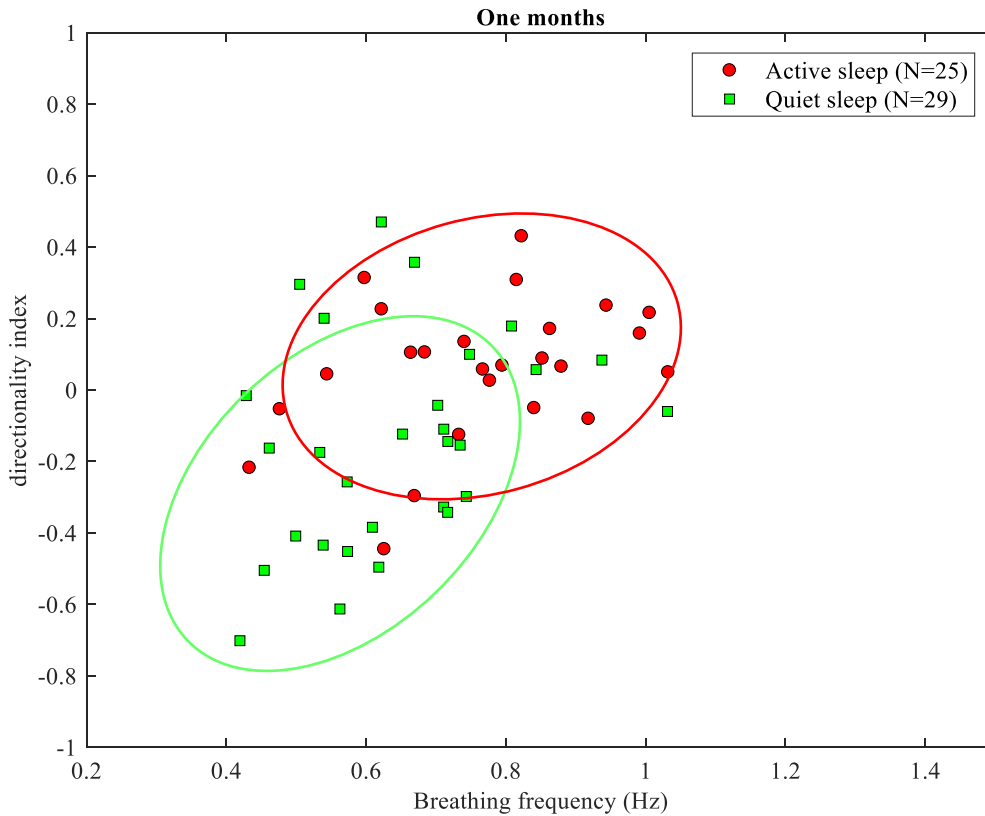


Figure 3.5.3 Scatter plot of breathing frequency and directionality index for one months

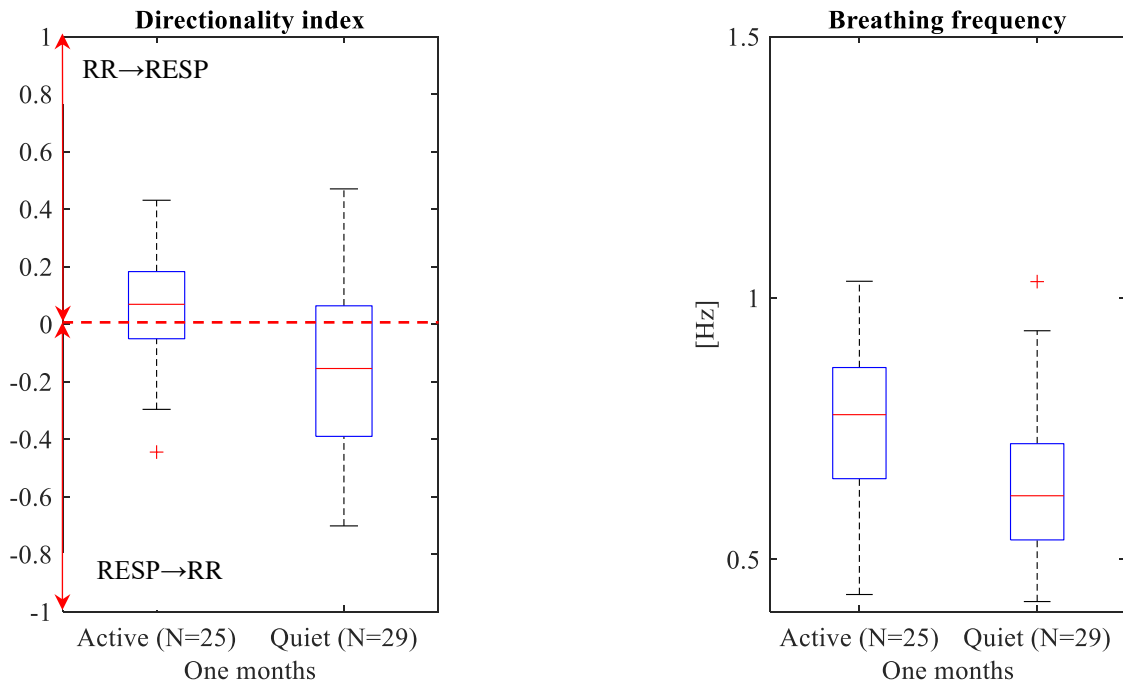


Figure 3.5.4 Boxplots of directionality index and breathing frequency in AS versus QS considering one months

Figure 3.5.4 depicts the breathing frequency and directionality index when one month infants are tested for differences between sleep states, both measurements are found statistically different.

Since directionality index sign is capable of discriminating the causal interactions between subsystems is important to highlight that directionality index mean is positive signed ($RR \rightarrow RESP$) and close to zero in AS while negative signed ($RESP \rightarrow RR$) in QS.

Regarding age-related analysis, no differences within same sleep state at different time points are found.

Considering both breathing frequency and directionality index for newborns and one month infants, neither of them turns out to be statistically different as reported in Table 3.5.2.

	Active sleep			Quiet sleep		
	Newborns	One months	<i>p-value</i>	Newborns	One months	<i>p-value</i>
Directionality index [s]	0.10 ± 0.30	0.06 ± 0.20	n.s.	-0.23 ± 0.30	-0.15 ± 0.29	n.s.
Breathing freq. [Hz]	0.82 ± 0.21	0.76 ± 0.16	n.s.	0.68 ± 0.14	0.64 ± 0.15	n.s.

Table 3.5.2 Extracted directionality index and breathing frequency computed. P-values are relative to statistics comparing same sleep state (AS or QS) parameters for the two different time points

Figure 3.5.5 and Figure 3.5.7 show scatter plots of age-related analysis. No clear differences between cohorts at different time points are present.

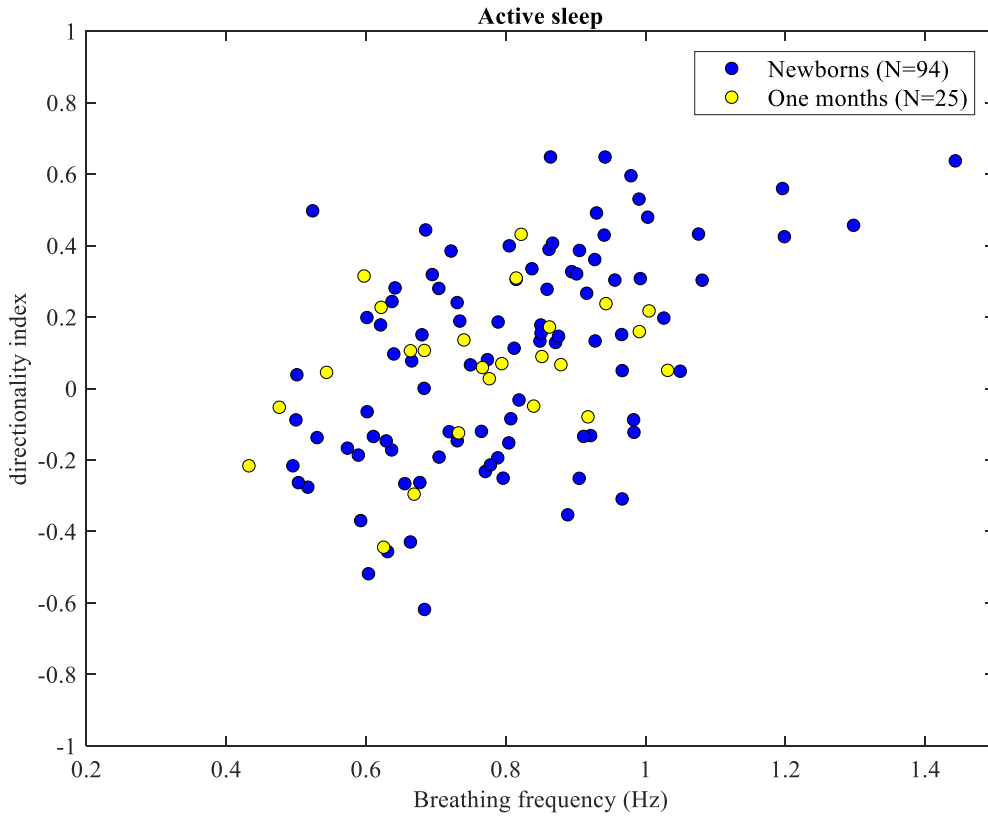


Figure 3.5.5 Scatter plot of breathing frequency and directionality index in AS for both newborns and one months

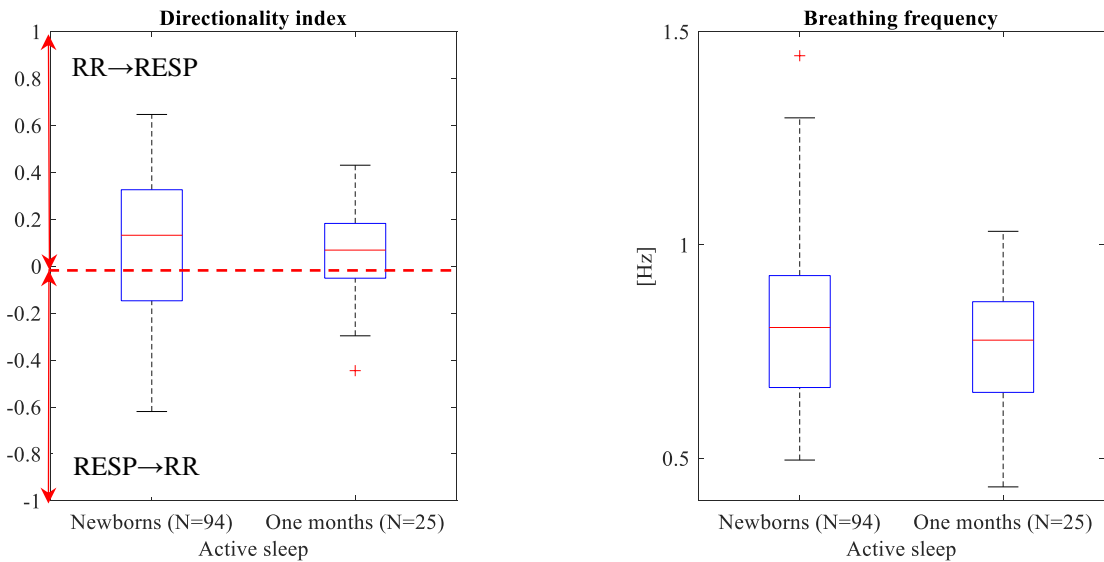


Figure 3.5.6 Boxplots of directionality index and breathing frequency comparing newborns versus one months in AS

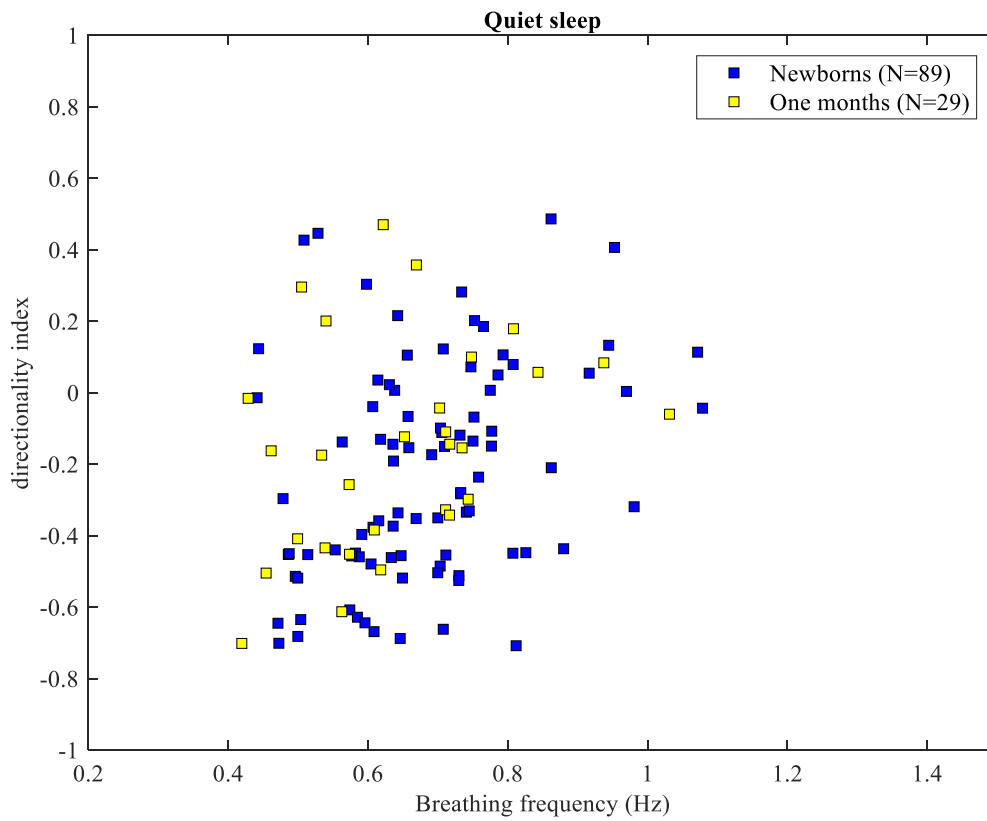


Figure 3.5.7 Scatter plot of breathing frequency and directionality index in QS for both newborns and one months

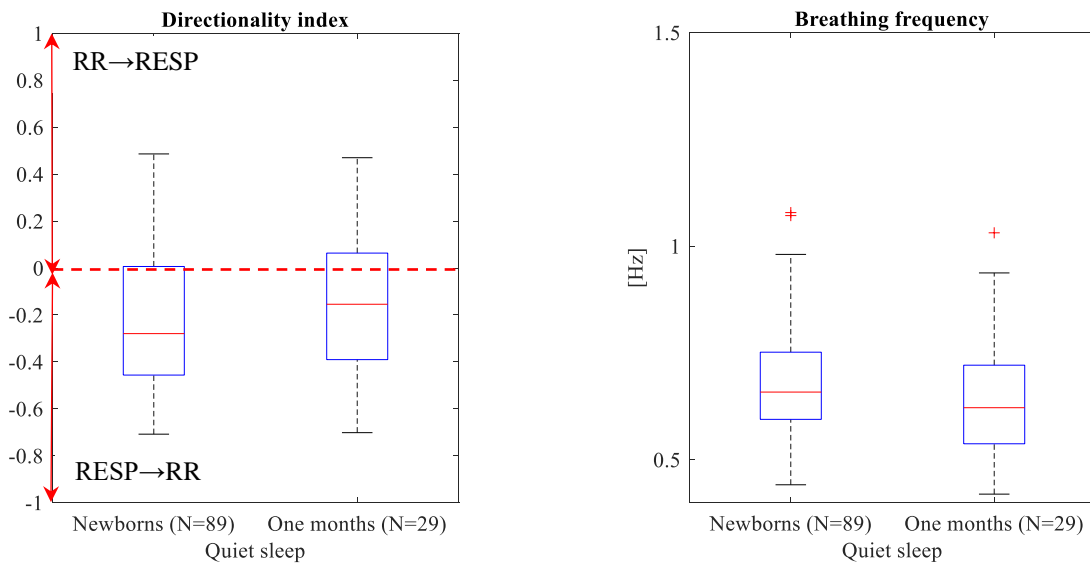


Figure 3.5.8 Boxplots of directionality index and breathing frequency comparing newborns versus one months in QS

As reported in the paper by Rosenblum et al. [65], it is possible to investigate directionality when the classification into groups is not performed based on sleep state but on breathing frequency. In this context, the breathing frequency threshold is set to 0.6 Hz.

As mentioned in Material and Method session, the assessment of directionality is based upon the directionality index sign, for this reason a negative and positive value refers to RESP→RR and RR→RESP direction respectively.

Table 3.5.3 shows the number of subjects (expresses as percentage) when newborns and one month infants are compared regardless the sleep stage and grouped based on directionality index sign.

In Table 3.5.4 directionality index and breathing frequency are shown when grouping is performed upon breathing frequency threshold of 0.6 Hz.

	Newborns		One months	
	RESP → RR	RR → RESP	RESP → RR	RR → RESP
Breathing freq. < 0.6	82.35%	17.65%	75.00%	25.00%
Breathing freq. ≥ 0.6	49.67%	50.33%	42.11%	57.89%

Table 3.5.3 Percentage indicating the portion of subjects associated with a negative directionality index and positive directionality index

	Newborns			One months		
	Breathing frequency < 0.6 Hz	Breathing frequency ≥ 0.6 Hz	<i>p-value</i>	Breathing frequency < 0.6 Hz	Breathing frequency ≥ 0.6 Hz	<i>p-value</i>
Directionality index [s]	-0.28 ± 0.34	0.00 ± 0.32	< 0.01	-0.20 ± 0.31	0.00 ± 0.24	< 0.01
Breathing freq. [Hz]	0.52 ± 0.04	0.81 ± 0.18	< 0.01	0.51 ± 0.06	0.78 ± 0.12	< 0.01

Table 3.5.4 Extracted breathing frequency and computed directionality index. P-values are relative to statistics comparing AS and QS parameters within the same age

Figure 3.5.9 shows the frequency distribution in terms of probability for directionality index. Considering breathing frequencies lower than the threshold of 0.6 Hz (blue), 82% of subjects exhibit a negative directionality index while the remaining 18% has positive values for directionality index. On the other hand, when breathing frequencies are equal or higher than the threshold (green), the population is distributed such as the 50% of subject has a negative value of the index while the remaining 50% has a positive value.

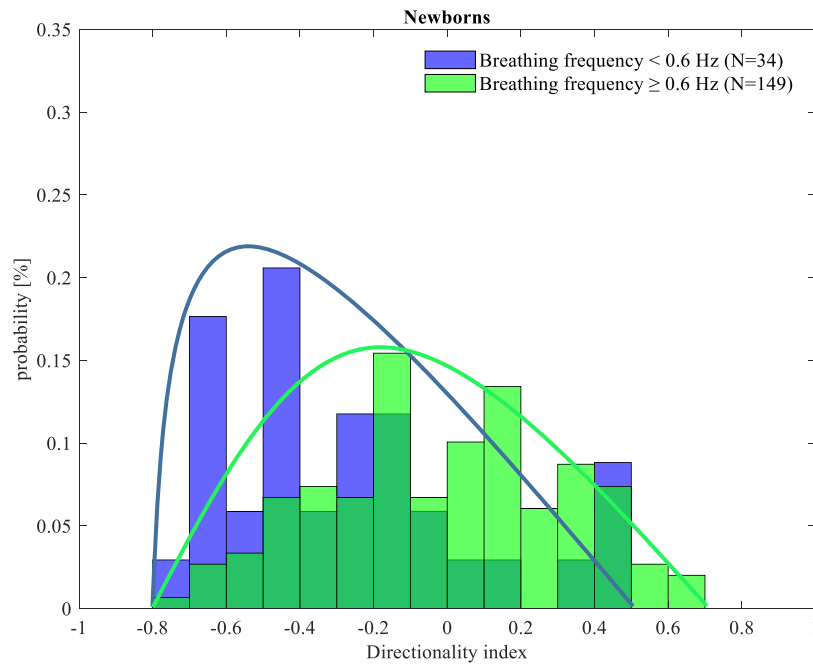


Figure 3.5.9 Histogram of newborn cohort grouped based on breathing frequency, darker green indicates bins where the distributions overlap

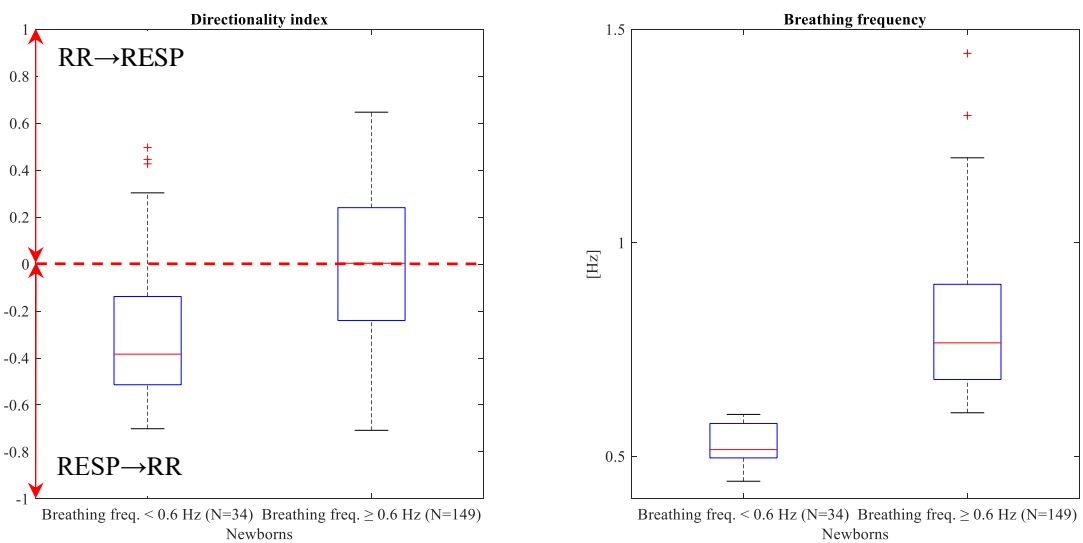


Figure 3.5.10 Boxplots of directionality index and breathing comparing newborns grouped based on breathing frequency

Figure 3.5.10 shows breathing frequency and directionality index comparison for state-related analysis, significant differences are found when comparing the two measurements in newborns for AS and QS.

Figure 3.5.11 shows the analogous histogram as Figure 3.5.9 when considering the one month cohort. Considering breathing frequencies lower than the threshold of 0.6 Hz (blue), 75% of subjects exhibit a negative directionality index while the remaining 25% has positive values for directionality index. On the other hand, when breathing frequencies are equal or higher than the threshold (green), the population is distributed such as the 42% of subject has a negative value of the index while the remaining 58% has a positive value.

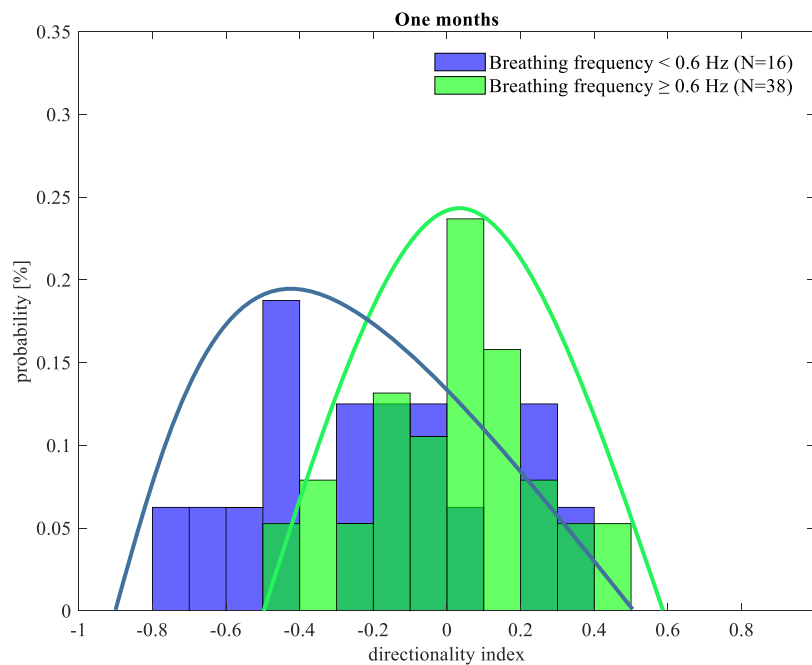


Figure 3.5.11 Histogram of one month cohort grouped based on breathing frequency, darker green area indicates bins where the distributions overlap

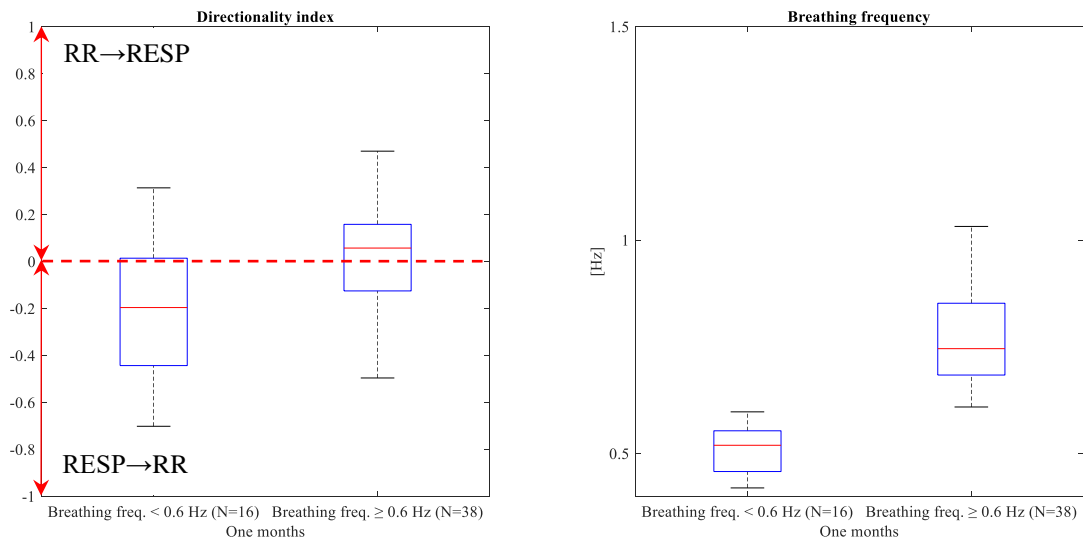


Figure 3.5.12 Boxplots of directionality index and breathing frequency comparing one months grouped based on breathing frequency

Figure 3.5.12 shows breathing frequency and directionality index comparison for state-related analysis, significant differences are found when comparing the two measurements for one month infants in AS and QS.

Table 3.5.5 shows the comparison of the two populations for both breathing frequency and directionality index. When these two quantities are tested at different time points no difference is found.

	Breathing frequency < 0.6 Hz			Breathing frequency ≥ 0.6 Hz		
	Newborns	One months	<i>p-value</i>	Newborns	One months	<i>p-value</i>
Directionality index [s]	-0.28 ± 0.34	-0.20 ± 0.31	n.s.	0.00 ± 0.32	0.00 ± 0.24	n.s.
Breathing freq. [Hz]	0.52 ± 0.04	0.51 ± 0.06	n.s.	0.81 ± 0.18	0.78 ± 0.12	n.s.

Table 3.5.5 Computed directionality index and extracted breathing frequency. P-values are relative to statistics comparing newborns and one months grouped based on breathing frequency threshold

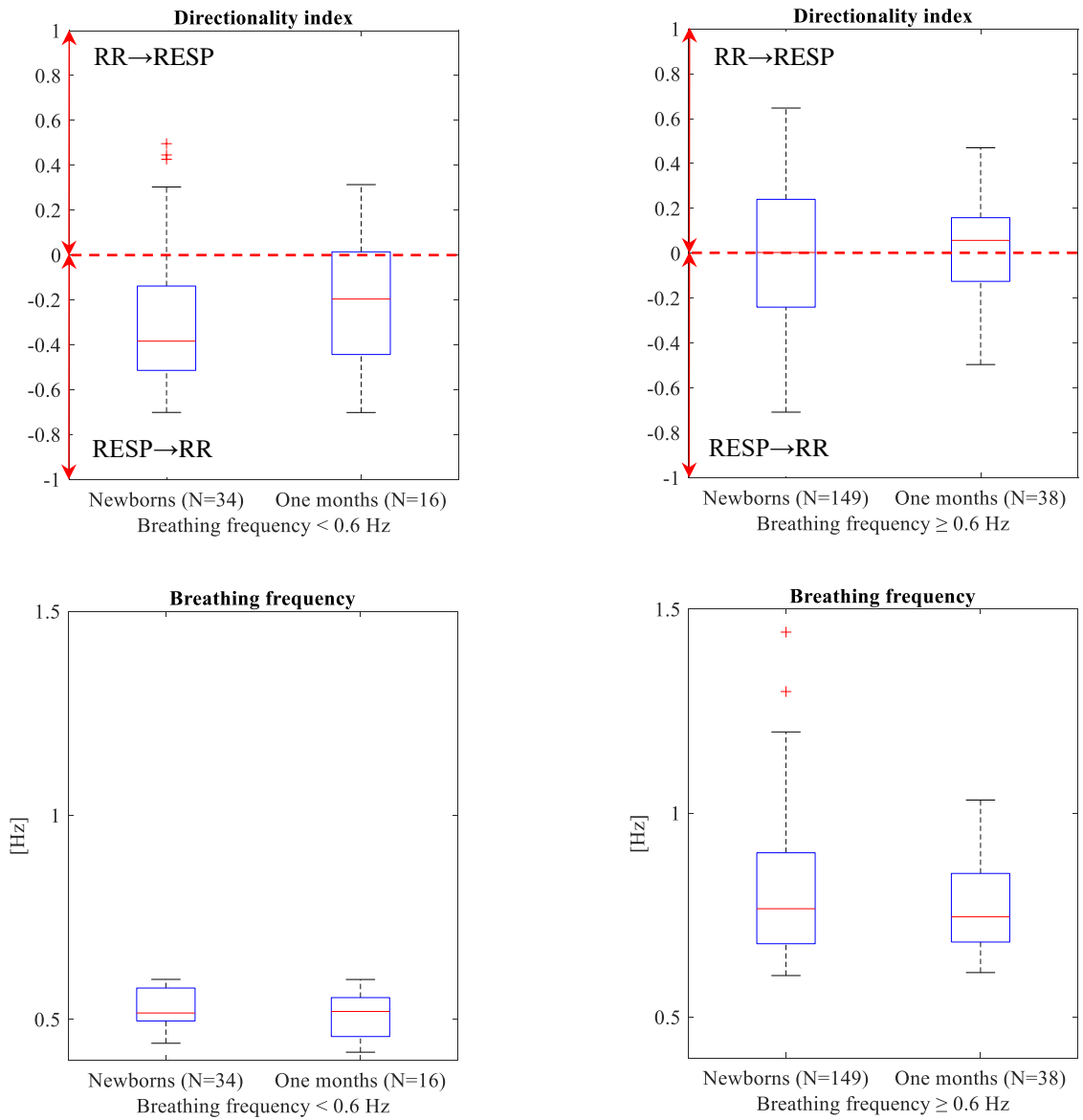


Figure 3.5.13 Boxplots of breathing and directionality index comparing newborns and one months at different time points

Chapter 4

In this chapter a discussion on the obtained results will be presented.

Computed parameters have shown abilities in discriminating Active Sleep versus Quiet Sleep and newborns versus one month infants.

Time domain and univariate entropy parameters, extracted from RR series and respiratory signal, confirmed results illustrated in literature about sleep states and evolution of Autonomic Nervous System with age.

Bivariate parameters showed a robust capability in discriminating sleep states based on information flow (Transfer Entropy), percentage and duration of synchronization (phase locking), directionality of interaction (Directionality Index) differences.

Afterwards, physiological interpretations of these results will be reported focusing on future applications of these method in SIDS investigation prospective.

Lastly, future developments and limitations of this work will be presented.

Discussions

4.1 Time and Frequency domain

The aim of the time domain analysis is to characterize RR series and respiratory signal depending on sleep states (AS versus QS) and age (newborns versus one month infants) by means of a univariate approach.

Despite the lack of a bivariate investigation of cardiorespiratory interaction, this preliminary analysis is capable of providing interesting insight on HR and respiratory dynamics.

In this work, time domain parameters relative to RR series are RR mean, RR IQR, SDNN and RMSSD. IBI mean and IBI IQR are computed analyzing the respiratory signal.

Time domain parameters from this data analysis indicate differences between AS and QS, with an increase of RR mean in QS with respect to AS in newborns only, and a decrease of HRV in both newborns and one month infants cohorts.

This is the normal expected behavior given that 1 month of age represents a transition between birth and later months, when the HR will settle on lower values and HRV increases, due to development of vagal regulation if subjects are in normal conditions [70].

Considering the comparison between sleep states, time domain parameters indicate an increase in overall variability in AS and QS (SDNN), while no difference was found in beat-to-beat variability (RMSSD) at birth and a slightly significant result at one month of age.

It is known from literature that the sympathetic system is the first to develop during pregnancy, while the parasympathetic system develops later and continues to adapt even during the first months of life [71]. The parasympathetic branch of the ANS is responsible of the HR decrease; its faster response is manifested in a more rapid, beat-to-beat control of the HR and this has emerged in the short-term variability parameters. The absence of significant differences in short term variability between sleep states in newborns can be a possible explanation for this parasympathetic immaturity.

To better identify the sources responsible for these changes in variability, power spectral estimation was performed and showed that RR variance distributes differently in High Frequency (HF), 0.35-1.5 Hz and Low Frequency (LF), 0.04-0.2 Hz depending on sleep states. HF is the major contribution in QS.

These results combined with time domain parameters suggest an increased parasympathetic activation in QS regardless of the age [51].

The mean distance between inspiratory onsets (IBI mean) and respiration variability (IBI IQR) show an increase and a decrease respectively when comparing AS versus QS for newborns and one month infants. These results are coherent with a slower respiratory rate and a lower variability associated to QS, as in this latter state the respiration is reported to be more regular with respect to AS.

Concluding, almost all the time domain parameters have proved their ability to find significant differences between sleep states.

Regarding the comparison between newborns and one month infants within the same sleep state, only time domain parameters computed on RR series show significant differences while parameters extracted from respiratory signal show a non-significant decreasing trend with age.

RR mean decreases from birth to one month of age in both active and quiet sleep.

This counterintuitive behavior has been reported by some studies highlighting the HR increase from birth to one month and then progressively decrease, with a stabilization at six months of age. HRV, SDNN and RMSSD decrease when comparing newborns and one month infants within the same sleep state [70].

Parameters computed from respiration do not show any change when comparing populations at different time points. This behavior shows the slower maturation and adaptation of respiratory system in term of development of both physical structures and control mechanisms.

4.2 Sample Entropy and Quadratic Sample Entropy

The univariate entropy has been computed on RR series by means of Sample Entropy (SampEn) and Quadratic Sample Entropy (QSE), in order to extrapolate information regarding complexity of the HR signal.

As described in literature, entropy is a measure of complexity that might help to highlight differences between populations such as healthy versus pathological subjects [36], [72].

As reported in Materials and Methods session, 300-beat segments are considered in order to achieve a reliable estimation, not affected by the segment length.

The use of these methods allows to explore HRV signals on a beat-to-beat scale, being the templates employed by SampEn and QSE related to embedding dimensions $m=1, 2, 3$.

Regulations occurring at this scale can be linked with vagus nerve activity, which change HR substantially within one cardiac cycle.

As a general consideration time domain parameters show a higher variability in AS rather than QS, on the other hand the complexity registered by SampEn and QSE is higher in QS. An entropy increase in QS with respect to AS has been found for both SampEn and QSE despite the embedding dimension, confirming the predominance of parasympathetic control in QS [51].

As a matter of fact, even previous studies have proposed that a simplification of HR dynamics and thus a lowering in entropy values, might follow a parasympathetic withdrawal and sympathetic activation [33].

These results also agree with previous results by Pincus et al. [36], who found higher values of approximated entropy (ApEn) in QS with respect to AS, and with another measure of complexity based on Mutual Information, AIF [73].

Regarding the age evolution of both entropy estimators no differences are found when comparing newborns and one month infants. This result is mainly attributed to the univariate investigation performed by measurements based on HR only.

Time domain parameters such as RR mean and RR IQR are successful in detecting HR changes based on mean and standard deviation but it is important to stress that this evolution does not necessarily imply changes in term of complexity.

From a methodological point of view, entropy measures tend to be influenced by the choice of the values for parameters r , m , N , as previously reported [35], [36].

In this work, the consistency of entropy measures can be observed, independently from the parameter choice. As a matter of fact, parameter m did not influence the results.

It is important to highlight that same analysis have been performed considering segments of length equal 100 beats and 200 beats. Obtained results are comparable with what reported for 300-beat length segments, this results shows the consistence of entropy estimation and their reliability in detecting complexity in presence of short records.

4.3 Transfer Entropy

Transfer entropy is a bivariate entropy estimator, which can be employed to assess the information flow between two time series. In this work the considered signals are the HR and respiratory signal. TE is a measure of predictability and complexity. In this analysis when considering the direction $1 \rightarrow 2$, TE quantifies the improvement in predicting the future of signal 2 when the prediction takes into consideration not only the past of signal 2 but also information from the past of signal [49].

It is possible to investigate differences in term of TE when AS and QS are compared within the same direction of information flow. Considering newborn population, an increase in TE from AS to QS can be seen both in $RR \rightarrow RESP$ and $RESP \rightarrow RR$ direction. The increase is more pronounced in QS than AS: QS can be seen as condition in which the cardiorespiratory coupling is more evident and the influence of RR over respiration and vice versa is noticeable. These findings suggest that cardio-respiratory interactions in QS transfer more information than in AS in healthy infants, as confirmed by Frasch et al [73].

Moreover, the main direction of the information flow when considering $RR \rightarrow RESP$ and $RESP \rightarrow RR$ within the same sleep state is from respiration to HR in QS, while in AS this not clearly recognizable.

Given that breathing in QS is slower and more regular, it potentially allows a more stable effect/relationship with HR.

The linear contribution of this relationship could be described in term of Respiratory Sinus Arrhythmia (RSA) phenomenon, that is the modulation of HR occurring during a breathing cycle. Giving the fact that respiration modulates HR, the past of respiratory signal is very informative in predicting the evolution of RR series because the effects of RSA modulation are seen on HR at a slightly delayed time scale. RSA is capable of explaining the linear aspect of this interaction only, it is important to underline that TE accounts for both linear and nonlinear interactions.

The analysis performed on one month cohort shows analogous results of the ones obtained considering newborns.

An age dependent evolution in terms of information flow happens only in QS for both RR→RESP and RESP→RR directions. AS is per se a state of lower coupling between HR and respiration and changes in TE are not dramatically affected by age. A bivariate and bidirectional approach to investigate entropy is capable of explaining age dependent evolutions those are instead more difficult to be extracted when a univariate entropy analysis is performed, such as the results obtained with SampEn and QSE.

TE analysis has provided an interesting insight in term of quantification of interaction and directionality but some questions are still in need to be addressed.

One limitation of this study is that the complexity of HR and respiration interaction operates on different time scales, which are not set a priori.

Thus, different rates of information production and exchange between length scales might affect the rate of information transfer, and consequently the values of TE obtained.

This issue can be addressed with further analysis, including TE estimation on signals with delays.

TE method of estimating entropy does not make any assumption about the interactions between subsystem, it would be interesting to separate linear and nonlinear contributions to pinpoint the prevalent working regime between the cardiac and respiratory systems.

4.4 Phase synchronization

Phase synchronization analysis allows quantifying the cardiorespiratory interaction between the cardiac and respiratory systems by means of oscillators' phase analysis.

The comparison can be performed considering AS versus QS within the newborn cohort. A significant increase in synchronization in QS is noticeable and in agreement with previous studies, which established that sleep state is a relevant aspect for cardio-respiratory synchronization, which occurs more frequently in QS. The above-mentioned increase is in term of both percentage of synchronization and duration of synchronization, considering a single breathing cycle or two breathing cycles.

It is important to highlight that the increase in synchronization is minor when two breathing cycles are considered, this is probably related to a more long term synchronization, a condition that is more difficult to be fulfilled over multiple breaths [69].

When one month population is analyzed, comparable trend of increase in synchronization are found. It is important to underline that in this case, the increase in synchronization is greater when comparing AS versus QS. It is possible to state that a more evident separation of the two sleep states in term of phase coupling is recognizable.

When age related analysis is performed, differences are found when considering the percentage of synchronization, whereas no differences are found in term of duration of synchronization. Focusing on synchronization occurrence, increasing trends are found in QS for both a single and two breathing cycles at different time points. This result is coherent with what previously found in time domain parameters and TE, reporting an evolution with age in QS only.

Given the result that one month infants percentage of synchronization is increasing in QS while the duration stays stable with respect to newborns, it is possible to assess that QS at one month is characterized by an increased number of coupling epochs with respect to QS in newborns. This conclusion is confirmed by the work of many authors reporting an increase in synchronization with age and a prevalence in synchronization in QS dependent on age [63].

The synchronization analysis on subjects with at least one AS segment and one QS segment during the 10-minute baseline shows a consistent trend of synchronization increase in QS for both newborns and one months despite the number of breathing cycles.

The slope of the synchronization increase from AS to QS appears to be independent from the percentage of synchronization in AS. This result may indicate that the increase in synchronization related to sleep state is an intrinsic property of the cardiorespiratory system and its investigation on a larger scale is needed in order to correlate its absence to SIDS risk.

The results obtain in this work regarding phase synchronization do present coupling as the sum of various ratios of n:m heartbeats and breathing cycles. A further analysis investigates the changes in synchronization when specific ratios are considered. It is important to stress that the mean HR increases from birth to one month of age as reported in time domain analysis [70]. This counter intuitive behavior is also shown by phase synchronization analysis where the occurrence of 3:1 ratio is more recurrent than 4:1 for newborns and vice versa for one month infants, despite the sleep state.

Thus, it is of particular interest to note a shift in the typical cardiorespiratory synchronization ratio when passing from a low risk period (birth) to a high risk one (2-4 months of age).

4.5 Directionality Index

Directionality index (DI) analysis performs a quantification of the causal directionality between HR and respiration similarly to Transfer Entropy.

This estimator is capable of assessing directionality by means of the phase analysis of the two considered signal, differently from TE that estimates probability in term of joint distribution of HR and respiration.

The analysis of DI and breathing frequency performed on newborns, comparing AS versus QS, shows slower breathing frequencies associated with QS and higher breathing frequencies with AS. QS is also characterized by a prevalence of RESP→RR directionality while AS exhibit no clear directionality of interaction. These results are similar with what found for TE: respiration is the main driver in QS.

On the other hand, the higher breathing frequencies associated with AS are no more capable of modulating the heart rate and the directionality shifts on the opposite direction (RR→RESP) or, to an absence of interaction [69].

The analogous analysis has been performed on one month infants. In this case, results are similar with what found for newborns.

In this work, differences between AS and QS in term of directionality have been found for both newborns and one month infants. This result is in contrast with other authors reporting the absence of significant differences between sleep states within the same age. The difference found when comparing AS versus QS is in agreement with results obtain in this work about TE and phase synchronization analysis. The hypothesis of two working regime in AS and QS can be seen in terms of both synchronization and directionality as hypothesizes by many authors [23], [74].

Age-related analysis shows no clear evolution in term of directionality of interaction when newborns and one months are compared within the same sleep state at different time points.

Despite the lack of significance it is possible to observe a slightly decrease of DI in AS, this trend is consistent with what found in [64] highlighting a decrease of DI with age, from birth up to six month of age when the directionality is reported to settle to a univocal direction: RESP→RR in both AS and QS.

The analysis of DI based on breathing frequency only, regardless sleep state, provides a confirmation of results by Rosenblum et al. [65], stating that respiratory frequencies of < 0.6 Hz are associated with a unidirectional interaction from RESP→RR.

On the contrary, respiratory frequencies ≥ 0.6 Hz exhibit the absence of a dominating directionality and interaction becomes nearly symmetrical. The mechanism for the latter condition may be explained by the low-pass behavior of the vagal-atrial transmission dynamics.

The dynamics include the release of acetylcholine from the nerve endings, its diffusion across the synaptic cleft, the action on sinoatrial pacemaker cells, the dynamics of

signal transduction in the pacemaker cells, and the degradation and reuptake processes of acetylcholine. Within these hypothesis, at physiological conditions, at higher breathing rates, the unidirectional working regime is abolished [64], [65].

These results are consistent in both newborns and one month infants populations, without changes related to age.

4.6 Conclusions

This work analyses has been performed on two databases composed of 151 newborns and 33 one month infants.

ECG and respiratory signals have been investigated by means of linear and nonlinear methods.

Time domain parameters constitutes a solid and established gold standard approach capable of highlighting sleep state and age differences when the two populations are compared. Despite a good discrimination capability, time domain parameters benefit from the integration with nonlinear parameters such as SampEn, QSE, TE, phase locking and DI to better describe the interrelationship between the cardiorespiratory circuit.

These newer descriptors are capable of addressing nonlinear phenomena of interaction that could lead to a better understanding of the controlling mechanism and a clear quantification of interaction.

It is crucial to fully characterize the physiological cardiorespiratory behavior with a joint linear and nonlinear analysis, in order to investigate its changes in pathological conditions.

Within this effort in characterizing the cardiorespiratory interrelationship, TE investigation performed in this work may be useful in revealing the causal relationship between subsystems.

The cardiorespiratory system of both newborns and one months may be modeled as closed-loop scheme with two different working regimes. In AS the HR and respiration are slightly perturbing each other so that a clear directionality cannot be seen, this result is coherent with the hypothesis of cardiac and respiration systems as two weakly coupled oscillators.

In QS instead, respiration becomes the main driver and its influence is clearly seen in the closed loop between HR and respiration. In this case, RSA can account for the linear contribution of this interaction, on the other hand cardiorespiratory synchronization takes into account the nonlinear oscillators' phase relationship.

If phase locking condition takes place, the interaction is transient and related to oscillators' phase, this behavior is in agreement with chaos theory regarding the weakly interacting systems.

Some of the most recent theories about SIDS started attributing the lack of cardiorespiratory control as the main driver of SIDS risk. In particular, the work by Bergman [23] addresses the interesting question about the role of supine sleep in preventing SIDS.

It has been reported by epidemiological investigation, as stated in the Introduction of this work, that the Back to Sleep campaign dramatically reduced the SIDS occurrence, indicating the supine position reduces SIDS risk with respect to prone sleep position.

As reported by many authors [1], [31] supine sleep is characterized by an increased occurrence of AS epochs, a reduced occurrence of QS, more frequent arousal, and more fragmented sleep. On the other hand, prone position reduces the occurrence of arousal, and it is characterized by more regular and pacified breathing patterns.

In light of these issues, many authors started to investigate the physiological determinants those make supine position capable to reduce SIDS occurrence.

It has been hypothesized that AS and QS are two conditions those differs in term of cardiorespiratory synchronization and the continuous alternation between lower and higher coupling condition is capable of stressing the ANS, making it more ready to face several challenges.

It has been also reported that the state change from AS to QS increases the occurrence of sighs and gaps, two mechanisms those are crucial in order to overcome cardiorespiratory challenges and the main drivers of the autoresuscitation mechanism [69].

The results obtained in this work could be interpreted with this hypothesis of ANS being the stressor of itself.

In this study, the healthy and full-term subjects analyzed were lying supine and their sleep was characterized by both AS and QS with a prevalence of AS for newborns.

AS and QS have been defined as two different sleep states with different characteristics in term of synchronization and also directionality. The alternation between these two sleep states constitutes a constant stressing condition that is probably capable of stimulating the ANS development.

Regarding the sleep state analysis, this work has highlighted QS as a state characterized by a clear preferential directionality of information flow and a net increase in synchronization with respect to AS. On the contrary, AS is defined as a state of low coupling between the cardiac and the respiratory system, differences between subjects are minor and often to be attributed to the quality of the signals.

These peculiar findings suggest to focus on QS rather than AS when analyzing cardiorespiratory coupling in infants. It should be emphasized that along with the analysis of QS, the sleep state patterns need to be investigated, in order to achieve a complete description of the cardiorespiratory interrelationship.

4.7 Further developments and future work

Despite the interesting results many questions are still to be addressed.

In order to deeper investigate the ANS evolution in term of both synchronization and directionality more time points are needed, the ideal situation would be tracking the ANS development from birth to one year of age to fully characterize the physiological behavior.

Once the quantification of interaction is established, an investigation on early and late preterm infants could help investigating the difference in term of ANS development on subjects born preterm.

The analysis on SIDS patients could highlight differences in coupling and synchronization and its quantification could open novel view about newborn state monitoring and care path by means of a noninvasive and reliable investigations.

An appealing prospective for future work is the analysis of the massive PASS database (available at CUMC), that comprises approximately 12,000 pregnant women from the United States and South Africa. It includes recordings of maternal, fetal, and neonatal signals, investigating pregnant women conditions' and following the development of their babies through pregnancy and the infants' first year of life. It is important to highlight that some infants included in the database died of SIDS.

The mission of the PASS Network is to perform community-linked studies to investigate the role of prenatal alcohol exposure in the risk for Sudden Infant Death Syndrome (SIDS) and adverse pregnancy outcomes, such as Stillbirth and Fetal Alcohol Spectrum Disorders (FASD).

A data-mining approach is required in order to discover hidden patterns in a such large dataset, involving methods of artificial intelligence and machine learning. It would be interesting to investigate which parameters and indexes are more capable of discriminating between healthy subjects and SIDS victims and the contribution of cardiorespiratory coupling in describing these differences.

Bibliography

- [1] M. M. Myers *et al.*, “Effects of sleeping position and time after feeding on the organization of sleep/wake states in prematurely born infants,” *Sleep*, vol. 21, no. 4, pp. 343–349, Jun. 1998.
- [2] W. G. Guntheroth and P. S. Spiers, “The Triple Risk Hypotheses in Sudden Infant Death Syndrome,” *Pediatrics*, vol. 110, no. 5, pp. e64–e64, 2002.
- [3] J. J. Filiano and H. C. Kinney, “A perspective on neuropathologic findings in victims of the sudden infant death syndrome: the triple-risk model,” *Neonatology*, vol. 65, no. 3–4, pp. 194–197, 1994.
- [4] P. N. Goldwater, “A perspective on SIDS pathogenesis. the hypotheses: plausibility and evidence.,” *BMC Med.*, vol. 9, no. 1, p. 64, 2011.
- [5] F. L. Trachtenberg, E. A. Haas, H. C. Kinney, C. Stanley, and H. F. Krous, “Risk Factor Changes for Sudden Infant Death Syndrome After Initiation of Back-to-Sleep Campaign,” *Pediatrics*, vol. 129, no. 4, pp. 630–638, 2012.
- [6] C. E. Leach *et al.*, “Epidemiology of SIDS and explained sudden infant deaths,” *Pediatrics*, vol. 104, no. 4, p. e43, 1999.
- [7] J. a Martin, M. J. K. Osterman, and P. D. Sutton, “Are preterm births on the decline in the United States? Recent data from the National Vital Statistics System.,” *NCHS Data Brief*, no. 39, pp. 1–8, 2010.
- [8] M. J. Davidoff *et al.*, “Changes in the gestational age distribution among U.S. singleton births: Impact on rates of late preterm birth, 1992 to 2002,” *Semin. Perinatol.*, vol. 30, no. 1, pp. 8–15, 2006.
- [9] K. Fyfe, S. R., and R. S.C., “Cardiovascular Consequences of Preterm Birth in the First Year of Life,” *Preterm Birth - Mother Child*, no. March 2017, 2012.

- [10] A. Kahn *et al.*, “Sudden infant deaths: Stress, arousal and SIDS,” *Pathophysiology*, vol. 10, no. 3–4, pp. 241–252, 2004.
- [11] M. Patel *et al.*, “Clinical associations with immature breathing in preterm infants: part 2-periodic breathing,” *Pediatr. Res.*, vol. 80, no. 1, pp. 28–34, 2016.
- [12] K. Fairchild *et al.*, “Clinical associations with immature breathing in preterm infants: part 1-central apnea,” *Pediatr. Res.*, pp. 1–7, 2015.
- [13] M. Willinger *et al.*, “Factors associated with the transition to nonprone sleep positions of infants in the United States: the National Infant Sleep Position Study,” *JAMA*, vol. 280, no. 4, pp. 329–335, 2015.
- [14] R. Y. Bhat, S. Hannam, R. Pressler, G. F. Rafferty, J. L. Peacock, and A. Greenough, “Effect of prone and supine position on sleep, apneas, and arousal in preterm infants,” *Pediatr. Res.*, vol. 118, no. 1, pp. 101–107, 2006.
- [15] R. Tuladhar, R. Harding, S. M. Cranage, T. M. Adamson, and R. S. C. Horne, “Effects of sleep position, sleep state and age on heart rate responses following provoked arousal in term infants,” *Early Hum. Dev.*, vol. 71, no. 2, pp. 157–169, 2003.
- [16] R. S. C. Horne, “Cardio-respiratory control during sleep in infancy,” *Paediatr. Respir. Rev.*, vol. 15, no. 2, pp. 163–169, 2014.
- [17] D. C. Galletly and P. D. Larsen, “The determination of cardioventilatory coupling from heart rate and ventilatory time series,” *Res. Exp. Med.*, vol. 199, no. 2, pp. 95–99, 1999.
- [18] G. E. Billman, “Heart rate variability - A historical perspective,” *Front. Physiol.*, vol. 2 NOV, 2011.
- [19] P. I. Terrill, S. J. Wilson, S. Suresh, and D. M. Cooper, “Characterising infant inter-breath interval patterns during active and quiet sleep using recurrence plot analysis,” *Proc. 31st Annu. Int. Conf. IEEE Eng. Med. Biol. Soc. Eng. Futur. Biomed. EMBC 2009*, pp. 6284–6287, 2009.

- [20] G. G. Haddad, H. J. Jeng, T. L. Lai, and R. B. Mellins, "Determination of sleep state in infants using respiratory variability.," *Pediatr. Res.*, vol. 21, no. 6, pp. 556–562, 1987.
- [21] L. J. Dierker, S. K. Pillay, Y. Sorokin, and M. G. Rosen, "Active and quiet periods in the preterm and term fetus.," *Obstet. Gynecol.*, vol. 60, no. 1, pp. 65–70, Jul. 1982.
- [22] T. E. Dick *et al.*, "Cardiorespiratory coupling: Common rhythms in cardiac, sympathetic, and respiratory activities," *Prog. Brain Res.*, vol. 209, pp. 191–205, 2014.
- [23] N. J. Bergman, "Proposal for mechanisms of protection of supine sleep against sudden infant death syndrome: an integrated mechanism review," 2014.
- [24] R. Haidmayer, K. P. Pfeiffer, T. Kenner, and R. Kurz, "Statistical Evaluation of Respiratory Control in Infants to Assess Possible Risk for the Sudden Infant Death Syndrome (SIDS)*," *Eur. J. Eur J Pediatr*, vol. 138, pp. 145–150, 1982.
- [25] J. Alfredo Garcia III, J. E. Koschnitzky, and J.-M. Ramirez, "The physiological determinants of Sudden Infant Death Syndrome," *Respir. Physiol. Neurobiol.*, vol. 189, pp. 288–300, 2013.
- [26] A. Fenner, U. Schalk, H. Hoenicke, A. Wendenburg, and T. Roehling, "Periodic breathing in premature and neonatal babies: incidence, breathing pattern, respiratory gas tensions, response to changes in the composition of ambient air.," *Pediatr. Res.*, vol. 7, no. 4, pp. 174–83, 1973.
- [27] P. Franco *et al.*, "Autonomic responses to sighs in healthy infants and in victims of sudden infant death.," *Sleep Med.*, vol. 4, pp. 569–577, 2003.
- [28] R. P. Bartsch, A. Y. Schumann, J. W. Kantelhardt, T. Penzel, and P. C. Ivanov, "Phase transitions in physiologic coupling," *Proc. Natl. Acad. Sci.*, vol. 109, no. 26, pp. 10181–10186, 2012.
- [29] M. Riedl, A. Mu, J. F. Kraemer, T. Penzel, J. Kurths, and N. Wessel, "Cardio-

- Respiratory Coordination Increases during Sleep Apnea,” *PLoS One*, vol. 9, no. 4, 2014.
- [30] R. M. Harper, H. C. Kinney, P. J. Fleming, and B. T. Thach, “Sleep influences on homeostatic functions: Implications for sudden infant death syndrome,” *Respir. Physiol.*, vol. 119, no. 2–3, pp. 123–132, 2000.
- [31] M. Progress, H. C. Kinney, B. T. Thach, and S. Africa, “The Sudden Infant Death Syndrome,” *Africa (Lond.)*, pp. 795–805, 2009.
- [32] M. Stefanski *et al.*, “A scoring system for states of sleep and wakefulness in term and preterm infants.,” *Pediatr. Res.*, vol. 18, no. 1, pp. 58–62, Jan. 1984.
- [33] M. Malik, “Heart Rate Variability: Standards of Measurement, physiological interpretations and clinical use,” *Circulation*, vol. 93, pp. 1043–1065, 1996.
- [34] A. Voss, S. Schulz, R. Schroeder, M. Baumert, and P. Caminal, “Methods derived from nonlinear dynamics for analysing heart rate variability.,” *Philos. Trans. A. Math. Phys. Eng. Sci.*, vol. 367, no. 1887, pp. 277–96, 2009.
- [35] S. Pincus and A. Goldberger, “Physiological time-series analysis: What does regularity quantify?,” *Am. J. Physiol.*, vol. 266, no. 4 Pt 2, pp. H1643–H1656, 1994.
- [36] S. Pincus, “Approximate entropy (ApEn) as a complexity measure.,” *Chaos*, vol. 5, no. 1, pp. 110–117, Mar. 1995.
- [37] J. S. Richman *et al.*, “Physiological time-series analysis using approximate entropy and sample entropy methods patterns Physiological time-series analysis using approximate entropy and sample entropy,” *Am J Physiol Hear. Circ Physiol*, pp. 2039–2049, 2000.
- [38] D. E. Lake and J. R. Moorman, “Accurate estimation of entropy in very short physiological time series: the problem of atrial fibrillation detection in implanted ventricular devices.,” *Am. J. Physiol. Heart Circ. Physiol.*, vol. 300, no. 1, pp. H319–H325, 2011.

- [39] D. E. Lake, "Renyi entropy measures of heart rate Gaussianity," *IEEE Trans. Biomed. Eng.*, vol. 53, no. 1, pp. 21–27, 2006.
- [40] T. Schreiber, "Measuring information transfer," *Phys. Rev. Lett.*, vol. 85, no. 2, pp. 461–464, 2000.
- [41] L. Faes, G. Nollo, and A. Porta, "Information domain approach to the investigation of cardio-vascular, cardio-pulmonary, and vasculo-pulmonary causal couplings," *Front. Physiol.*, vol. 2 NOV, 2011.
- [42] S. Nemati, B. A. Edwards, J. Lee, B. Pittman-Polletta, J. P. Butler, and A. Malhotra, "Respiration and heart rate complexity: Effects of age and gender assessed by band-limited transfer entropy," *Respir. Physiol. Neurobiol.*, vol. 189, no. 1, pp. 159–163, 2013.
- [43] R. Vicente, M. Wibral, M. Lindner, and G. Pipa, "Transfer entropy—a model-free measure of effective connectivity for the neurosciences," *J. Comput. Neurosci.*, vol. 30, no. 1, pp. 45–67, 2011.
- [44] J. Lee, S. Nemati, I. Silva, B. A. Edwards, J. P. Butler, and A. Malhotra, "Transfer Entropy Estimation and Directional Coupling Change Detection in Biomedical Time Series," *Biomed. Eng. Online*, vol. 11, p. 19, 2012.
- [45] I. Vlachos and D. Kugiumtzis, "Nonuniform state-space reconstruction and coupling detection," *Phys. Rev. E - Stat. Nonlinear, Soft Matter Phys.*, vol. 82, no. 1, 2010.
- [46] V. C. V. Raykar, "Probability density function estimation by different methods," *Enee 739Q Spring*, vol. 94, pp. 23–24, 2002.
- [47] K. Hlaváčková-Schindler, M. Paluš, M. Vejmelka, and J. Bhattacharya, "Causality detection based on information-theoretic approaches in time series analysis," *Phys. Rep.*, vol. 441, no. 1, pp. 1–46, 2007.
- [48] A. Kraskov, H. Stögbauer, and P. Grassberger, "Estimating mutual information," *Phys. Rev. E - Stat. Nonlinear, Soft Matter Phys.*, vol. 69, no. 6 2, 2004.

- [49] A. Montalto, L. Faes, and D. Marinazzo, “MuTE: A MATLAB toolbox to compare established and novel estimators of the multivariate transfer entropy,” *PLoS One*, vol. 9, no. 10, 2014.
- [50] T. M. Cover and P. E. Hart, “Nearest Neighbor Pattern Classification,” *IEEE Trans. Inf. Theory*, vol. 13, no. 1, pp. 21–27, 1967.
- [51] M. Lucchini, N. Pini, W. P. Fifer, N. Burtchen, and M. G. Signorini, “Entropy information of cardiorespiratory dynamics in neonates during sleep,” *Submitt. to Entropy*, 2017.
- [52] S. Schulz *et al.*, “Cardiovascular and cardiorespiratory coupling analyses: a review.,” *Philos. Trans. A. Math. Phys. Eng. Sci.*, vol. 371, p. 20120191, 2013.
- [53] T. E. Dick *et al.*, “Cardiorespiratory Coupling: Common Rhythms in Cardiac, Sympathetic, and Respiratory Activities,” *Prog Brain Res*, vol. 209, pp. 191–205, 2014.
- [54] A. Angelone and N. A. J. Coulter, “Respiratory Sinus Arrhythmia: a Frequency Dependent Phenomenon.,” *J. Appl. Physiol.*, vol. 19, no. 3, pp. 479–482, 1964.
- [55] A. Pikovsky, M. Rosenblum, and U. Kurths, “Phase Synchronization in Regular and Chaotic Systems,” *Tutorials Rev. Int. J. Bifurc. Chaos*, vol. 10, no. 10, pp. 2291–2305, 2000.
- [56] C. Schäfer, M. G. Rosenblum, H. H. Abel, and J. Kurths, “Synchronization in the human cardiorespiratory system.,” *Phys. Rev. E. Stat. Phys. Plasmas. Fluids. Relat. Interdiscip. Topics*, vol. 60, no. 1, pp. 857–870, 1999.
- [57] M. G. Rosenblum, J. Kurths, A. Pikovsky, C. Schäfer, P. Tass, and H. H. Abel, “Synchronization in noisy systems and cardiorespiratory interaction,” *IEEE Engineering in Medicine and Biology Magazine*, vol. 17, no. 6, pp. 46–53, 1998.
- [58] C. Hamann, R. P. Bartsch, A. Y. Schumann, T. Penzel, S. Havlin, and J. W. Kantelhardt, “Automated synchrogram analysis applied to heartbeat and reconstructed respiration,” *Chaos*, vol. 19, no. 1, 2009.

- [59] P. Tass *et al.*, “Detection of $n:m$ Phase Locking from Noisy Data: Application to Magnetoencephalography,” *Phys. Rev. Lett.*, vol. 81, no. 15, pp. 3291–3294, 1998.
- [60] C. Schäfer, M. G. Rosenblum, J. Kurths, and H. H. Abel, “Heartbeat synchronized with ventilation.,” *Nature*, vol. 392, no. 6673, pp. 239–240, 1998.
- [61] C. D. Nguyen, C. Dakin, M. Yuill, S. Crozier, and S. Wilson, “The effect of sigh on cardiorespiratory synchronization in healthy sleeping infants.,” *Sleep*, vol. 35, no. 12, pp. 1643–50, 2012.
- [62] D. Cysarz, H. Bettermann, S. Lange, D. Geue, and P. van Leeuwen, “A quantitative comparison of different methods to detect cardiorespiratory coordination during night-time sleep.,” *Biomed. Eng. Online*, vol. 3, no. 1, p. 44, 2004.
- [63] R. Mrowka, A. Patzak, and M. Rosenblum, “Quantitative Analysis of Cardiorespiratory Synchronization in Infants,” *Int. J. Bifurc. Chaos*, vol. 10, no. 11, pp. 2479–2488, 2000.
- [64] R. Mrowka, L. Cimponeriu, A. Patzak, and M. G. Rosenblum, “Directionality of coupling of physiological subsystems: age-related changes of cardiorespiratory interaction during different sleep stages in babies.,” *Am. J. Physiol. Regul. Integr. Comp. Physiol.*, vol. 285, no. 6, pp. R1395-401, 2003.
- [65] M. G. Rosenblum, L. Cimponeriu, A. Bezerianos, A. Patzak, and R. Mrowka, “Identification of coupling direction: application to cardiorespiratory interaction,” *Phys. Rev. E. Stat. Nonlin. Soft Matter Phys.*, vol. 65, no. 4, p. 11, 2002.
- [66] M. G. Rosenblum and a S. Pikovsky, “Detecting direction of coupling in interacting oscillators.,” *Phys. Rev. E. Stat. Nonlin. Soft Matter Phys.*, vol. 64, no. 4 Pt 2, p. 45202, 2001.
- [67] B. Kralemann, L. Cimponeriu, M. Rosenblum, A. Pikovsky, and R. Mrowka, “Phase dynamics of coupled oscillators reconstructed from data,” *Phys. Rev. E - Stat. Nonlinear, Soft Matter Phys.*, vol. 77, no. 6, pp. 1–16, 2008.
- [68] B. Kralemann, L. Cimponeriu, M. Rosenblum, A. Pikovsky, and R. Mrowka,

- “Uncovering interaction of coupled oscillators from data,” *Phys. Rev. E - Stat. Nonlinear, Soft Matter Phys.*, vol. 76, no. 5, pp. 1–4, 2007.
- [69] M. Lucchini, N. Pini, W. P. Fifer, N. Burtchen, and M. G. Signorini, “Cardio-respiratory phase locking in newborn and one month infants as a function of sleep state,” in *EMBEC & NBC*, 2017.
- [70] M. Lucchini, W. P. Fifer, R. Sahni, and M. G. Signorini, “Novel heart rate parameters for the assessment of autonomic nervous system function in premature infants.,” *Physiol. Meas.*, vol. 37, no. 9, pp. 1436–46, 2016.
- [71] S. W. Porges and S. A. Furman, “The early development of the autonomic nervous system provides a neural platform for social behaviour: A polyvagal perspective,” *Infant Child Dev.*, vol. 20, no. 1, pp. 106–118, 2011.
- [72] D. E. Lake, J. S. Richman, M. P. Griffin, and J. R. Moorman, “Sample entropy analysis of neonatal heart rate variability,” *Am J Physiol Regul Integr Comp Physiol*, vol. 283, no. 3, pp. R789-97, 2002.
- [73] M. G. Frasch, U. Zwiener, D. Hoyer, and M. Eiselt, “Autonomic organization of respirocardial function in healthy human neonates in quiet and active sleep,” *Early Hum. Dev.*, vol. 83, no. 4, pp. 269–277, 2007.
- [74] P. Indic, E. Bloch-Salisbury, F. Bednarek, E. N. Brown, D. Paydarfar, and R. Barbieri, “Assessment of cardio-respiratory interactions in preterm infants by bivariate autoregressive modeling and surrogate data analysis,” *Early Hum. Dev.*, vol. 87, no. 7, pp. 477–487, 2011.